Wabash CarbonSAFE

Static and Dynamic Modeling
Task 9.0
Technical Report

February 1, 2019 through March 31, 2022

Richard Dessenberger, Roland Okwen, Mansour Khosravi, Scott Frailey, James Damico, Carl Carman

Prairie Research Institute
University of Illinois
Urbana-Champaign, IL 61820

Report Issued: February 13, 2022

Report Number: DOE-FE0031626-8
U.S. DOE Cooperative Agreement Number: DE-FE0031626

Principal Investigator: Mr. Christopher Korose
Business Contact: Illinois State Geological Survey
615 E Peabody Drive
Champaign, IL 61820-7406

DISCLAIMER

Table of Contents

List of Figures

List of Tables

Executive Summary

The objective of the Wabash CarbonSAFE project's static and dynamic modeling task is to assess the feasibility of storing 50 million tonnes (1.67 million metric tonnes annually; MMTA) of industrially-sourced carbon dioxide (CO_2) in a commercial-scale geological storage complex at Wabash Valley Resources LLC (WVR) gasification facility near Terre Haute, Indiana over a period of 30 years. The targeted formations for storing CO_2 are: 1). Mt Simon Sandstone (MSS) and the 2). Potosi Dolomite (Knox Group). Also evaluated was storing 20 million tonnes (1.67 MMTA) of CO_2 over 12 years, to address current commercial scenarios based on 45Q laws, which are driving commercial activity generally.

All of the available data from the recently drilled Wabash #1 stratigraphic test well (now plugged and abandoned) were used in the construction of both the static and dynamic models. Geologic models were constructed to characterize both the Mt Simon Sandstone and Potosi Dolomite storage complexes. Dynamic simulation models were constructed and used to assess the feasibility of injecting CO_2 into the Mt Simon and Potosi formations. The geocellular models for the Potosi Dolomite and Mt. Simon Sandstone were built using Petrel™, Schlumberger's reservoir modeling software. The dynamic simulations were run using Landmark's *Nexus*® reservoir simulation software

The general workflow for developing the geocellular models for the Mt. Simon Sandstone and Potosi Dolomite can be characterized as comprising six principal steps: 1) compile structure surfaces, formation tops, petrophysical data, core and well test data; 2) develop separate 3-D structural frameworks for the Mt. Simon Sandstone and Potosi Dolomite and their overlying formations; 3) define zones and layers for the injection zones and confining units; 4) scale up the porosity and permeability data into the zones and layers using mathematical averaging methods; 5) analyze well data and define the variograms for the porosity and permeability data; 6) populate grids with the porosity and permeability utilizing geostatistical algorithms. Sequential Gaussian Simulation (SGS) algorithms were utilized to populate the grids with porosity and permeability data for the Potosi and Mt. Simon models.

For constructing the Mt. Simon model, in addition to Wabash #1 well data, the petrophysical log data of over 20 wells that penetrated the Lower Mt. Simon were imported into the Petrel™ software. The data were used to correlate the formation tops, build the surfaces, thickness maps, and estimate the spatial distribution of porosity and permeability data. In addition to the porosity and permeability data of the Wabash #1 well, the porosity data of 28 wells and permeability data of 6 wells were imported into a regional static model for 1) data analysis and defining the vertical and horizontal variograms through the Illinois Basin, and 2) using the parameters for distributing porosity and permeability into the Mt. Simon model. The model is centered on Wabash #1 and covers a 22 by 22 mile area.

The input data for the Potosi model comprise: the petrophysical log data of Wabash #1 at half-ft (0.15 m) intervals including Gamma ray, resistivity, porosity, photoelectric, and sonic logs, and structure surfaces, thickness maps, well test data, and permeability data. The Potosi static model is a layer cake model, and the grids were propagated with the porosity and permeability data of Wabash #1. The model boundary covers a surface area of about 22 x 22 miles and includes Wabash #1 and two proposed wells (Well 1-North; Well 2-South) locations. The Potosi Dolomite consists of streaks with high porosity and permeability values and thick dolomite intervals with lower property values, therefore the Potosi zones were subdivided into thinner layers to reproduce the reservoir properties from the 0.5-ft porosity and permeability data from Wabash #1 logs. It is uncertain if the permeability of the Potosi Dolomite is consistent within the project boundary, but the presence of vuggy intervals and lost circulation zones in almost all wells that encounter the Potosi throughout the Illinois Basin suggest that the pore throat systems of vuggy intervals are highly connected. Thus, the Potosi static model was built by assuming the spatial connectivity of the vugs in the horizontal direction and discontinuity of pore systems in the vertical direction.

A *Nexus*® dynamic simulation model for the Mt Simon sandstone was constructed using the geologic model exported from Petrel™. Porosity and permeability were populated within the Petrel™ model and exported

to *Nexus*®. Two permeability models were considered: Core-correlated and DST-correlated models which are low-perm and high-perm realizations; respectively. The Core-correlated permeability model matches the permeability measured on Wabash #1 cores. The DST-correlated permeability model matches the permeability from Wabash #1 well tests.

Dynamic simulations were performed to assess the CO_2 injectivity of the Mt Simon. Single well and multiple well injection scenarios were considered. Learnings from the Mt Simon simulation study are as follows:

- It is not possible to inject 1.67 MMTA of CO_2 for 30 years into the Mt Simon at Wabash #1 with a single well.
- A single vertical well (with various completion intervals) and a single 1,000 m long horizontal well (at various depths) were considered. None were capable of injecting 1.67 MMTA for 30 years.
- It is possible to inject 1.67 MMTA of CO_2 for 30 years into the Mt Simon with multiple wells, but the well count differs substantially between the DST-correlated and Core-correlated permeability models.
- DST-correlated permeability model results indicate that two wells spaced 1.5 to 3 miles apart are capable of injecting 1.67 MMTA of CO_2 for 30 years into the Mt Simon.
- Core-correlated permeability model results indicate that considerably more wells are necessary for the injection of 1.67 MMTA of CO_2 for 30 years into the Mt Simon.
- Due to the lower injectivity of the Mt Simon at Wabash #1 (relative to the higher injectivity typically observed in the central portion of the Illinois basin), the focus of this project was shifted toward injection of 1.67 MMTA of CO_2 for 30 years into the Potosi Dolomite.

A *Nexus*® dynamic simulation model for the Potosi Dolomite was constructed using the geologic model exported from Petrel™. The model includes the Potosi Dolomite, underlying Davis Formation, and the overburden formations (listed in descending order) the Maquoketa Group, Trenton Limestone, Platteville (Black River) Group, Dutchtown Limestone, St. Peter Sandstone, Shakopee Dolomite, and Oneota Dolomite.

Dynamic simulations were performed to assess the CO_2 injectivity of the Potosi Dolomite for several injection scenarios. Each simulation includes an injection period of either 12 or 30 years, followed by a 50 year post-injection observation period. The four injection scenarios simulated include: two-well injection of 1.67 MMTA of CO_2 for 30 years and 12 years, and single-well injection of 1.67 MMTA of CO_2 into Wabash #1 for 30 years and 12 years. Learnings from the Potosi simulation study are as follows:

- The Potosi has adequate injectivity to support a large scale CO_2 injection project at the Wabash site; as it is possible to inject over 5 MMTA for 30 years without exceeding the fracture pressure of the Potosi.
- CO_2 plume radius for injecting 1.67 MMTA for 12 years into Wabash #1 is 2.8 miles.
- CO_2 plume radius for injecting 1.67 MMTA for 30 years into Wabash #1 is 3.8 miles.
- CO_2 plume radius for injecting 1.67 MMTA for 12 years into two wells that are 5 miles apart is 2.2 miles.
- CO_2 plume radius for injecting 1.67 MMTA for 30 years into two wells that are 5 miles apart is 3.0 miles.
- The pressure increase from injection does not substantially propagate vertically past the Dutchtown formation; which results in a negligible increase in pressure in any overlying formations above the Dutchtown.

1. Introduction

The objective of the Wabash CarbonSAFE project's static and dynamic modeling task is to assess the feasibility of storing 50 million tonnes (1.67 million metric tonnes annually; MMTA) of industrially-sourced carbon dioxide (CO_2) in a commercial-scale geological storage complex at Wabash Valley Resources LLC (WVR) gasification facility near Terre Haute, Indiana over a period of 30 years. The targeted formations for storing CO_2 are: 1). Mt Simon Sandstone (MSS) and the 2). Potosi Dolomite (Knox Group). Also evaluated was storing 20 million tonnes (1.67 MMTA) of CO_2 over 12 years, to address current commercial scenarios based on 45Q laws, which are driving commercial activity generally.

All of the available data from the recently drilled Wabash #1 stratigraphic test well (now plugged and abandoned) were used in the construction of both the static and dynamic models. The next sections of the report describe the geologic models that were constructed to characterize both the Mt Simon Sandstone and Potosi Dolomite storage complexes. Later sections describe the dynamic simulation models that were constructed and used to assess the feasibility of injecting CO_2 into the Mt Simon and Potosi formations.

2. Static Modeling

The geologic potential of the Mt. Simon Sandstone and Potosi Dolomite for injection of CO_2 was assessed through reservoir modeling processes. Building an accurate 3-D geocellular model for the injection intervals and their overlying formations was the primary objective of this task. The goal was to develop two separate models with sufficient details to represent the vertical and lateral heterogeneity at the injection zones in the site area which could be used as tools for simulation model and management.

The general workflow for developing the geocellular models for the Mt. Simon Sandstone and Potosi Dolomite shown in Figure 1 can be characterized as comprising six principal steps: 1) compile structure surfaces, formation tops, petrophysical data, core and well test data; 2) develop separate 3-D structural frameworks for the Mt. Simon Sandstone and Potosi Dolomite and their overlying formations; 3) define zones and layers for the injection zones and confining units; 4) scale up the porosity and permeability data into the zones and layers using mathematical averaging methods; 5) analyze well data and define the variograms for the porosity and permeability data; 6) populate grids with the porosity and permeability utilizing geostatistical algorithms.

2.1 Data Collection and Methods

The geocellular models for the Potosi Dolomite and Mt. Simon Sandstone were built using Petrel™, Schlumberger's reservoir modeling software. The input data for the Potosi model comprise: the petrophysical log data of the Wabash #1 at half-ft (0.15 m) intervals including Gamma ray, resistivity, porosity, photoelectric, and sonic logs, and structure surfaces from the top of the Maquoketa Shale to the Eau Claire Formation, thickness maps, well test data, and permeability data. The permeability data were estimated using the Lucia (1983, 1995) equations. The surfaces were constructed by formation from wells in the Illinois Basin. The Potosi static model is a layer cake model, and the grids were propagated with the porosity and permeability data of the Wabash #1 well.

For constructing the Mt. Simon model, in addition to Wabash #1 well data, the petrophysical log data of over 20 wells that penetrated the Lower Mt. Simon were imported into the Petrel™ software. The data were used to correlate the formation tops, build the surfaces, thickness maps, and estimate the spatial distribution of porosity and permeability data. The permeability data at the Wabash #1 were estimated using cementation factor derived from resistivity logs and sandstone grain sizes (Khosravi et al., 2022). After estimating the permeability data, the results were correlated against the core analysis data and drill stem test (DST) results from Wabash #1. Eventually, because of discrepancies between the core data and

DST data, two permeability models were proposed: a core-correlated permeability model and a DST-correlated permeability model. Porosity values in several selected wells were obtained on a limestone matrix (2.71 g/cc); they were then calibrated to a sandstone matrix (2.65 g/cc). For several wells with density-porosity and neutron- porosity, cross-plot of neutron-density porosity logs were calculated and imported into the model. In some cases where porosity logs were not available, porosity values were computed from bulk density logs (see Asquith and Krygowski 2004). The structural surfaces from top of the Eau Claire shale to Precambrian and the thickness map of the intervals were used to build the structural framework of the static model. Sequential Gaussian Simulation (SGS) algorithms were utilized to populate the grids with porosity and permeability data for the Potosi and Mt. Simon models.

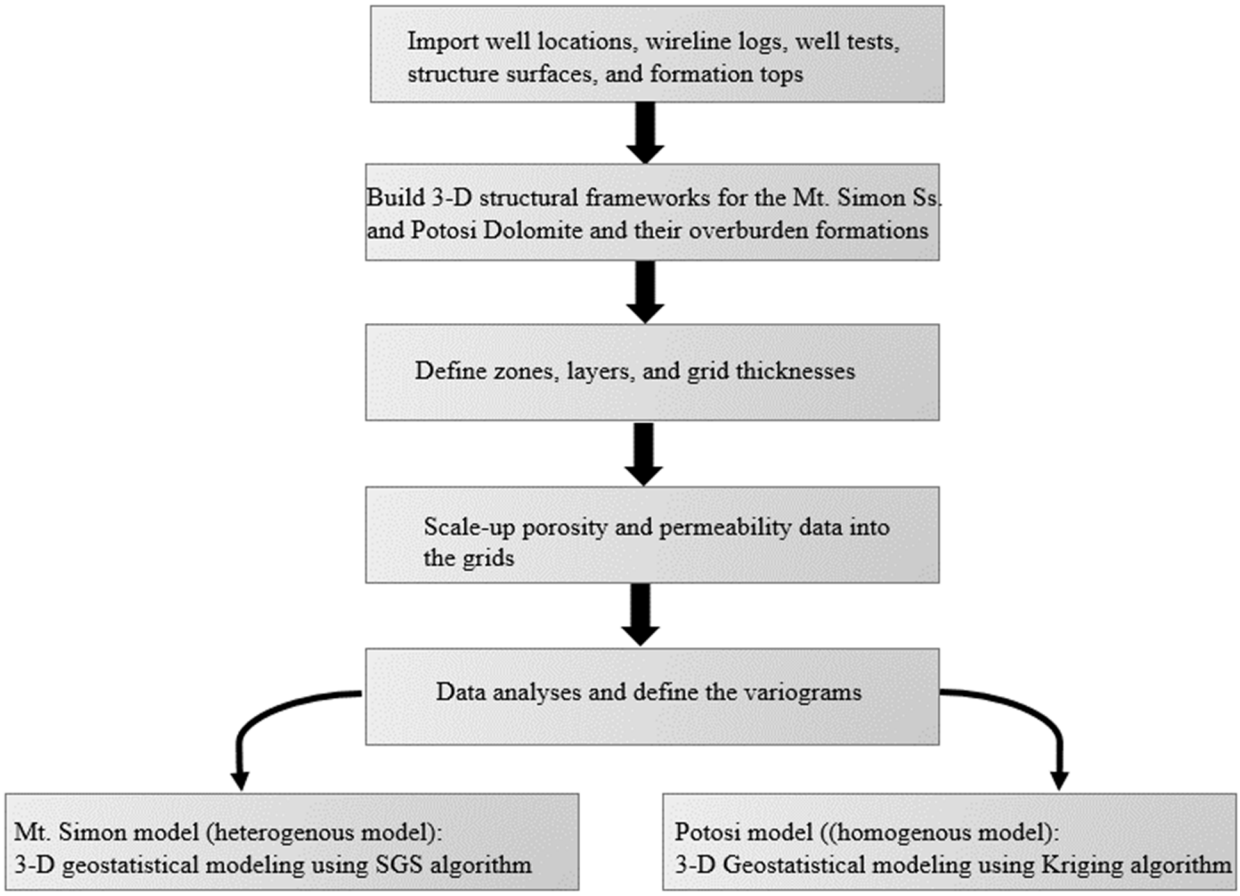

Figure 1*. Workflow for developing geocellular models for the Mt. Simon Sandstone and Potosi Dolomite.*

2.2 Mt Simon Sandstone

2.2.1 Structural framework

For construction of the structural framework of the Mt. Simon Sandstone, regional structural surfaces from the top of the Eau Claire Formation to top of the Precambrian crystalline basement were utilized. The structural framework of the Mt. Simon model includes the surfaces of the Eau Claire, Upper Mt. Simon, Middle Mt. Simon, Lower Mt. Simon, Argenta, and Precambrian crystalline basement (Figure 2).

The model boundary covers a surface area of 22 x 22 mile (35.4 x 35.4 km) centered on Wabash #1 (Figure 3). The model includes 60 cells in X direction and 60 cells in Y direction with grid spacing of 2000 ft x 2000 ft (608 x 608 m). The overall thickness of the geocellular model is approximately 3413 ft (1040 m).

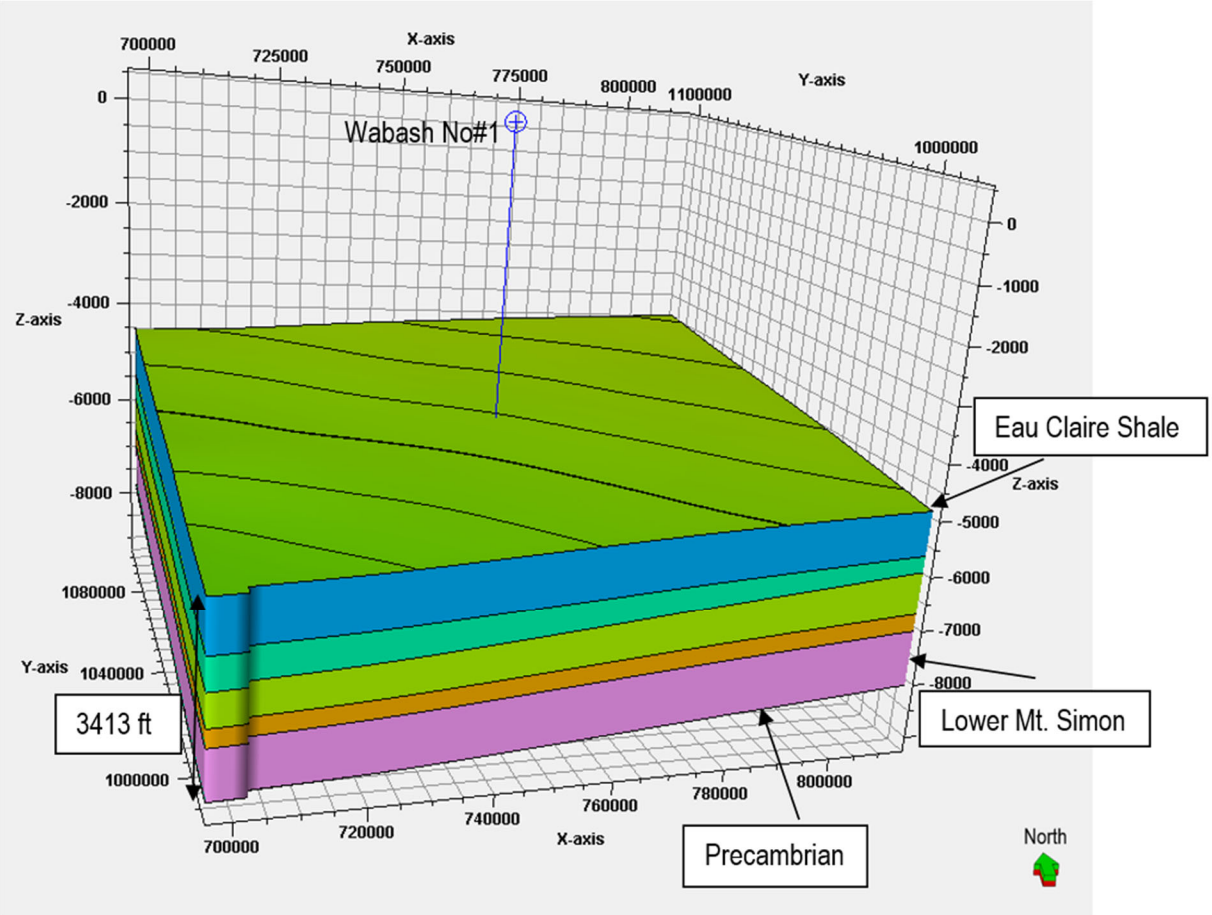

Figure 2. *3-D structural framework of the Mt. Simon model. The top of the project is the Eau Claire Shale structure surface, and the base is the top of the Precambrian.*

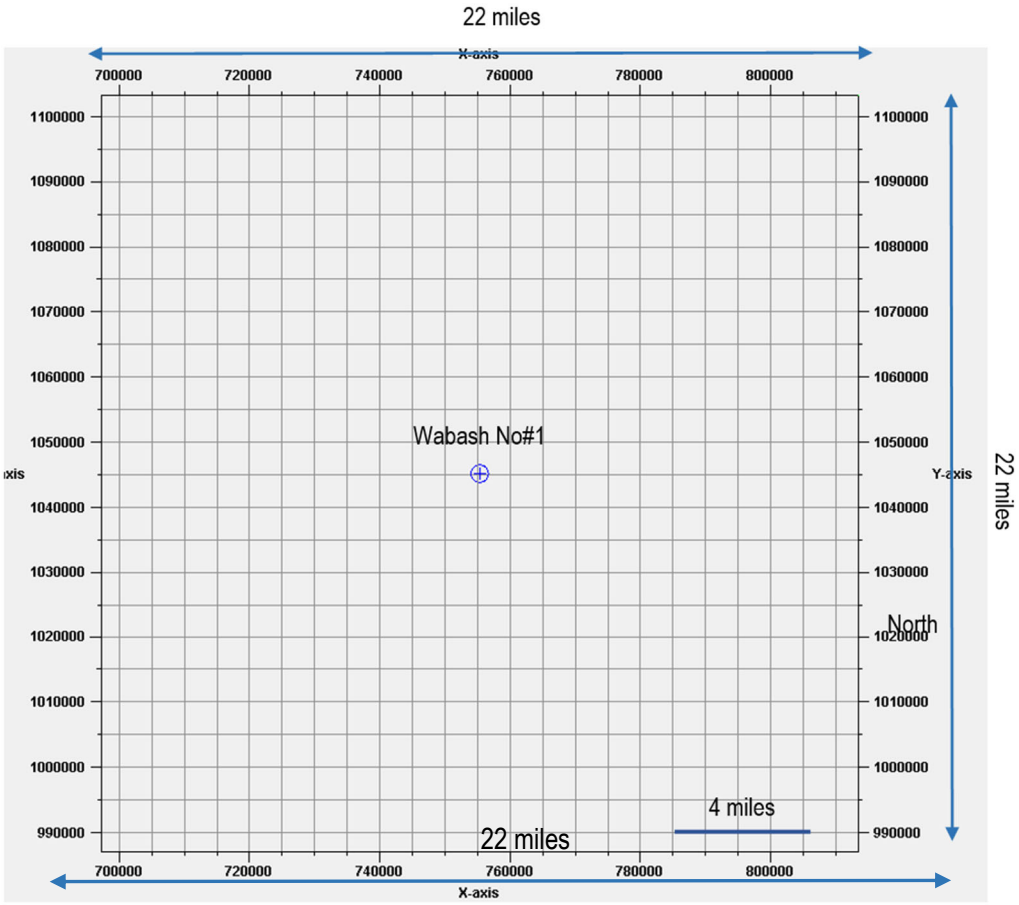

Figure 3. *Dimensions of the Mt. Simon model boundary, centered on the Wabash #1 well.*

2.2.2 Model Zonation

The structural framework for the model was built based on structural surfaces from Eau Claire Formation to Precambrian crystalline basement, and formations top of the wells penetrate the Mt. Simon Sandstone in Illinois. The Lower Mt. Simon intervals were differentiated from the Middle and Upper Mt. Simon at the Illinois Basin – Decatur Project (IBDP) site regarding reservoir quality, lithology, and depositional environments (Freiburg et al., 2016). Accordingly, the correlative tops of the Lower, Middle, and Upper Mt. Simon were picked at the Wabash #1 (Figure 4). The Lower Mt. Simon interval with high porosity ranges is the main injection zone and the Middle and Upper Mt. Simon with low porosity ranges act as a baffle. The Lower Mt. Simon was divided into two zones: the upper zone and the Arkose zone. The Arkose zone is underlain by 20-ft intrusive basalt interval and considered as a separate zone. Below the basalt zone there are two intervals of 9 ft and 23 ft with high porosity ranges. The Eau Claire Formation was divided into two main zones, the upper part, which mostly consists of dolomitic intervals,

interbedded with limestone, sandstone and the lower part which is predominately comprised of shaly intervals. The top and the bottom of the model are constrained by structure surface on the top of the Eau Claire Formation and Precambrian crystalline basement, respectively. Table 1 shows the thickness and porosity range of the Mt. Simon static model zones:

Table 1. *Number, thickness, and porosity range of different zones of Mt. Simon model.*

Formations/Zone	Thickness/ Thickness range (ft)	Total Porosity range (%)
Eau Claire	256	0-8
Eau Claire Shale	699	0-45
Upper Mt. Simon	473.55	2-17
Middle Mt. Simon	667.54	2-15
Lower. Mt. Simon	315.1	1-16
Lower. Mt. Simon-Arkose	781.22	2-28
Basalt	20.58	0-15
Below basalt	200.07	4-39
Precambrian (Base of the model)	Model base	-

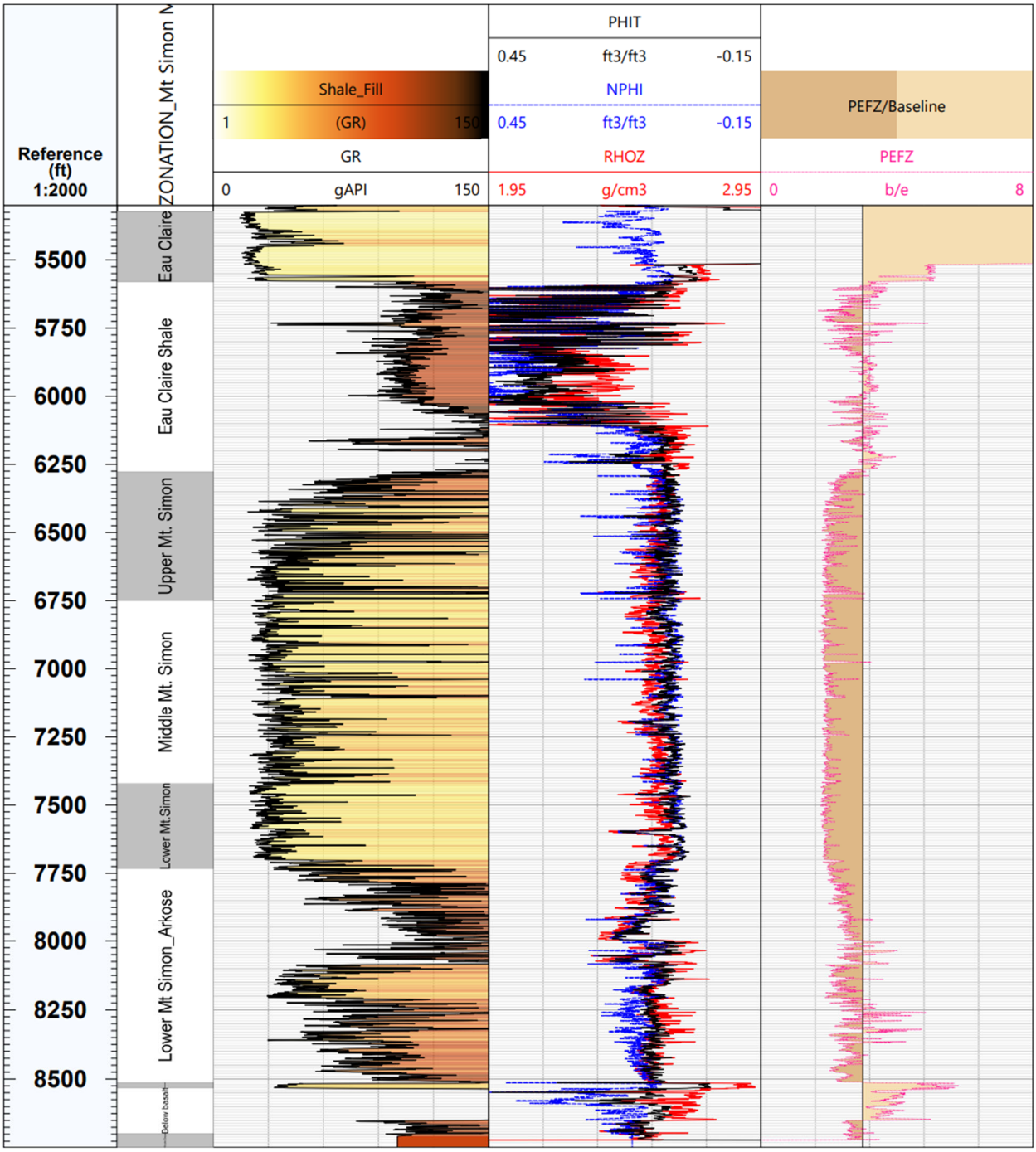

Figure 4. *Mt. Simon model zones with petrophysical logs. Log abbreviations: GR: Gamma ray; PHIT: density porosity; RHOZ: density; NPHI: Neutron porosity; PEFZ: photoelectric.*

2.2.3 Data Scale-up

The lower part of the Mt. Simon Sandstone has the highest range of porosity and permeability relative to the Middle and Upper Mt. Simon. The variogram data analyses were performed on porosity and permeability data to estimate the vertical variogram ranges of the values and determine the optimal number of model layers. Therefore, from the top of the Lower Mt. Simon to the base of the model the zones were subdivided into 5-ft layers to reproduce the reservoir properties from the 0.5-ft porosity and permeability data. The Eau Claire, and Upper and Middle Mt. Simon formations were layered coarsely since the intervals are composed of rocks with low porosity and permeability. As a result of data analysis, 739 layers were defined form the top to the base of the model. Table 4 shows the number of zones and layers for each interval. The Mt. Simon model boundary covers a surface area of 22 x 22 mile (35.4 x 35.4 km) with 9 zones. As a result, the 3-D geocellular model contains 2,616, 060 grid cells, including 59 columns, 60 rows, and 739 layers.

Error! Reference source not found.-A shows the histogram of the 0.5-ft porosity data relative to upscaled data. The histograms of upscaled data depict a reasonable correlation with the log data, except for in the intervals that coarsely layered with a porosity range of 1 to 4%.

Figures 5-B and 5-C show a high correlation between the histograms of log of upscaled permeabilities except for the intervals with less than 0.5 mD. The inconsistency of permeability log data and upscaled data within the range of 0.05 to 0.5 mD is related to the large thickness of overburden units.

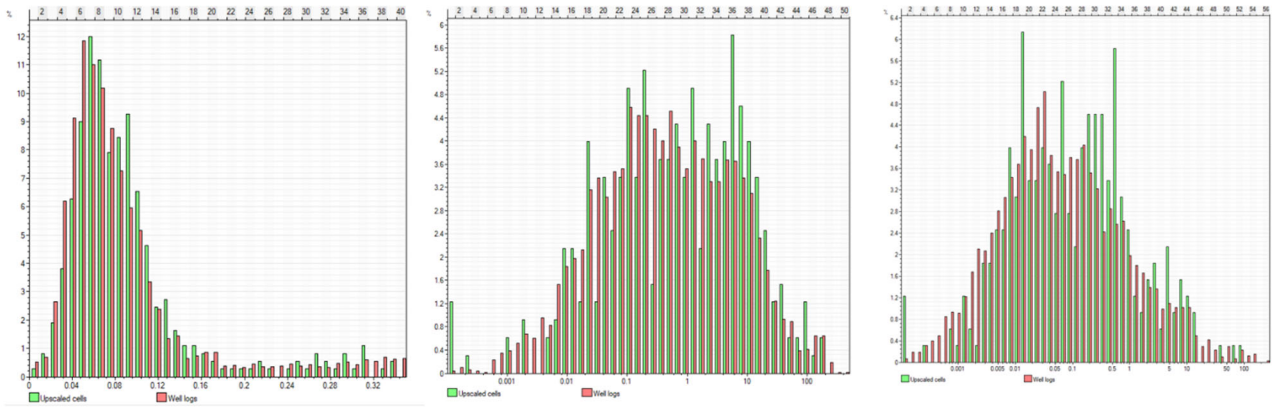

Figure 5*. 5-A, to left) Histogram of upscaled porosity (red) vs. well log porosity (green). 5-B, middle) histogram of upscaled DST-correlated permeability data (red) vs. well log permeability data (green). 5-C, to right) histogram of upscaled core-correlated permeability data (red) vs. well log permeability data (green).*

2.2.4 Mt. Simon 3D Geocellular Model

In addition of the porosity and permeability data of the Wabash #1 well, the porosity data of 28 wells and permeability data of 6 wells were imported into a regional static model for 1) data analysis and defining the vertical and horizontal variograms through the Illinois Basin, and 2) using the parameters for distributing porosity and permeability into the Mt. Simon model. Variogram models of the porosity and permeability data were constructed to establish data stationarity and spatial correlation of the data over the regional area where Mt. Simon Sandstone is present. The correlation distance allows for the use of geostatistical approaches to extrapolate the porosity and permeability data into the static model. Three types of variogram models—spherical, exponential, and Gaussian—are generally utilized for the

experimental model-fitting process (Dubrule, 2003). In this model the spherical model indicated a high correlation with the experimental variograms. A sequential Gaussian simulation (SGS) (Deutsch 2002) method was employed to distribute porosity and permeability using variogram parameters created for each interval. Table 2 and Table 3 show the porosity and permeability variograms' major, minor, and vertical ranges for each zone.

Table 2. *Major, minor, and vertical porosity of the derived variograms for the various zones of the Mt. Simon model.*

Zone	Major (ft)	Minor (ft)	Vertical (ft)
Eau Claire Fm. (upper part)	420,000	400,000	24
Eau Claire Shale	200,000	180,000	28
Upper Mt. Simon	580,000	390,000	53
Middle Mt. Simon	490,000	430,000	67
Lower Mt. Simon	560,000	388,000	46
Arkose zone	470,000	320,000	32
Basalt zone	100,000	50,000	10
Interval below the basalt	450,000	320,000	45

Table 3. *Major, minor, and vertical permeability of the derived variograms for the various zones of the Mt. Simon model.*

Zone	Major (ft)	Minor (ft)	Vertical (ft)
Eau Claire Fm. (upper part)	-	-	-
Eau Claire Shale	-	-	-
Upper Mt. Simon	570,000	470,000	61
Middle Mt. Simon	280,000	270,000	74
Lower Mt. Simon	560,000	420,000	54
Arkose zone	525,000	511,000	45
Basalt zone	100,000	50,000	10
Interval below the basalt	520,000	470,000	61

Error! Reference source not found. through Figure 8 depict cross sections of the distribution of porosity and permeability in the regional models, intersecting with 6 wells including Wabash #1. The locations of the wells in Illinois and Indiana are shown in Figure 9. In the porosity cross section, the areas with high porosity are shown in red, whereas the areas with low porosity are shown in blue (**Error! Reference source not found.**). In the permeability models cross sections, the areas with high permeability are shown in red, whereas the areas with low permeability are shown in purple (Figure 8 and Figure 8).

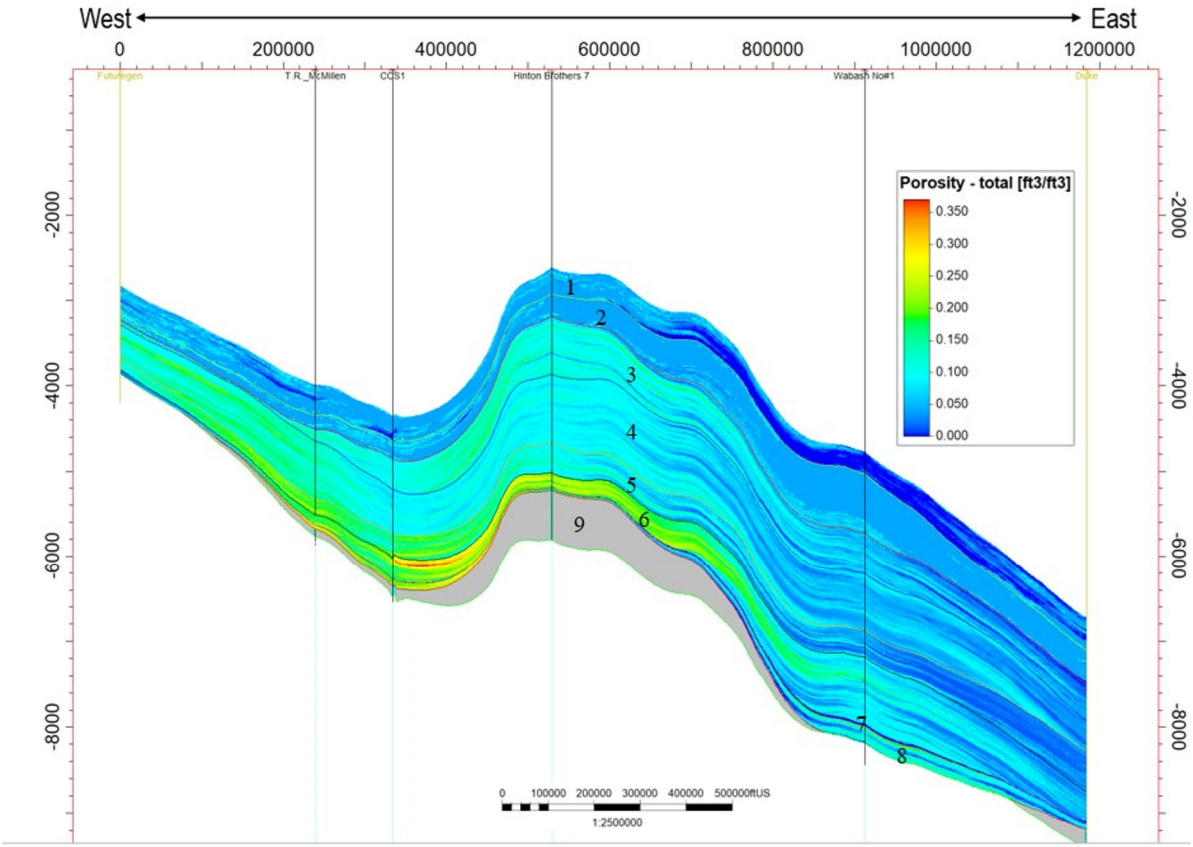

Figure 6. *West-East cross section of porosity model showing the distribution and trend of the porosity. The vertical exaggeration (Z scale) of the model is 100 scale to better show the depth of the model and the trend of porosity. Formation codes: 1: Eau Claire Fm.; 2: Eau Claire shale; 3: Upper Mt. Simon; 4: Middle Mt. Simon; 5: Lower Mt. Simon; 6: Arkose zone; 7: Basalt; 8: interval below basalt ; 9: Precambrian.*

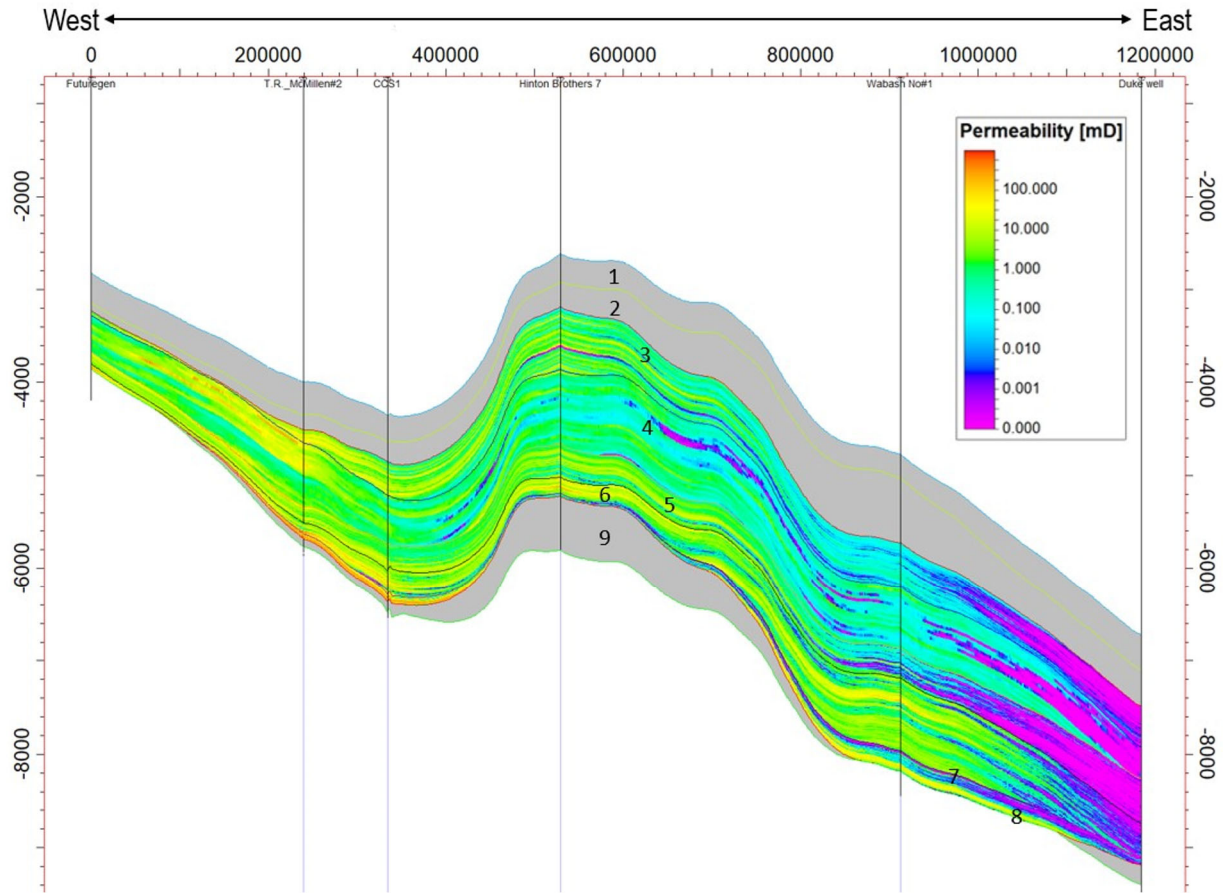

Figure 7. *West-East cross section of DST-correlated permeability model showing the distribution and trend of the permeability. The vertical exaggeration (Z scale) of the model is 100 used to better show the depth of the model and the trend of permeability. Formation codes: 1: Eau Claire Fm.; 2: Eau Claire shale; 3: Upper Mt. Simon; 4: Middle Mt. Simon; 5: Lower Mt. Simon; 6: Arkose zone; 7: Basalt; 8: interval below basalt ; 9: Precambrian.*

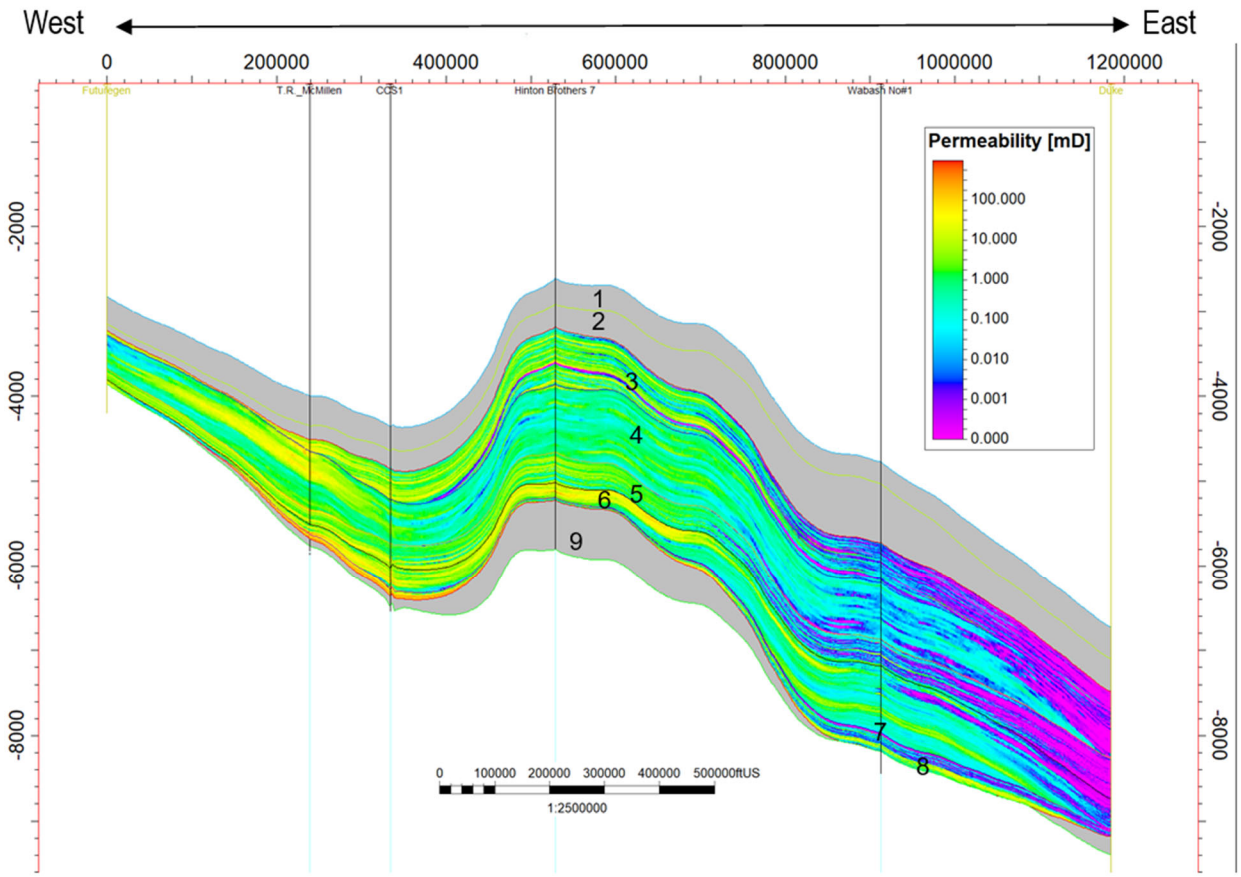

Figure 8. *West-East cross section of core-correlated permeability model showing the distribution and trend of the permeability. The vertical exaggeration (Z scale) of the model is 100 used to better show the depth of the model and the trend of permeability. Formation codes: 1: Eau Claire Fm.; 2: Eau Claire shale; 3: Upper Mt. Simon; 4: Middle Mt. Simon; 5: Lower Mt. Simon; 6: Arkose zone; 7: Basalt; 8: interval below basalt ; 9: Precambrian.*

The cross sections depict the arkose zone as having the highest porosity and permeability ranges with an increasing trend toward the CCS1 well in central Illinois. However, in the vicinity of the Wabash #1 well the estimated permeability matched with core data shows lower ranges relative to the estimated permeability correlated with DST data from the well. The porosity and permeability of the intervals decrease toward Duke well in the southern part of Indiana. The upper portion of the Lower Mt. Simon shows 12 to 18% porosity and 10-30 mD permeability through central and western Illinois but the reservoir properties dramatically reduce toward Indiana. The Middle Mt. Simon regionally consists of tight sandstones, except in western Illinois where the FutureGen and T. R. McMillen#2 wells are located. The Upper Mt. Simon porosity is less than 10% close to Wabash #1 and about 3-5% at the Duke well. However, the porosity ranges increase toward CCS1 and T.R. Mc Millen#2 to about 12%. The permeability cross section shows a similar trend to the porosity model for the Upper Mt. Simon, indicating an increase in permeability ranges from east to west. The Eau Claire Formation consists of thick intervals of shale with a low range of effective porosity (1-3%) and thin intervals of dolomite, silt and sand with less than 5% porosity. These intervals with low porosity and permeability in the model act as barrier to fluid flow.

The Mt. Simon static model was constructed using the regional trend of the porosity and permeability models. Figure 10 through Figure 12 show the porosity and permeability models and E-W cross sections. The model is centered the Wabash #1 and covers a 22 by 22 mile area. The porosity of the Eau Claire Formation is incredibly low, and the formation acts as a barrier to flow. The intervals of the Upper and Middle Mt. Simon show a low range of porosity and permeability. The Lower Mt. Simon and the Arkose part show high porosity and permeability ranges. In the Wabash #1 well, there is a basalt zone below the Lower Mt. Simon with extremely low porosity and permeability ranges. However, the basalt zone is regionally discontinuous and is modeled only around the Wabash #1 well. Two regionally discontinuous sandstone intervals below the basalt zone with thicknesses of 9 and 23 ft show high porosity and permeability ranges near the Wabash #1 well. Because of their thickness, extent, and reservoir properties in the Wabash #1 well area, the two intervals below the basalt interval and the Arkose zone can be considered locally as injection intervals.

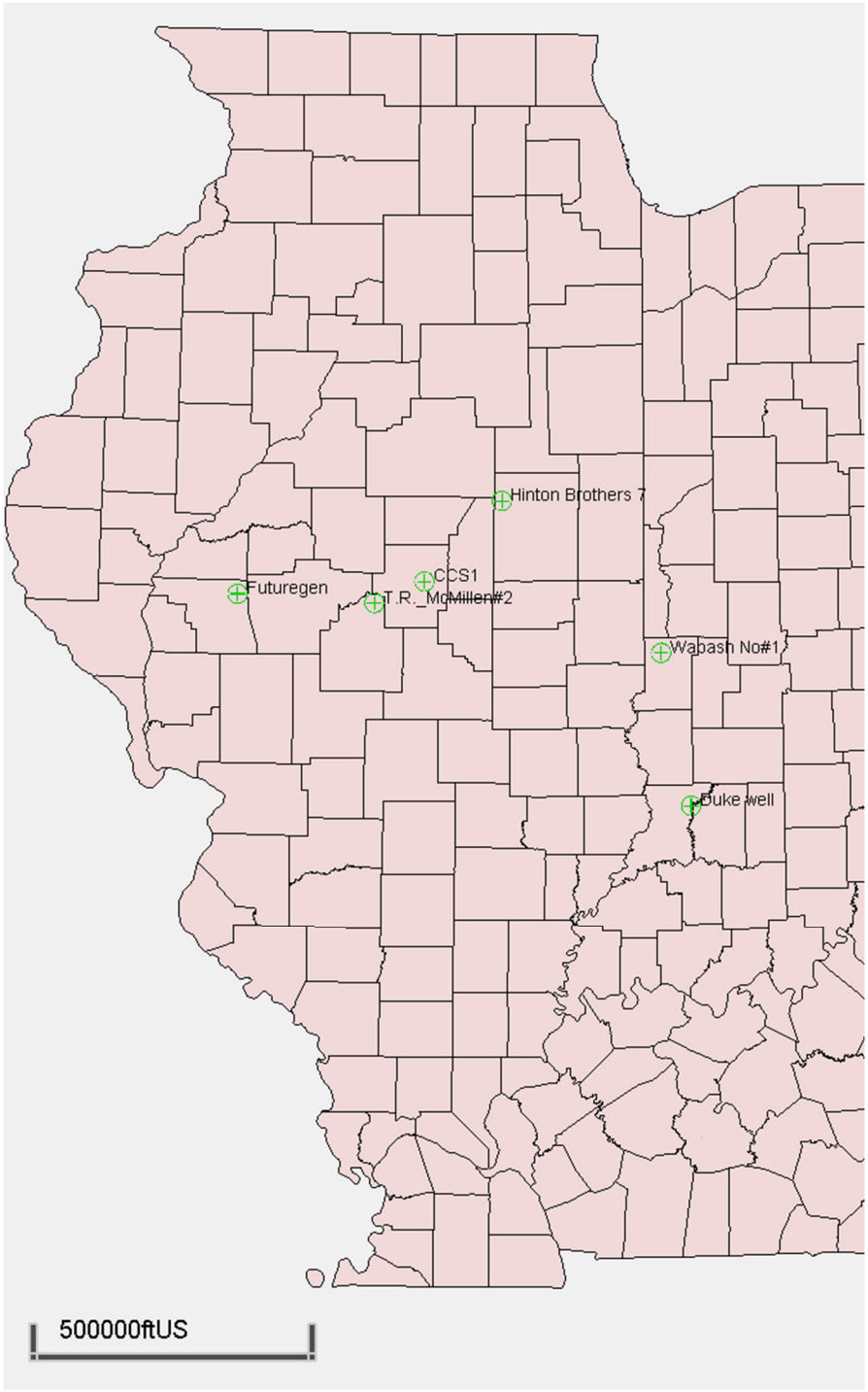

Figure 9. *The locations of the wells in E-W cross section of regional porosity and permeability models.*

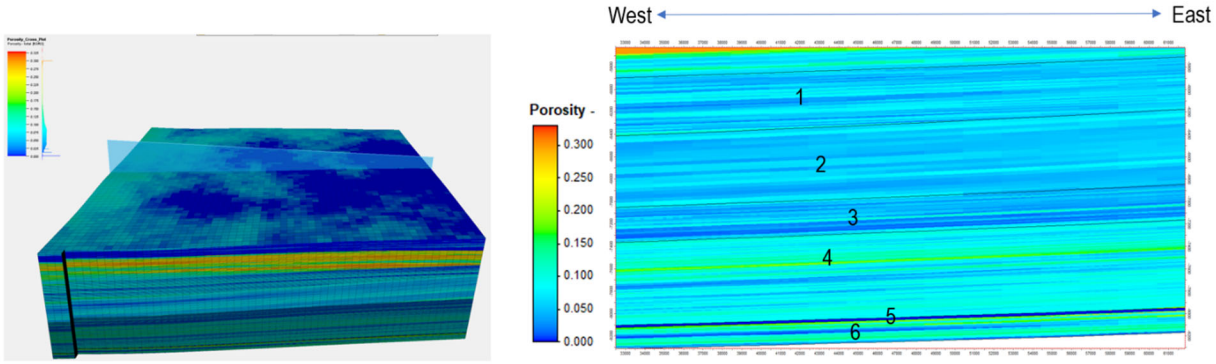

Figure 10. *The 22 by 22 mile porosity model from top of the Eau Claire Formation to Precambrian Crystalline basement. The Wabash #1 is at the center of the model. The E-W cross section shows the porosity of the Upper and Middle, Lower Mt. Simon, and basalt zone. Note: Two intervals below the basalt show high porosity ranges. Zone codes: 1: Upper Mt. Simon; 2: Middle Mt. Simon; 3: Lower Mt. Simon; 4: Arkose zone; 5: Basalt; 6: interval below the basalt.*

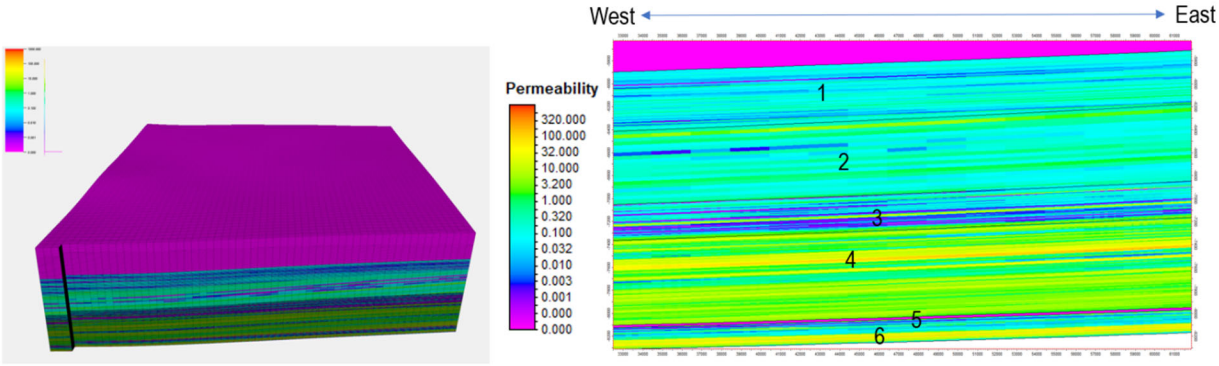

Figure 11. *The 22 by 22 mile DST- correlated permeability model from top of the Eau Claire Formation to Precambrian crystalline basement. The Wabash #1 is at the center of the model. The E-W cross section shows the porosity of the Upper and Middle, Lower Mt. Simon, and basalt zone. Note two intervals below the basalt show high permeability ranges. Zone codes: 1: Upper Mt. Simon; 2: Middle Mt. Simon; 3: Lower Mt. Simon; 4: Arkose zone; 5: Basalt; 6: interval below the basalt.*

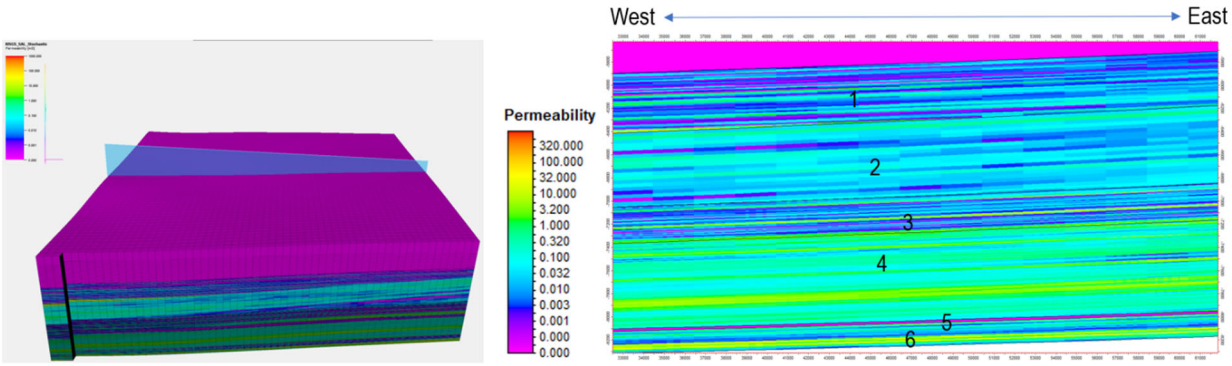

Figure 12. *The 22 by 22 mile core- correlated permeability model from top of the Eau Claire Formation to Precambrian crystalline basement. The Wabash #1 is at the center of the model. The E-W cross section shows the porosity of the Upper and Middle, Lower Mt. Simon, and basalt zone. Note two intervals below the basalt show high permeability ranges. Zone codes: 1: Upper Mt. Simon; 2: Middle Mt. Simon; 3: Lower Mt. Simon; 4: Arkose zone; 5: Basalt; 6: interval below the basalt.*

2.3 Potosi Dolomite

2.3.1 Structural framework

Regional structural surfaces from the top of the Maquoketa Shale (Maquoketa Group) to the top of the Eau Claire Formation and thickness maps of the formations were utilized to prepare the structure framework of the model. Thickness maps were subtracted from the structure map on the top of the Maquoketa to provide surfaces for all intervals including Trenton Limestone, Platteville (Black River) Group, Shakopee Dolomite, Oneota Dolomite, Potosi Dolomite, Davis Formation, and Eau Claire Formation (Figure 13). The model boundary covers a surface area of about 22 x 22 miles (35.4 x 35.4 km) and includes Wabash #1 and also two proposed wells (Well 1-North; Well 2-South) locations. The model is comprised of 116 cells in X direction and 116 cells in Y direction with grid spacing of 1000 ft x 1000 ft (304 x 304 m; Figure 14). Ground elevation is approximately 552 ft (168 m) above mean sea level. The overall thickness of the geocellular model is approximately 2936 ft (895 m).

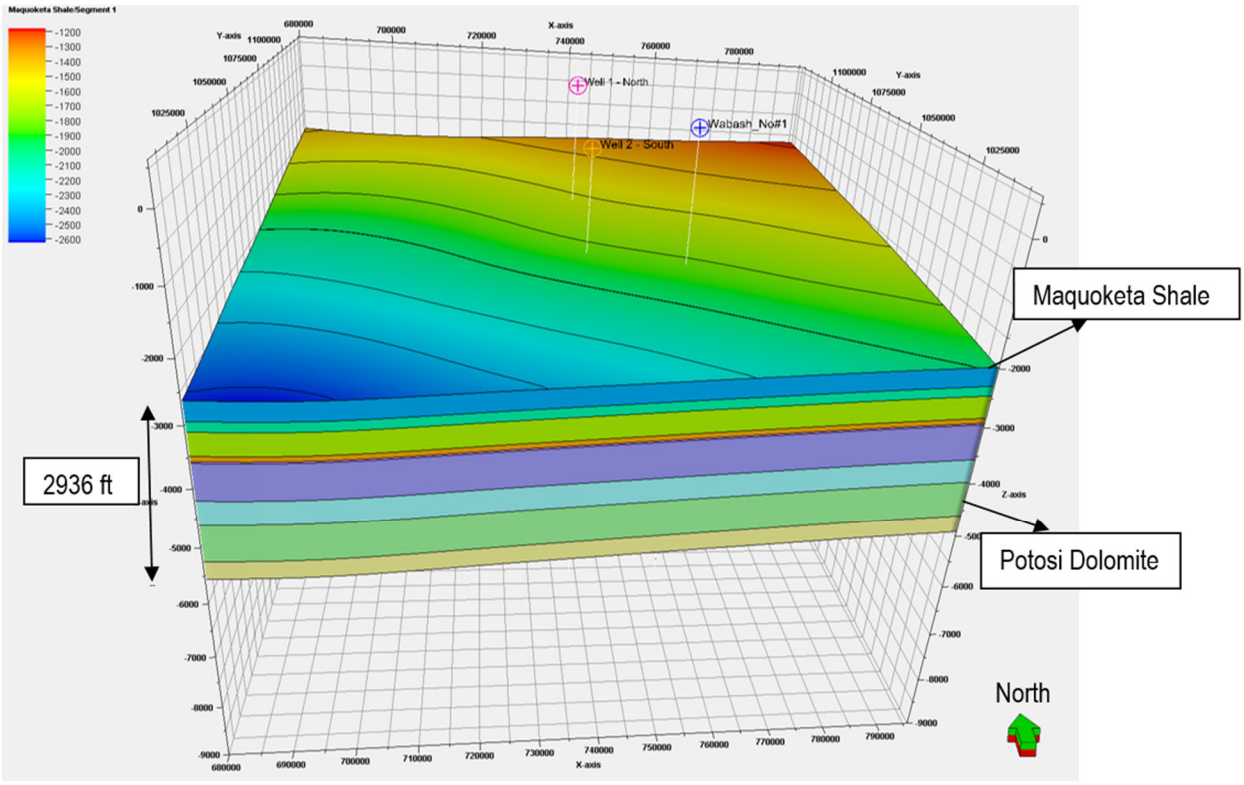

Figure 13. *3-D structural framework of the Potosi model, the top of the project is the Maquoketa Shale structure surface, and the base is the top of the Eau Claire Formation. The Potosi Dolomite interval is shown with green color.*

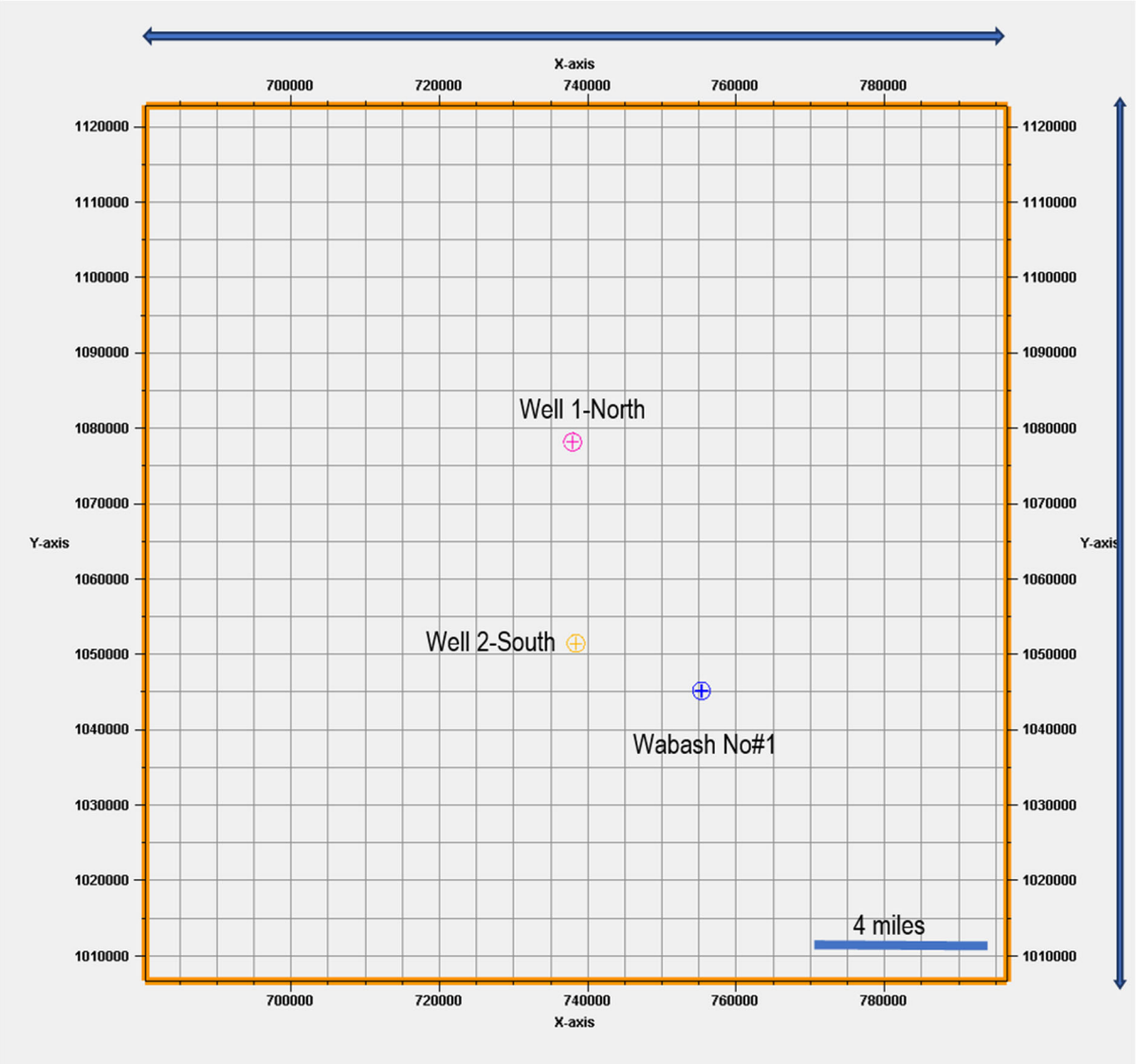

Figure 14. *Dimensions of the Potosi model boundary and location of drilled well (Wabash #1), and proposed wells (Well 1-North; Well 1- South).*

2.3.2 Model Zonation

The petrophysical analyses and previous studies of the Potosi Dolomite (Lasemi and Khorasgani, 2020) indicate the Potosi Dolomite contains cavernous and fracture porosities. The is no core interval from the Potosi Dolomite at the Wabash #1 well, but the core intervals from equivalent intervals at the IBDP site contains large vugs and fracture porosities (Adushita and Smith, 2014). The lateral extent of the vuggy intervals (streaks) is unknown, but mud circulation losses reported from wells in north-central and western Illinois and a low percentage of core recovery from equivalent intervals suggests continuity of the intervals. The secondary porosities of the streaks as vugs or fractures were estimated by subtracting sonic porosity logs from neutron-density cross plot, showing over 20% porosity. The petrophysical analyses indicate that the streaks have a range of 20% to over 50% porosity. In the Wabash #1 well, a 20-ft interval (from 4505 to 4525 ft.) in the upper part of the Potosi Dolomite showed over 40% porosity, and well testing in this zone indicated a permeability of 45,000 mD or greater (Khosravi et al., 2022). The tight zones between high-porosity streaks show less than 10% porosity with a thickness range of 10 to over 50 ft. To differentiate the streaks from the tight zones, the top and the base of the streaks were picked and treated as separate zones in the static model. Accordingly, the Potosi Dolomite divided into 14 zones to confine the vertical extension of tight intervals and high-porosity zones (Figure 15). The Shakopee and Oneota Dolomite were each divided into 9 zones based on lithology and porosity ranges. The overlying formations from the St. Peter to the Maquoketa shale show low porosity ranges, and each of these formations was considered as one separate zone. Table 4 shows the thickness and porosity ranges of the zones for the Potosi model.

Table 4. *Number, thickness, and porosity range of different zones of Potosi model.*

Formations/Zone	Thickness/ Thickness range (ft)	Total Porosity range (%)
Maquoketa Shale	314	0-8
Trenton	163	0-5
Platteville	378.61	0-6
Dutchtown	84.39	0-12
St. Peter	28	0-8
Shakopee	21-150	1-19
Oneota	12-95	1-12
Potosi Zone1	7.38	5-16
Potosi Zone2	6.85	15-35
Potosi Zone3	112.68	1-22
Potosi Zone4	7.46	13-28
Potosi Zone5	2.61	>50
Potosi Zone6	9.46	10-23
Potosi Zone7	64.15	3-16
Potosi Zone8	3.04	31-47
Potosi Zone9	198.61	2-18
Potosi Zone10	2.69	20-34
Potosi Zone11	23.26	3-15
Potosi Zone12	2.69	18-27
Potosi Zone13	85.33	3-18
Potosi Zone14	4.34	20-45

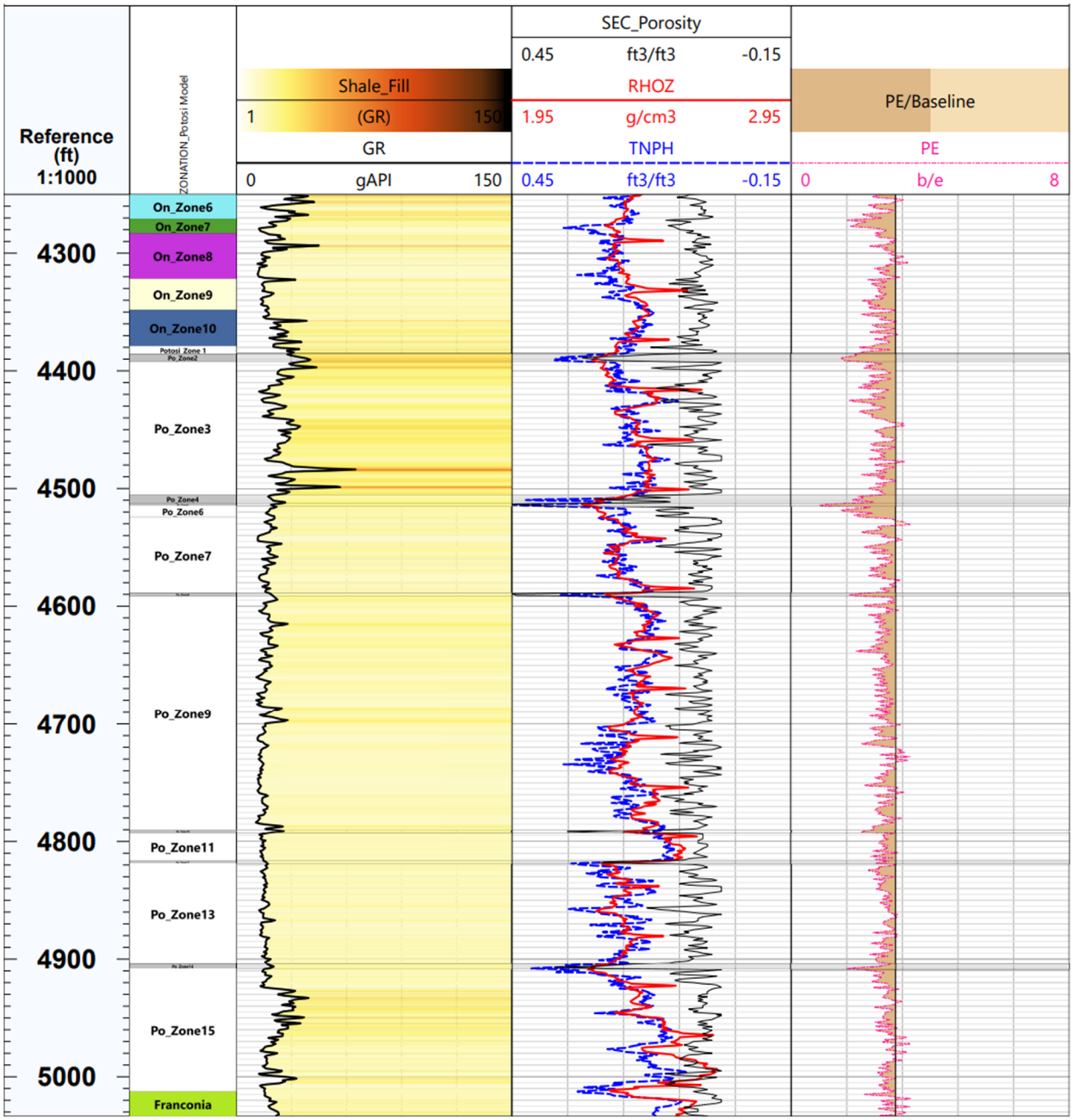

Figure 15. *Potosi zones and porosity logs. The streaks are shown by light gray color. Log abbreviations: GR: Gamma ray; Sec. porosity: secondary porosity; RHOZ: density; TNPH: Neutron porosity; PE: photoelectric.*

2.3.3 Data Scale-up

Because of the poor reservoir quality of the formations overlying the Potosi from the upper part of the Knox Group to the Maquoketa, each formation above the Shakopee Dolomite was considered as one separate layer. The Potosi Dolomite consists of streaks with high porosity and permeability values and thick dolomite intervals with lower property values, therefore the Potosi zones were subdivided into thinner layers to reproduce the reservoir properties from the 0.5-ft porosity and permeability data from the Wabash #1 well logs. To determine the optimal number of layers that would reproduce the vertical heterogeneity of the Potosi model, data analyses were performed on the porosity and permeability data. These analyses assist in subdividing each zone proportionally into layers with the appropriate thicknesses. The porosity and permeability data analyses indicate that subdividing Potosi zones into 2-ft intervals can reproduce layers with similar porosity and permeability values as the 0.5-ft intervals from the log data. The Potosi model boundary covers a surface area of 22 x 22 miles (35.4 x 35.4 km) with 14 zones. With subdividing the Potosi zones into 2-ft intervals, the 3-D geocellular model contains 3,242, 896 grid cells, which included 116 columns, 116 rows, and 241 layers. Table 5 shows the number of zone and layers for the Potosi Dolomite and overlying formations. In addition, an arithmetic averaging method was used to upscale the half-ft interval porosity raw log data into the model layers. Horizontal and vertical permeabilities were calculated for each layer using geometric and harmonic mean sampling methods, respectively.

Table 5. *Number of zone and layers of Potosi model.*

Formations	Zones	Layers
Maquoketa Shale	1	1
Trenton	1	1
Platteville	1	1
Dutchtown	1	1
St. Peter	1	1
Shakopee	9	9
Oneota	9	9
Potosi	14	218

Figure 16-A shows the histogram of the 0.5-ft interval porosity log data relative to upscaled data. The upscaled data are reasonably consistent with the log data. The upscaled porosity appears to have overrepresentation in the range of 4 to 10%. The main reason for the overrepresentation of those values is the presence of overburden formations which are layered coarsely, and thus the porosity is averaged for a relatively thicker interval.

The histogram of upscaled permeability (Figure 16-B) indicates a trend and ranges similar to the log permeability data, except for the 1-5 mD ranges due to large thickness of overburden. For the vuggy intervals with a higher range of permeability there is a reasonable correlation between the upscaled and the log-based data.

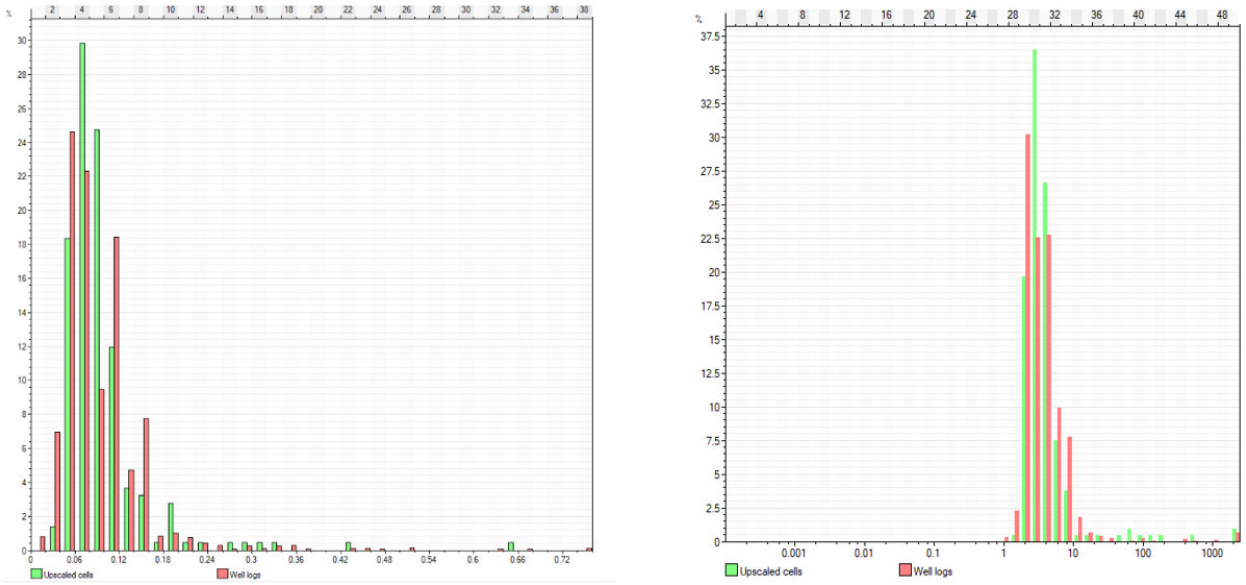

Figure 16. *16-A, to left) Histogram of upscaled porosity (red) vs. well log porosity (green); 16-B, to right) histogram of upscaled permeability data (red) vs well log permeability data (green).*

2.3.4 Potosi 3D Geocellular Model

It is uncertain if the permeability of the Potosi Dolomite is consistent within the project boundary, but the presence of vuggy intervals and lost circulation zones in almost all wells that encounter the Potosi throughout the Illinois Basin suggest that the pore throat systems of vuggy intervals are highly connected. Thus, the Potosi static model was built by assuming the spatial connectivity of the vugs in the horizontal direction and discontinuity of pore systems in the vertical direction.

An early in situ well test at Wabash #1 provided a permeability value of 2,400 mD for an injection unit within the Potosi Dolomite (24,000 md-feet over 10 feet [3 m]). Although subsequent, longer, well testing indicated much higher permeabilities of 45,000 mD or greater exist within the Potosi Dolomite (Khosravi et al., 2022), the low permeability value of 2,400 mD was used in the geocellular model and was assigned to the 2-ft intervals with the highest porosity ranges. Accordingly, a proportion of permeability was assigned to intervals with lower porosity ranges. Figure 17 and Figure 18 show the porosity and permeability models, and the accompanying east-west cross sections depict the porosity and permeability ranges of the Potosi Dolomite with higher resolution. The vuggy intervals with high porosity and high permeability are shown with warmer colors. The model shows at least 7 zones with high porosity and permeability values which could be considered for CO_2 injection.

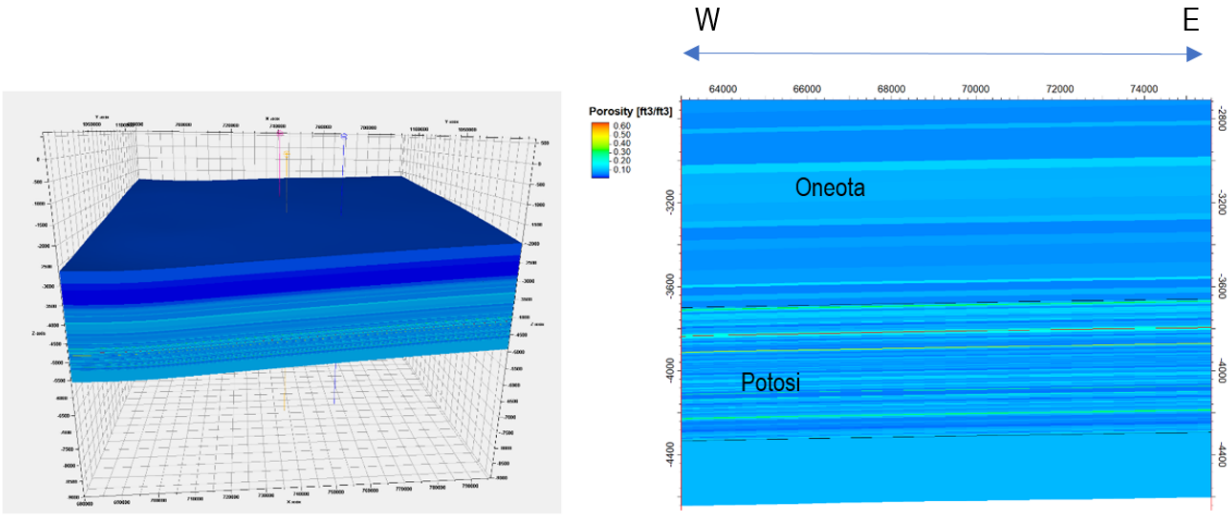

Figure 17. *The 22 by 22 mile porosity model from top of the Maquoketa Shale to Eau Claire Formation. The E-W cross section shows the porosity Oneota Dolomite and Potosi Dolomite.*

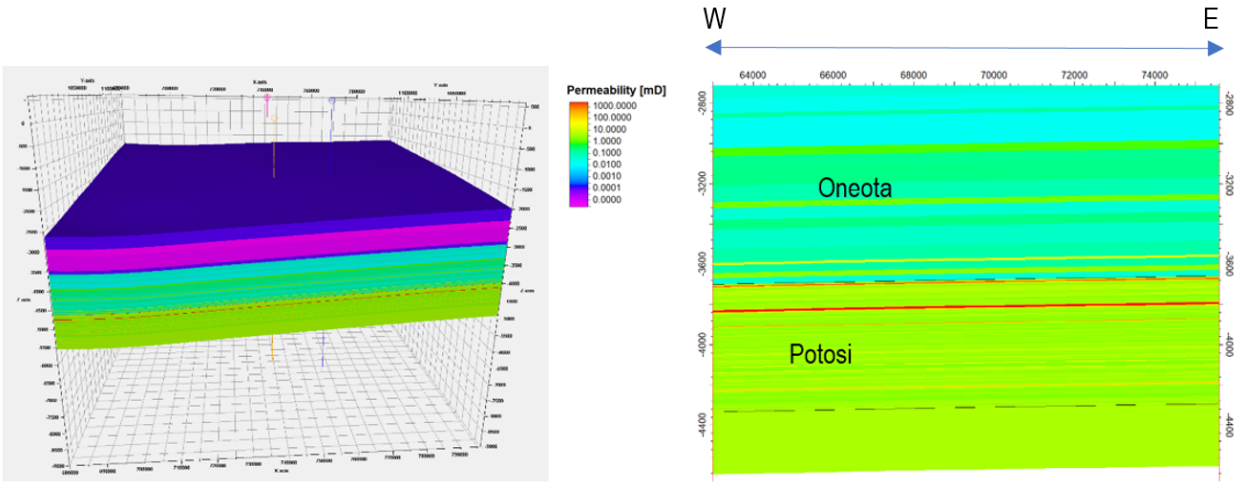

Figure 18. *The 22 by 22 mile permeability model from top of the Maquoketa Shale to Eau Claire Formation. The E-W cross section shows the porosity Oneota Dolomite and Potosi Dolomite.*

3. Dynamic Modeling

Dynamic reservoir simulation models were built and used to assess several scenarios for the feasibility of storing up to 50 million tonnes (1.67 million tonnes per year), over a period of up to 20 years, of industrially-sourced carbon dioxide (CO_2) in a commercial-scale geological storage complex at Wabash Valley Resources LLC (WVR) gasification facility near Terre Haute, Indiana. Simulation results include: CO_2 injectivity, CO_2 plume size, and pressure distribution as a function of time. The pressure front and CO_2 plume sizes from the dynamic simulation results are also used to estimate the area of review (AoR).

The dynamic simulations were run using Landmark's *Nexus*® reservoir simulation software. Separate simulation models were created to model the Mt Simon Sandstone and Potosi Dolomite. The simulation input, model construction and simulation results are discussed in the following sections. The Mt Simon Sandstone model is discussed in the next section, followed by the Potosi Dolomite models.

3.1 Mt Simon Sandstone

3.1.1 Model Input

A geological model for the Mt Simon Sandstone (Mt Simon) was created in Petrel™, and the grid and property arrays were exported to *Nexus*® for dynamic reservoir simulation. The Petrel™ model is described in an early section of the report. This section describes the reservoir engineering data and assumptions used in building the Mt Simon *Nexus*® simulation model. The reservoir engineering data include fluid PVT data and rock property data.

3.1.1.1 Fluid PVT Data

The Mt Simon *Nexus*® model is a gas-water model. PVT data are required for both CO_2 and brine. A water sample was obtained from Wabash #1, and the salinity was measured to be 169,000 ppm. The initial reservoir pressure and temperature were measured during Wabash #1 well testing; and are interpreted to be 3,351 psia and 144°F at 6,796 ft, MD (6,244 ft, TVDss).

The brine properties were calculated for a brine salinity of 169,000 ppm at a reservoir temperature of 144°F, using water property correlations (McCain, 1991). The brine properties used in the *Nexus*® model are shown in Table 6.

CO_2 PVT properties are from an internal Python code. *Nexus*® gas-water CO_2 PVT properties are entered in tabular form, as a function of pressure. CO_2 properties are shown in Figure 19.

***Table 6**. Summary of brine fluid properties used in the Mt Simon Nexus® model.*

Parameter	units	Value
Stock Tank Water density	lb/ft3	70.2376
Water Compressibility	1/psia	2.86E-06
Water Viscosity	cp	0.778
Water Formation Volume Factor	rb/stb	1.0156
Pressure Derivative of Water Viscosity	1/psia	5.435E-05
Reference Pressure	psia	3,351
Reservoir Temperature	F	144

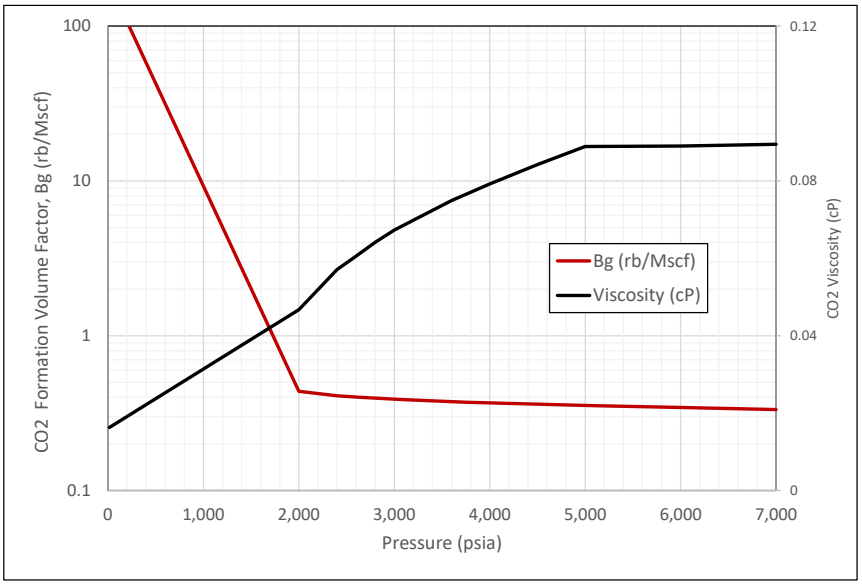

***Figure 19.** CO_2 properties at 144°F used in the Mt Simon Nexus® model.*

3.1.1.2 Rock Properties

No site-specific laboratory measurements of relative permeability, capillary pressure and rock compressibility were available. Rock compressibility was estimated using Newman's correlation for sandstones (Newman, 1973), using the median porosity within the Mt Simon. The median porosity is 15.25%, which corresponds to a rock compressibility value of $3.9 * 10^{-6}$ psi^{-1}. The relative permeability curves used in the simulations were generated based on general knowledge from the literature using Brooks-Corey functions (Krevor et.al., 2012), see Figure 20.

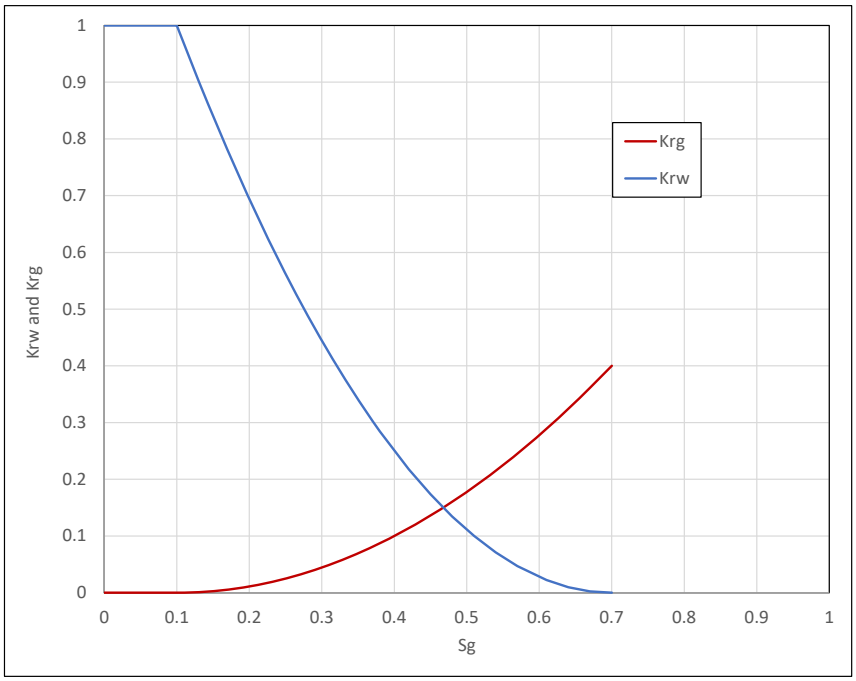

Figure 20. *Relative permeability curves used in the Mt Simon simulation model.*

3.1.2 Simulation Cases

Dynamic simulations were performed to assess the CO_2 injectivity of the Mt Simon. The Mt Simon simulation model is based on the geologic model and reservoir engineering input, as described in the previous sections.

The simulation model is 22 x 22 miles areally, and includes the Mt Simon Sandstone and the overlying Eau Claire Formation, which is the upper confining unit. The model is centered over Wabash #1. The model is heterogenous in both the lateral and vertical directions. The grid block dimensions are 666 x 666 ft areally, having been refined 3:1 relative to the static model lateral grid size of 2,000 x 2,000 ft. The cell thickness is variable and ranges from 5 to 15 ft. There are 577 layers in the model. The number of grid blocks in the x, y, and z directions are 177 x 177 x 577; respectively. There is a total of 18 million cells in the simulation model. Figure 21 shows a 3-D image of the Mt Simon *Nexus*® model, the blocks are colored by grid cell thickness.

Porosity and permeability were populated within the Petrel™ model and exported to *Nexus*®. Two permeability models were considered: Core-correlated and DST-correlated models which are low-perm and high-perm realizations; respectively. The Core-correlated permeability model matches the permeability measured on the Wabash #1 cores. The DST-correlated permeability model matches the permeability from Wabash #1 well tests. Figure 22 shows the horizontal ($k_x = k_y$) permeability distribution for the Core-correlated model (low perm realization). The warmer colors are high permeability, and the cooler colors are low permeability. Figure 23 shows the horizontal permeability distribution for the DST-correlated model (high perm realization). These two images illustrate that the DST-correlated permeability is significantly higher than the Core-correlated permeability.

The top and bottom surfaces of the model are sealed, no flow boundaries. An infinite-acting aquifer is attached to the edges (lateral) of the model. The infinite-acting aquifer was calibrated prior to running CO_2 injection scenarios. The fracture gradient of 0.75 psi/ft is an average of measurements from Step Rate Tests that were performed on the Mt Simon formation at the T.R. McMillen #2 well (Frailey, 2021). In the simulation model, the maximum bottom-hole-pressure (BHP) is constrained to 90% of the fracture gradient

to prevent fracturing the rock during CO_2 injection. The maximum BHP constraint is applied at the top of the perforated interval.

The reservoir rock is an aquifer, with a water saturation of 100%. *Nexus*® requires a gas-water contact and an initial pressure at a reference depth to initialize the simulation model. The simulation model is initialized with a gas-water contact placed just above the top of the model and an initial pressure at datum depth of 3,351 psia at 6,796 ft MD (6,244 ft, TVDss), which was measured during the well tests in Wabash #1.

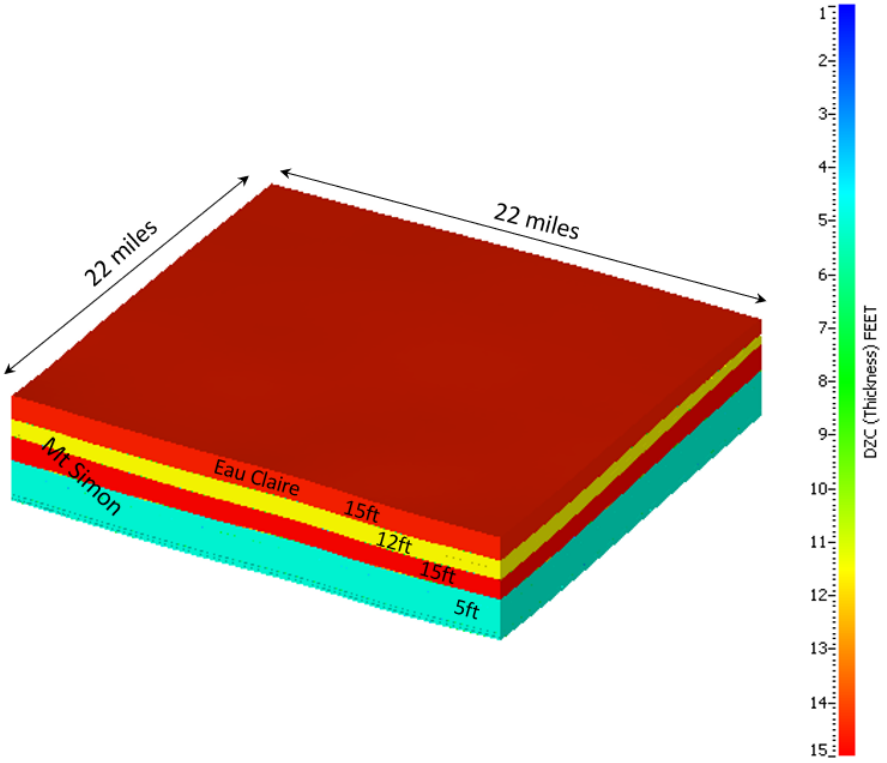

Figure 21. *Mt Simon simulation model, showing the 22 x 22 mile model with blocks colored by cell thickness. The Mt Simon is 2,400 ft thick and the Eau Claire is 700ft thick.*

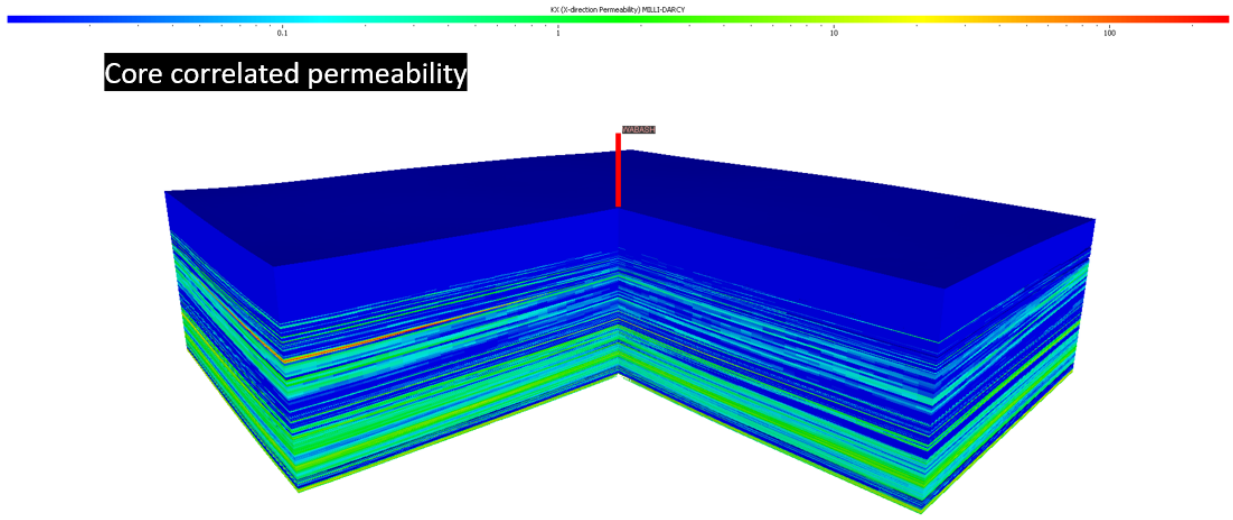

Figure 22. *Mt Simon Nexus® model 3-D display showing Core-correlated permeabilities.*

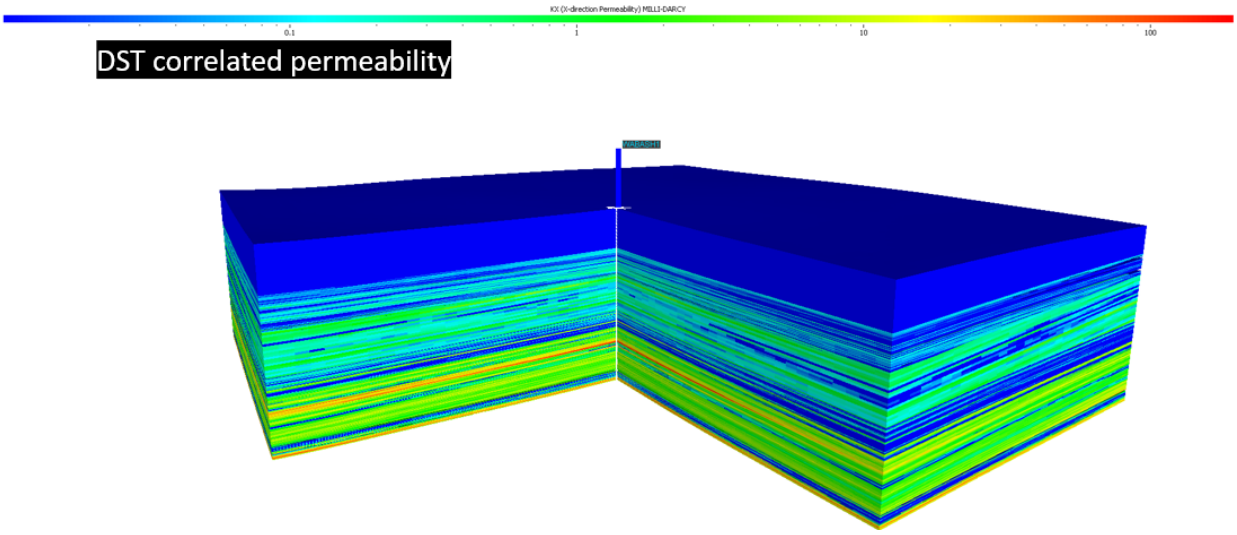

Figure 23. *Mt Simon Nexus® model 3-D display showing DST-correlated permeabilities.*

3.1.3 Single Well Injection Scenarios

Multiple CO_2 injection scenarios were run on the Mt Simon model to assess single well injectivity for different completion intervals using both the DST-correlated and Core-correlated permeability models. The Mt Simon permeability is lower than pre-drilling expectations. It is a challenge to inject 1.67 MMTA for 30 years. As a result, different completion intervals were tested. All simulations were run by constraining the well maximum BHP to 90% of the fracture pressure.

Table 7 describes five single well injection cases; including well type, perforated interval and perforation length. Three vertical well and two horizontal well cases are described. Each of the five cases were run on both the Core-correlated and DST-correlated permeability models. Figure 24 shows a partial cross section (5,300 ft in length) through the model at Wabash #1 from both the Core-correlated and DST-correlated permeability models. In the images, the overlying Eau Claire has been removed from the model to emphasize the Mt Simon interval, and the vertical scale is greatly exaggerated by 25 times. The cross

sections show the locations of the two well test intervals (DST1 and DST2) and the perforation intervals for all five simulation cases.

Case 3 was set-up to optimize the productivity of the well relative to the fracture pressure. In all the cases considered, the well BHP is constrained by fracture pressure, and the fracture pressure increases with depth. Therefore, targeting deeper injection intervals will yield larger injection rates. Figure 25 shows cumulative permeability thickness (KH) in mD-ft for Wabash #1 from the DST-correlated permeability model. Using a perforation depth of 7,280 – 8,155' ss captures 88% of the cumulative KH of the Mt Simon, which is the perforated interval for Case 3.

The simulation results are summarized in Table 8. The table contains the average injection rate over 30 years, the total amount of CO_2 injected after 30 years and the CO_2 plume radius at 30 years. None of the cases are able to inject 1.67 MMTA for 30 years, as indicated by the 30 year average injection rates. The DST-correlated model's average 30 year injection rates are 2 to 14 times higher than the Core-correlated model rates.

The results show that Case 3 has the highest injectivity relative to the other vertical well cases. Figure 26 and Figure 27 show simulation results from Case 3 for both the DST-correlated and Core-correlated models; respectively. Figure 26 shows a map view of the plume radius at 30 years, a cross section of the plume at 30 years, and a cross section of the permeability for the DST-correlated model. After 30 years of injection, a total a 34.8 million tonnes (MMtonnes) of CO_2 is injected at an average rate of 1.16 MMTA, resulting in a CO_2 plume radius of 1.51 miles. Figure 27 shows a map view of the plume radius at 30 years, a cross section of the plume at 30 years, and a cross section of the permeability for the Core-correlated model. After 30 years of injection, a total a 6 MMtonnes of CO_2 is injected at an average rate of 0.2 MMTA, resulting in a CO_2 plume radius of 1.32 miles. The DST-correlated model is able to inject 5.8 times the volume of the Core-correlated model over the 30 year injection period. Even though the DST-correlated model injects 5.8 times more CO_2 than the Core-correlated model, the plume radius is similar: 1.51 vs. 1.32 miles for the DST-correlated and Core-correlated models; respectively. The similar CO_2 plume radius is related to the injection profile, which is a result of the permeability distribution. The DST-correlated model shows three high-perm intervals that capture a majority of the CO_2, as shown in Figure 26. The three intervals have very similar CO_2 plume radii at 30 years. In, contrast, the Core-correlated model shows four high-perm intervals that capture a majority of the CO_2, as shown in Figure 27. The thin sandstone interval below the basalt captures the largest quantity of CO_2, and results in the large CO_2 radius at 30 years.

The horizontal well in the DTS1 interval with the DST-correlated permeability model, Case 4, has the highest CO_2 injection rate. Case 4 injects a total of 48.9 MMtonnes of CO_2 over 30 years with an average injection rate of 1.63 MMTA and a plume radius of 2.02 miles at 30 years. This rate is 14.8 times the rate observed from Case 4 for the Core-correlated model. The Core-correlated model injects a total of 3.3 MMtonnes of CO_2 over 30 years with an average injection rate of only 0.11 MMTA and shows a plume radius of 0.82 miles at 30 years. As both the DST-correlated and Core-correlated models are equally probable, the injectivity of a horizontal well has a large range of uncertainty. Furthermore, horizontal well performance is strongly influenced by vertical permeability. Within a vertically heterogenous interval, such as the Mt Simon, a vertical well can be advantageous as it crosses more of the thin-bedded high permeability streaks within the formation.

Table 7. *Mt Simon single well simulation cases.*

Case	Interval	Perforation Length ft
1	Vertical well, All of Mt Simon (5,721' - 7,958')	2,237
2	Vertical well, All of Mt Simon + sandstone below Basalt (5,721' - 8,155')	2,434
3	Vertical well, Lower Mt Simon + sandstone below Basalt (7,280' - 8,155')	877
4	1,000 m Horizontal well, within DST1 interval (7,415')	3,281
5	1,000 m Horizontal well, in sandstone below basalt (8,127')	3,281

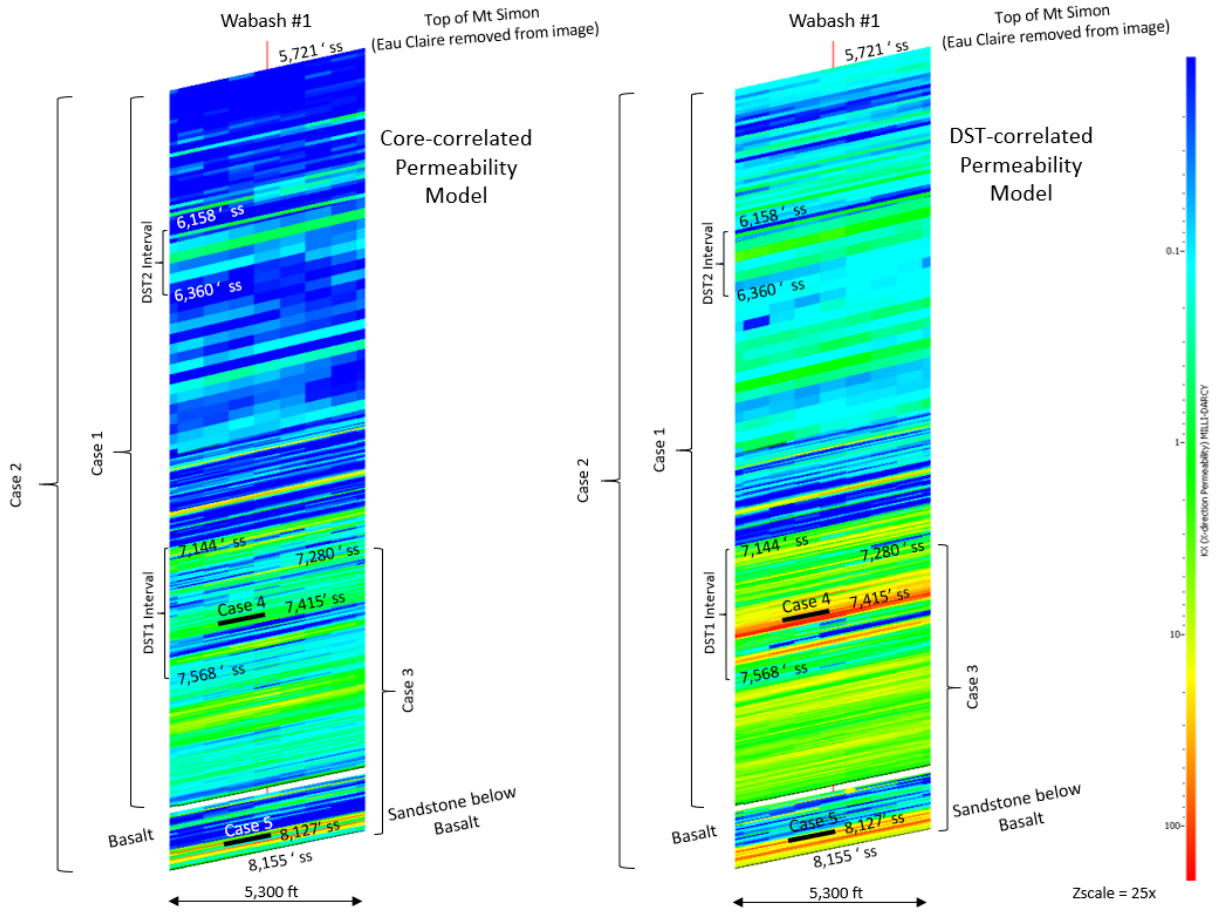

Figure 24. *Partial cross section through Wabash #1 from both the Core-correlated and DST-correlated models showing horizontal permeability on a log scale, with well perforation and DST locations denoted.*

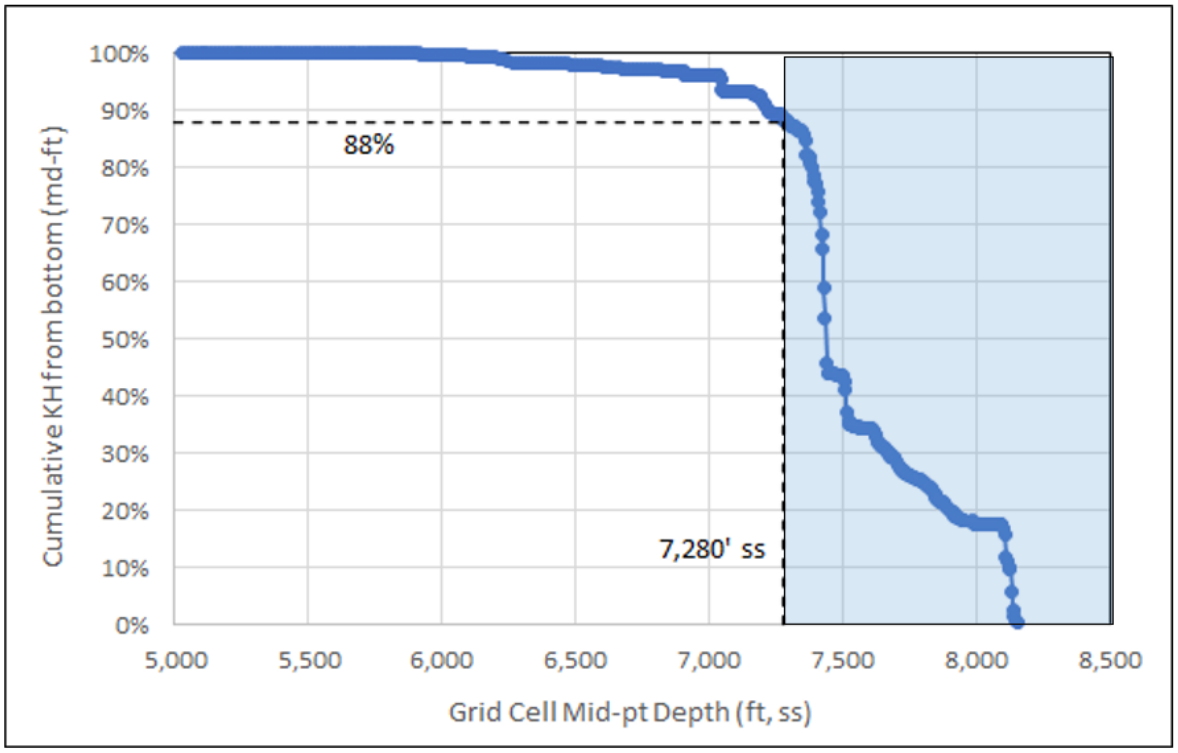

Figure 25. *Wabash #1 cumulative permeability thickness (KH) for the DST-correlated model from the bottom upwards, originating at the base of the sandstone below the basalt. Showing that 88% of the cumulative KH is included in a completion interval from 7,280' to 8,155' ss, which is the perforated interval for Case 3.*

Table 8. *Simulation results: single well injection for 30 years at maximum BHP.*

		DST-Correlated Model			Core-Correlated Model		
Case	Perforation Interval	Avg Injection Rate	Total CO2 injected	Plume Radius at 30 years	Avg Injection rate	Total CO2 injected	Plume Radius at 30 years
	ft, ss	MMTA	MMtonnes	miles	MMTA	MMtonnes	miles
1	All Mt Simon (5,721' - 7,958')	0.68	20.4	1.2	0.11	3.3	1.01
2	All Mt Simon + SS Below Basalt (5,721' - 8,155')	0.84	25.2	1.2	0.18	5.4	1.13
3	Lower Mt Simon + SS below Basalt (7,280' - 8,155')	1.16	34.8	1.51	0.2	6	1.32
4	1,000 m horziontal well, DST1 Interval (7,415')	1.63	48.9	2.02	0.11	3.3	0.82
5	1,000 m horizontal well, SS below Basalt (8,127')	0.57	17.1	2.27	0.23	6.9	1.77

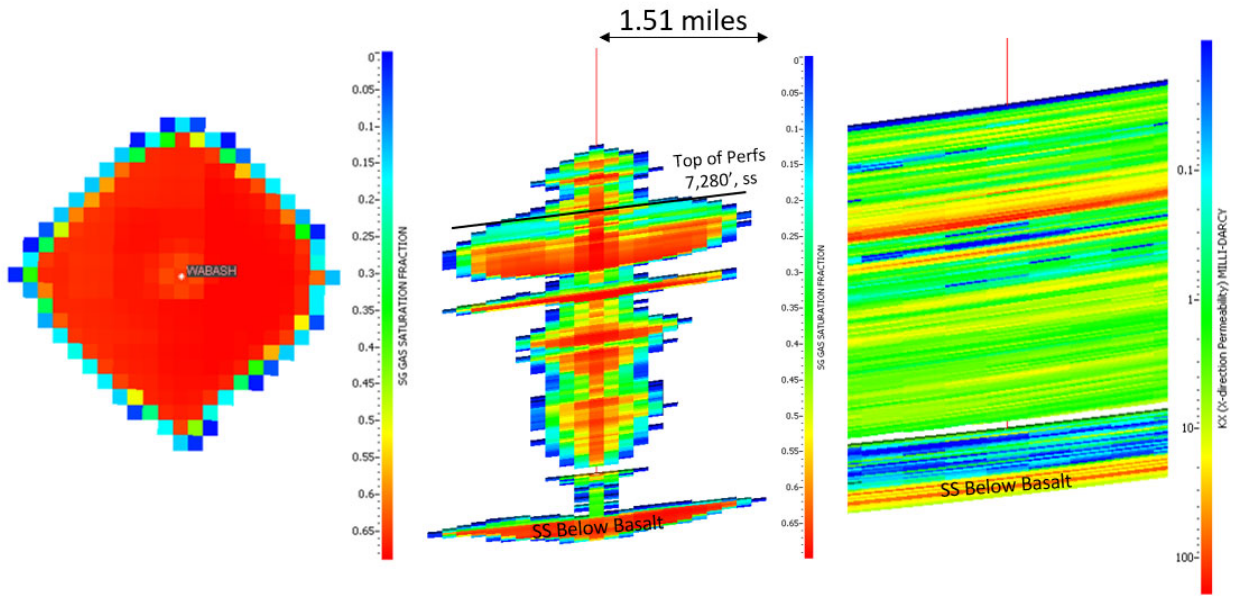

Figure 26. *Case 3, DST-correlated permeability model results after 30 years of injection, showing plume radius, plume cross section and permeability cross section.*

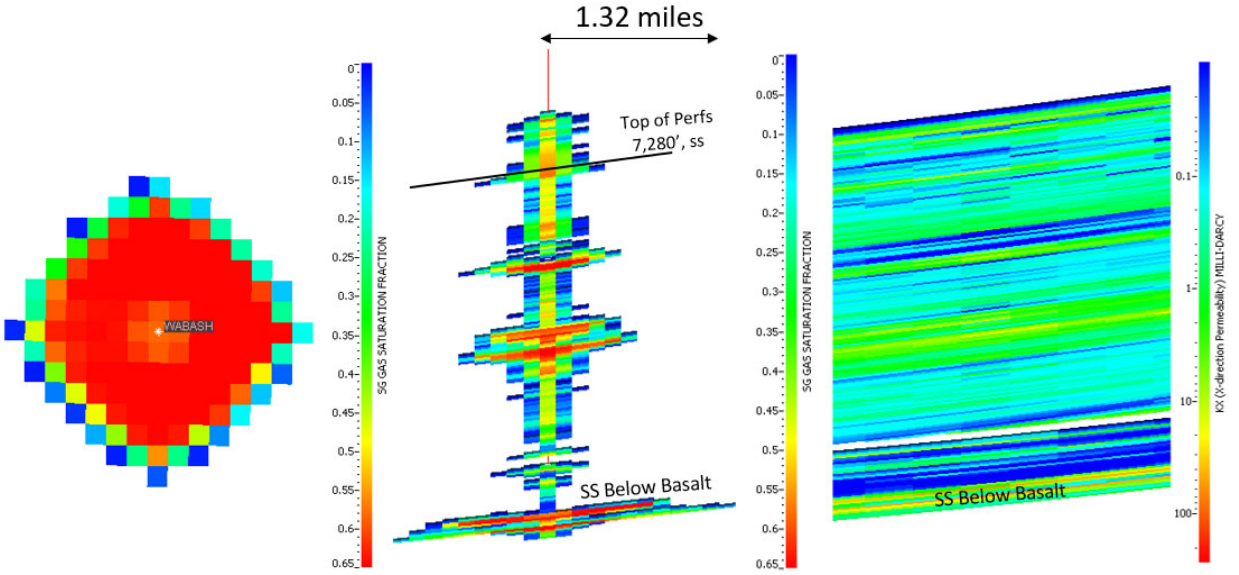

Figure 27. *Case 3, Core-correlated permeability model results after 30 years of injection, showing plume radius, plume cross section and permeability cross section.*

3.1.4 Multiple Well Injection Scenarios

Unfortunately, none of the single well injection scenarios, as discussed in the previous section, are capable of injecting 1.67 MMTA of CO_2 for 30 years. In this section, multiple well injection scenarios are investigated on both the DST-correlated and Core-correlated permeability models to assess the number of wells and the well spacing required to inject 1.67 MMTA of CO_2 for 30 years.

3.1.4.1 Two Well Injection Scenario: DST-correlated Model

For the DST-correlated model, the previous results show that a single vertical well is capable of injecting an average of 1.16 MMTA for 30 years. This suggests that two wells are required to inject 1.67 MMTA for 30 years. Simulations were run using the DST-correlated model with two injection wells, both constrained by 90% of the fracture pressure gradient (0.90 * 0.75 psi/ft). Both injection wells are vertical and the perforated interval is 7,280' – 8,155' ss, same as Case 3 in the prior section which showed the largest injectivity (See Table 7 and Table 8).

As the 3-D Mt Simon simulation model is heterogenous in both the lateral and vertical directions, a total of four 2nd-well locations were considered. The 2nd well was placed west, South, east and North of Wabash #1. Two simulation cases were run for each 2nd well location: one with well KH (mD-ft) as populated from the geomodel, and a second with the KH (mD-ft) of the 2nd well modified to be the same as Wabash #1. The rationale for the second case with the same KH is that the well data is very sparse in this area and it is equally possible that the properties at the 2nd well could be very similar to the properties measured at Wabash #1. A KH multiplier was applied at the 2nd well location to match the KH (mD-ft) at Wabash #1.

Simulations were run using variable well spacing to determine the well spacing required to inject 1.67 MMTA for 30 years. Table 9 shows the minimum well spacing required to inject 1.67 MMTA for 30 years using two wells for the DST-correlated permeability model. The magnitude of the multiplier applied to the 2nd well to match the KH at Wabash #1 indicates that the reservoir properties are lower in the model away from Wabash #1. The results indicate that the 2nd well needs to be located 1.5 to 3.0 miles away from Wabash #1. Figure 28 and Figure 29 show gas saturation at 30 years along a west-east cross section through the injection wells for the case of 2nd well KH from the geologic model and 2nd well KH the same as Wabash #1; respectively. Well interference between the two wells is indicated by the asymmetric shape of the CO_2 plumes. The CO_2 plume radius is 1.3 miles after 30 years of injection at 1.67 MMTA (total injection of 50 MMtonnes of CO_2) for both cases.

Table 9. *DST-correlated simulation results showing the minimum well spacing required to inject 1.67 MMTA for 30 years using two vertical wells.*

	Well Spacing Required to Inject 1.67 MMTA for 30 years		
2ndWell Direction	KH from Geomodel	KH same as Wabash #1	KH Multiplier on 2nd Well
West	10,000' (1.9 mi)	8,000' (1.5 mi)	1.162
South	9,000' (1.8 mi)	8,000' (1.5 mi)	1.174
East	16,000' (3.0 mi)	11,000' (2.0 mi)	1.295
North	13,000 (2.5 mi)	9,000 (1.8 mi)	1.258

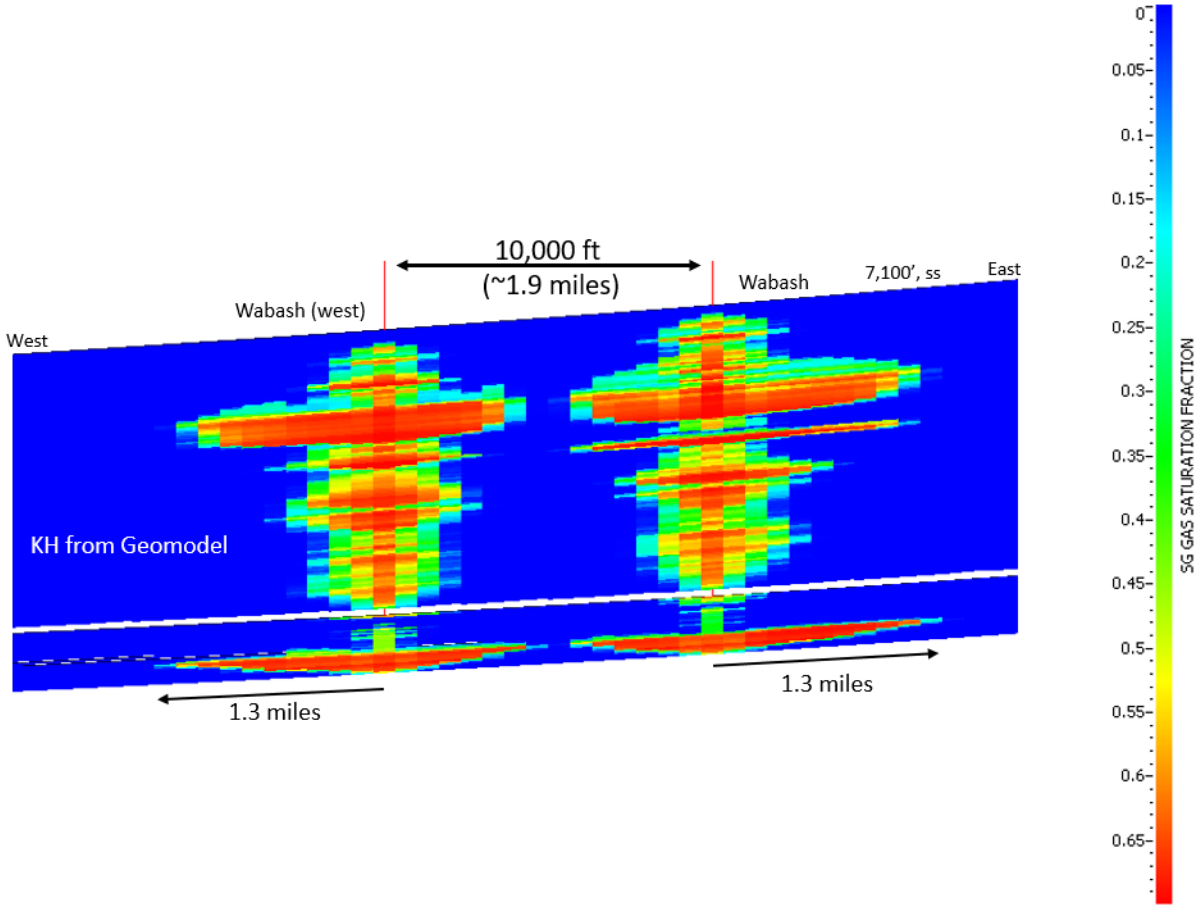

Figure 28. *Gas saturation at 30 years along a west-east cross section through the injection wells for the case with the 2nd well placed to the west of Wabash #1 and using the well KH from the geologic model, showing the minimum well spacing of 1.9 miles required to inject 1.67 MMTA for 30 years.*

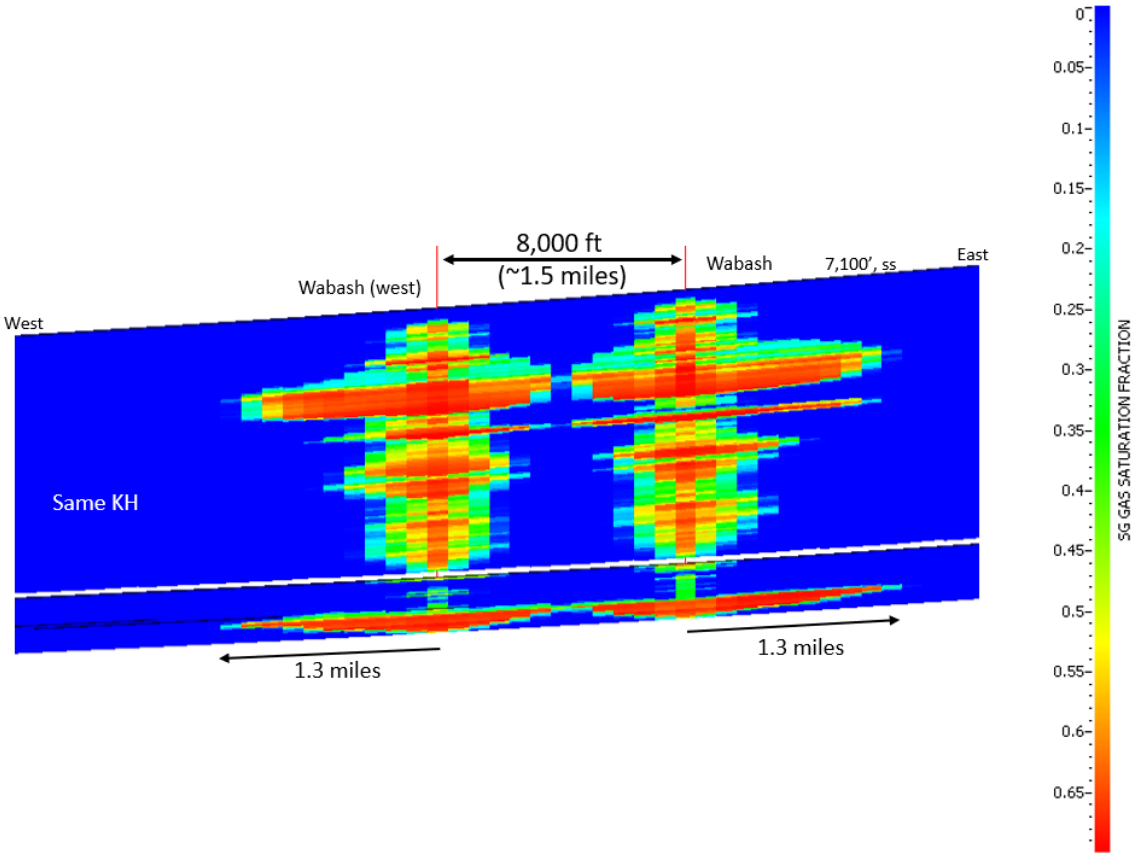

Figure 29. *Gas saturation at 30 years along a west-east cross section through the injection wells for the case with the 2nd well placed to the west of Wabash #1 and using the 2nd well KH the same as Wabash #1, showing the minimum well spacing of 1.5 miles required to inject 1.67 MMTA for 30 years.*

3.1.4.2 Multiple Well Injection Scenario: Core-correlated Model

For the Core-correlated model, the previous results show that a single vertical well is capable of injecting an average of 0.2 MMTA for 30 years. This suggests that multiple wells are required to inject 1.67 MMTA for 30 years. Numerous multiple well simulations were run using the Core-correlated model with various well counts and well spacings to determine the well count and spacing required to inject 1.67 MMTA for 30 years. The maximum injection pressure of each well is constrained to 90% of the fracture pressure gradient (0.90 * 0.75 psi/ft). All of the wells inject simultaneously and continuously for the entire 30 year period. Total injection is constrained at 1.67 MMTA at the well group level. Each well injects proportional to its individual injection capacity relative to the maximum allowable injection pressure. All the wells are vertical and the perforated interval is 7,280' – 8,155' ss, same as Case 3 in the prior section which showed the largest injectivity (See Table 7 and Table 8). The wells are placed in a 5-spot pattern, centered around Wabash #1.

The simulation results indicate that 17 wells, spaced 3 miles apart in a 5-spot pattern are required to inject 1.67 MMTA for 30 years with the Core-correlated simulation model. Figure 30 shows the well locations for the 17 well case, the number on the x and y axis are the grid cell numbers in the I and J directions; respectively. The overall footprint of the well locations is 12.75 x 12.75 miles, with each 5-spot pattern being 4.25 x 4.25 miles. The wells are diagonally three miles apart.

Figure 31 shows a map view of the CO_2 plumes after 30 years of injection at 1.67 MMTA for model layer 567 (high perm layer) within the sandstone below the basalt. Only cells with gas saturation ≥ 1% are shown.

The individual CO_2 plume radii are denoted by the values next to each plume. The results indicate that the plume size varies with layer in the model, but the maximum plume size is in layer 567. The CO_2 plume radii vary from 0.7 to 1.0 miles at 30 years of injection. Figure 32 shows the initial and final pressure (at 30 years) along a South-North cross section through a column of injectors toward the west of the model (first column of 4 injectors on the left in Figure 30). The wells along the cross-section are wells: W14, W9, W6 and W16 as denoted in Figure 31 and Figure 32. The pressure distribution shows that a majority of the CO_2 is captured within the sandstone interval below the basalt, as previously observed in the single well simulations. The pressure increase is highest between the wells, and lowest at the wells located at the outer edge of the injection pattern. The pressure distribution also reflects the heterogenous nature of the Mt Simon.

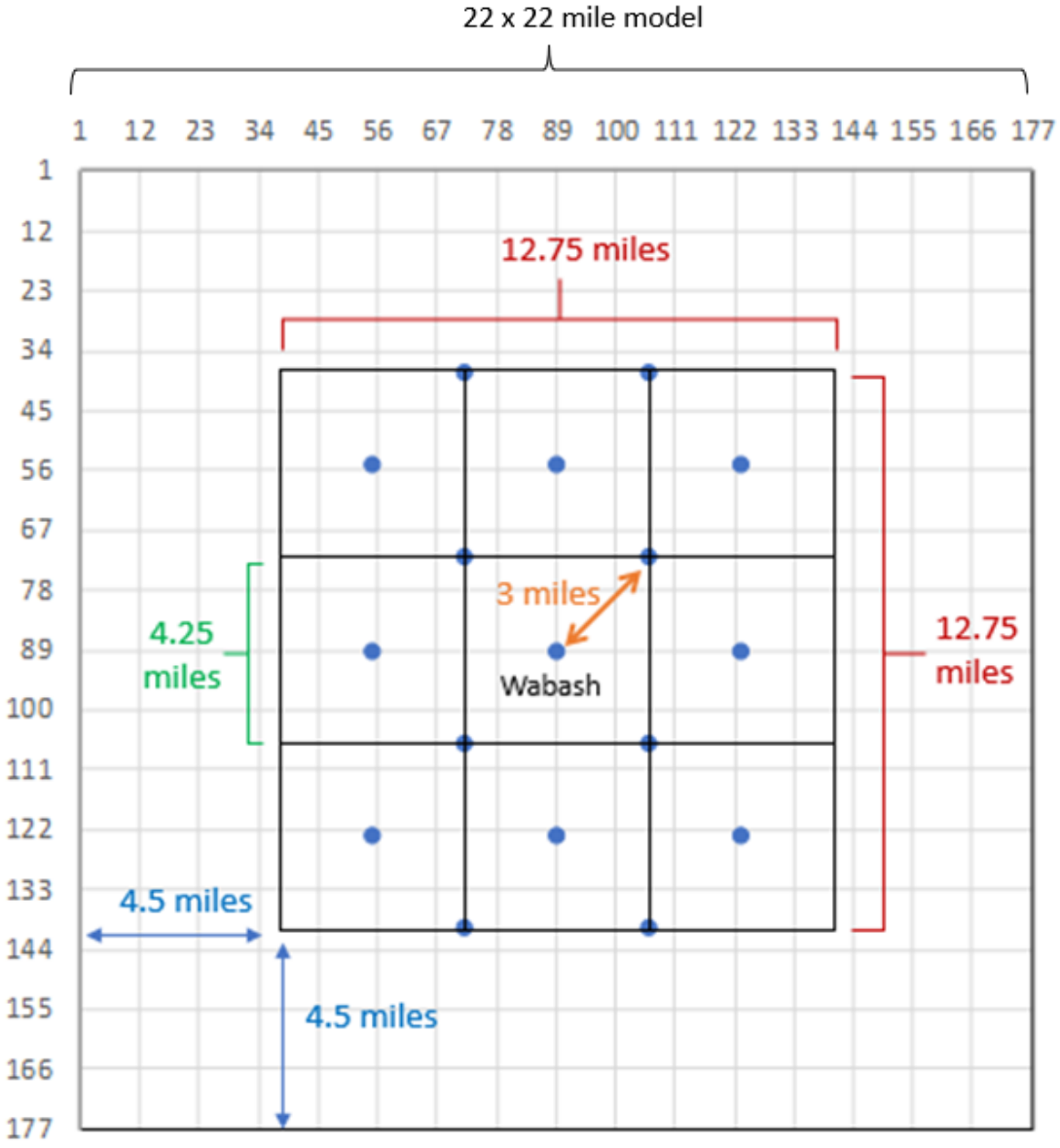

Figure 30. *Well locations for the 17 wells spaced 3 miles apart that are required to inject 1.67 MMTA for 30 years with the Core-correlated permeability model. The blue circles denote injection well locations.*

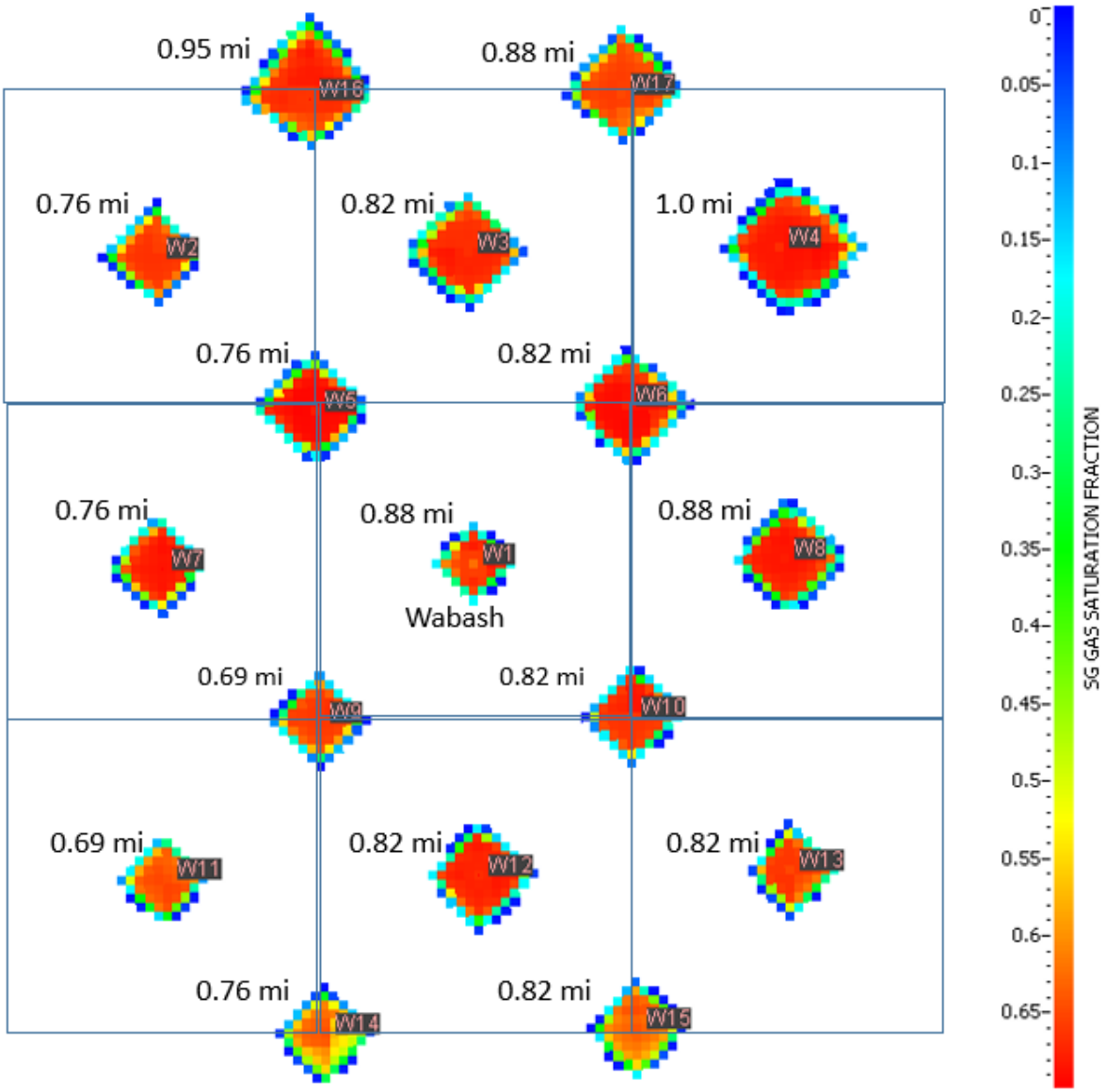

Figure 31. *Map view of CO_2 plumes after 30 years of injection at 1.67 MMTA for layer 567 (high perm layer) within the sandstone below the basalt, showing plume size for each of the 17 wells. Only cells with gas saturation ≥ 1% are shown.*

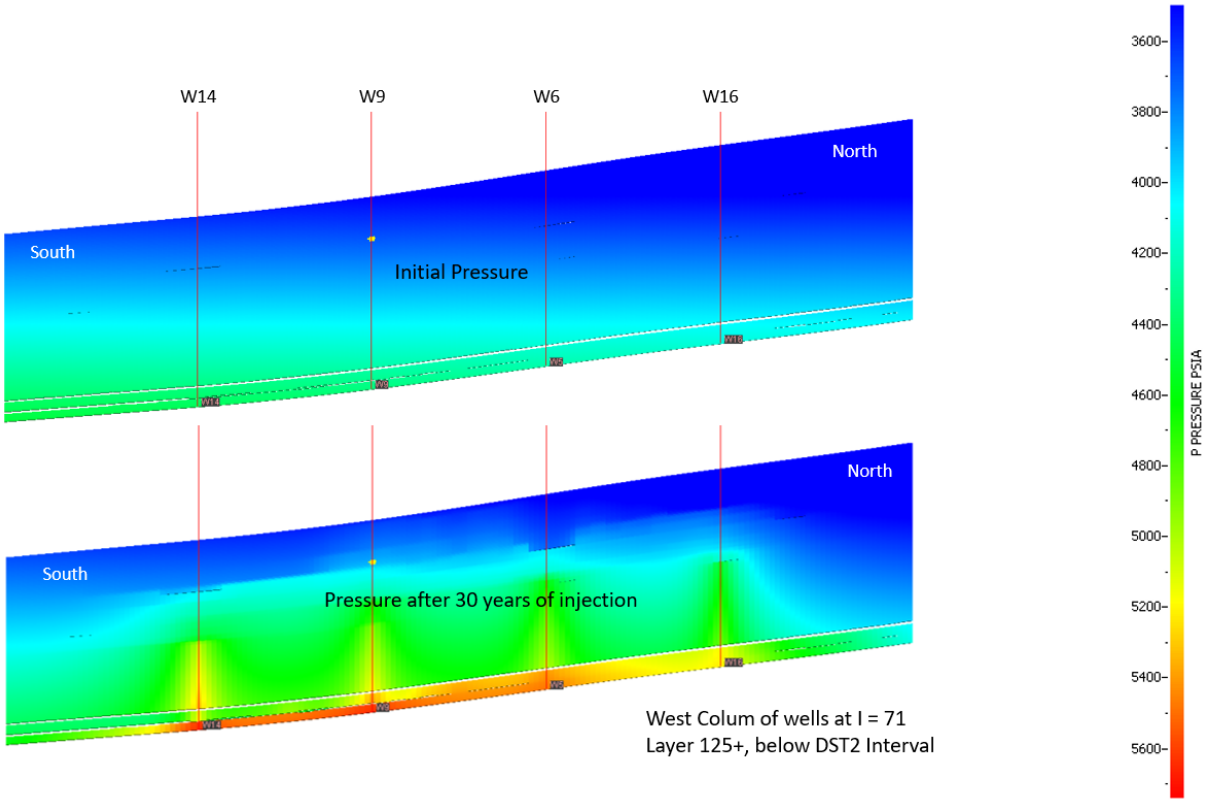

Figure 32. *Initial and final pressure at 30 years along a South-North cross section through a column of injectors towards the west of the model (first column of 4 injectors on the left).*

3.1.5 Summary of Mt Simon Simulations

A *Nexus*® dynamic simulation model for the Mt Simon sandstone was constructed using the geologic model exported from Petrel™. The model is based on all the available data and includes the Mt Simon sandstone and the overlying Eau Claire. Porosity and permeability were populated within the Petrel™ model and exported to *Nexus*®. Two permeability models were considered: Core-correlated and DST-correlated models which are low-perm and high-perm realizations; respectively. The Core-correlated permeability model matches the permeability measured on Wabash #1 cores. The DST-correlated permeability model matches the permeability from Wabash #1 well tests.

Dynamic simulations were performed to assess the CO_2 injectivity of the Mt Simon. Single well and multiple well injection scenarios were considered. Learnings from the Mt Simon simulation study are as follows:

- It is not possible to inject 1.67 MMTA of CO_2 for 30 years into the Mt Simon at Wabash #1 with a single well.
- A single vertical well (with various completion intervals) and a single 1,000 m long horizontal well (at various depths) were considered. None were capable of injecting 1.67 MMTA for 30 years.
- It is possible to inject 1.67 MMTA of CO_2 for 30 years into the Mt Simon with multiple wells, but the well count differs substantially between the DST-correlated and Core-correlated permeability models.
- DST-correlated permeability model results indicate that two wells spaced 1.5 to 3 miles apart are capable of injecting 1.67 MMTA of CO_2 for 30 years into the Mt Simon.

- Core-correlated permeability model results indicate that considerably more wells are necessary for the injection of 1.67 MMTA of CO_2 for 30 years into the Mt Simon.
- Due to the lower injectivity of the Mt Simon at Wabash #1 (relative to the higher injectivity typically observed in the central portion of the Illinois basin), the focus of this project was shifted toward injection of 1.67 MMTA of CO_2 for 30 years into the Potosi Dolomite.

There are many sources of uncertainty in the model and results, several are listed below:

- Well data is relatively sparse in the region surrounding Wabash #1. The drilling of additional wells in the area would help reduce uncertainty in both the static and dynamic models.
- There is a significant uncertainty associated with the permeability in the Mt Simon at Wabash #1. A large difference was observed between laboratory core measured and well-test derived permeability. Two permeability models were developed and used in the dynamic simulations. Additional core testing and/or well tests are required to help resolve the difference in permeability.
- No core measured relative permeability or capillary pressure data are available for either the Mt Simon or Eau Claire intervals. Recommend that core be obtained and laboratory measurements be conducted in the future.
- CO_2 solubility in brine and chemical reactions of the CO_2 with the reservoir rock were not considered in this study.

3.2 Potosi Dolomite

3.2.1 Model Input

A geologic model for the Potosi was created in Petrel™, and the grid and property arrays were exported to *Nexus*® for dynamic reservoir simulation. The Petrel™ model is described in an early section of the report. This section describes the reservoir engineering data and assumptions used in building the Potosi *Nexus*® simulation model. The reservoir engineering data include: fluid PVT data and rock property data.

3.2.1.1 Fluid PVT Data

The Potosi *Nexus*® model is a gas-water model. PVT data are required for both CO_2 and brine. A water sample was obtained from Wabash #1, and the salinity was measured to be 34,250 ppm. The initial reservoir pressure and temperature were measured during Wabash #1 well testing; and are 1,954 psia and 108°F at 4,500 ft, MD (3,948 ft, TVDss).

The brine properties were calculated for a brine salinity of 34,250 ppm at a reservoir temperature of 108°F, using water property correlations (McCain, 1991). The brine properties used in the *Nexus*® model are shown in Table 10.

CO_2 PVT properties are from the online National Institute of Standards and Technology (NIST) Chemistry WebBook (Lemmon et.al, 2021). *Nexus*® gas-water CO_2 PVT properties are entered in tabular form, as a function of pressure. CO_2 properties are shown in Figure 33.

Table 10. *Summary of brine fluid properties used in the Potosi Nexus® model.*

Parameter	units	Value
Stock Tank Water density	lb/ft3	63.889
Water Compressibility	1/psia	2.79E-06
Water Viscosity	cp	0.70575
Water Formation Volume Factor	rb/stb	1.00876
Pressure Derivative of Water Viscosity	1/psia	4.998E-05
Reference Pressure	psia	1,954
Reservoir Temperature	F	108

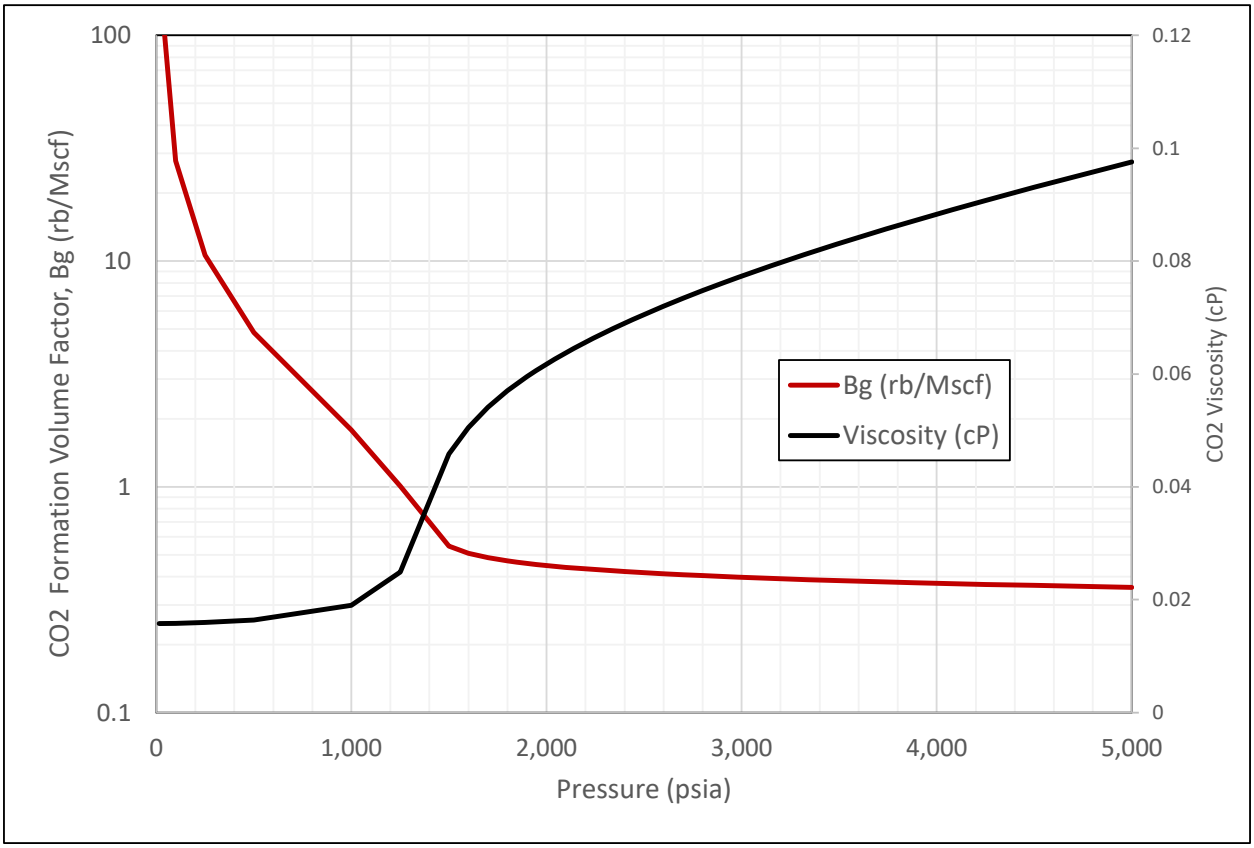

Figure 33: *CO_2 properties at 108°F used in the Potosi Nexus® model.*

3.2.1.2 Rock Properties

No core was obtained from the Potosi Dolomite from Wabash #1, thus no site-specific laboratory measurements of relative permeability, capillary pressure and rock compressibility were available. Rock compressibility was estimated using Newman's correlation for limestone (Newman, 1973), using the

median porosity within the Potosi Dolomite. The median porosity is 7.75%, which corresponds to a rock compressibility value of 1.043 x 10^{-5} psi^{-1}. The relative permeability tables used were obtained from an earlier Potosi simulation study, "The Potosi Reservoir Model 2013" (Adushita and Smith, 2014), Report DOE/FE0002068-14. The Potosi contains vuggy intervals, so two sets of relative permeability curves were used in the model: one set of curves for the matrix rock and a second set for the vuggy intervals (Figure 34). The matrix relative permeability data is based on relative permeability measured on the Nisku #2 sample from Bennion and Bachu (2010). The vuggy relative permeability data are vertical equilibrium curves, sometimes also called straight-line or stick curves. This type of curve is also commonly used to model flow within fractures. Vuggy layers in the model were defined as layers having secondary porosity greater than 8%.

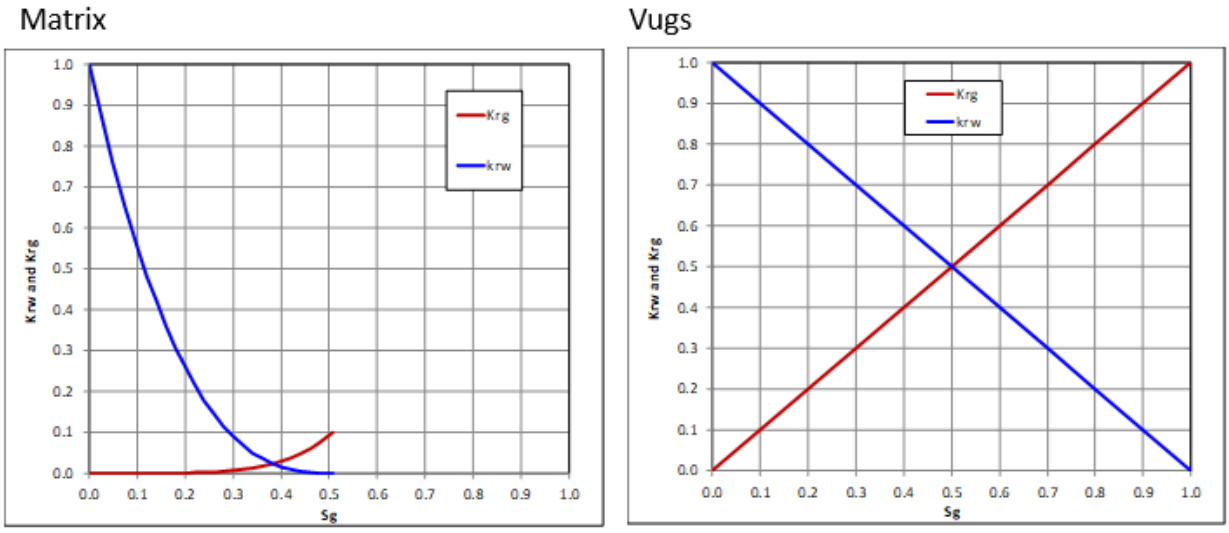

Figure 34. *Relative permeability curves for matrix rocks and vuggy intervals as used in the Potosi simulation model.*

3.2.2 Preliminary Potosi Dolomite Models

Preliminary simulations were performed to assess the CO_2 injectivity of a single well into the Potosi. This model is based on the geologic model and reservoir engineering input, as described in the previous sections.

The simulation model is 22 x 22 miles areally and consists of the Potosi formation only. The model is center over Wabash #1. The overburden and underlying formations are not included in the preliminary model. It is a layer cake model, with constant properties within each layer but the properties varying vertically from layer-to-layer. The grid block dimensions are 1000 x 1000 ft areally, and ~3 ft thick. The number of grid blocks in the x, y and z directions are 116 x 116 x 219; respectively. There is a total of 2.9 million cells in the simulation model. Figure 35 shows a 3-D image of the preliminary Potosi *Nexus*® model, with the blocks colored by depth.

Porosity and permeability in both the x-direction (k_x) and vertical direction (k_z) were populated within the Petrel™ model. Within *Nexus*®, permeability in the y-direction (k_y) was set to the values of k_x. Figure 36 shows the horizontal permeability ($k_x = k_y$) distribution along a west-east cross section through the center of the preliminary Potosi simulation model. The warmer colors are high permeability, and the cooler colors are low permeability. The Potosi contains vuggy intervals with high permeability (10 to 2,400 mD), surrounded by matrix rock with lower permeability (on the order of 1 to 62 mD). One 10 ft thick vuggy interval from 4,506 to 4,516 ft, MD was tested in Wabash #1. The actual interval tested in situ was 4,505

ft to 4,525 ft, MD, and interpretation of an early well test indicates a permeability-thickness of 24,000 mD-ft (over 10 feet). The details of the well test analyses are contained in a separate report (Khosravi et al., 2022). Although subsequent, longer, well testing indicated much higher permeabilities exist within the Potosi Dolomite, the low permeability value of 2,400 mD is assigned to the tested vuggy interval. Other vuggy intervals are assigned a permeability value proportional to their thicknesses. The cross section shows several vuggy intervals.

The top and bottom surfaces of the model are sealed, no flow boundaries. An infinite-acting aquifer is attached to the edges (lateral) of the model. The infinite-acting aquifer was calibrated prior to running CO_2 injection scenarios. The fracture gradient of 0.71 psi/ft was measured from Step Rate Tests that were performed on the Potosi Dolomite at Wabash #1 (Khosravi et al., 2022). In the simulation model, the maximum bottom-hole-pressure (BHP) is constrained to 90% of the fracture gradient to prevent fracturing the rock during CO_2 injection. The maximum BHP constraint is applied at the top of the perforation interval.

The reservoir rock is an aquifer, with a water saturation of 100%. *Nexus*® requires a gas-water contact and an initial pressure at a reference depth to initialize the simulation model. The simulation model is initialized with a gas-water contact placed just above the top of the model and initial pressure at datum depth of 1,954 psia at 3,938 ft, TVDss (4,500 ft, MD). Again, the pressure at this depth was measured during the well tests in Wabash #1.

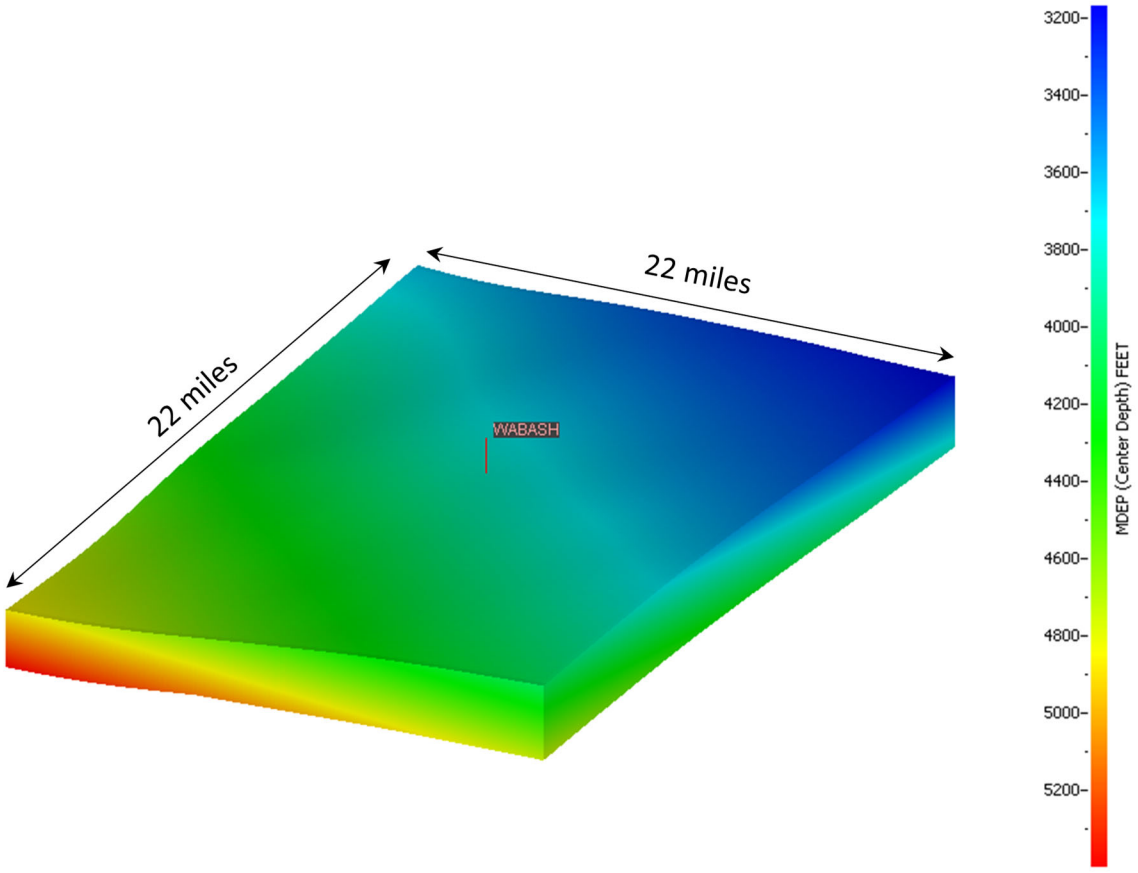

Figure 35. *Preliminary Potosi simulation model, showing the 22 x 22 mile model with blocks colored by depth.*

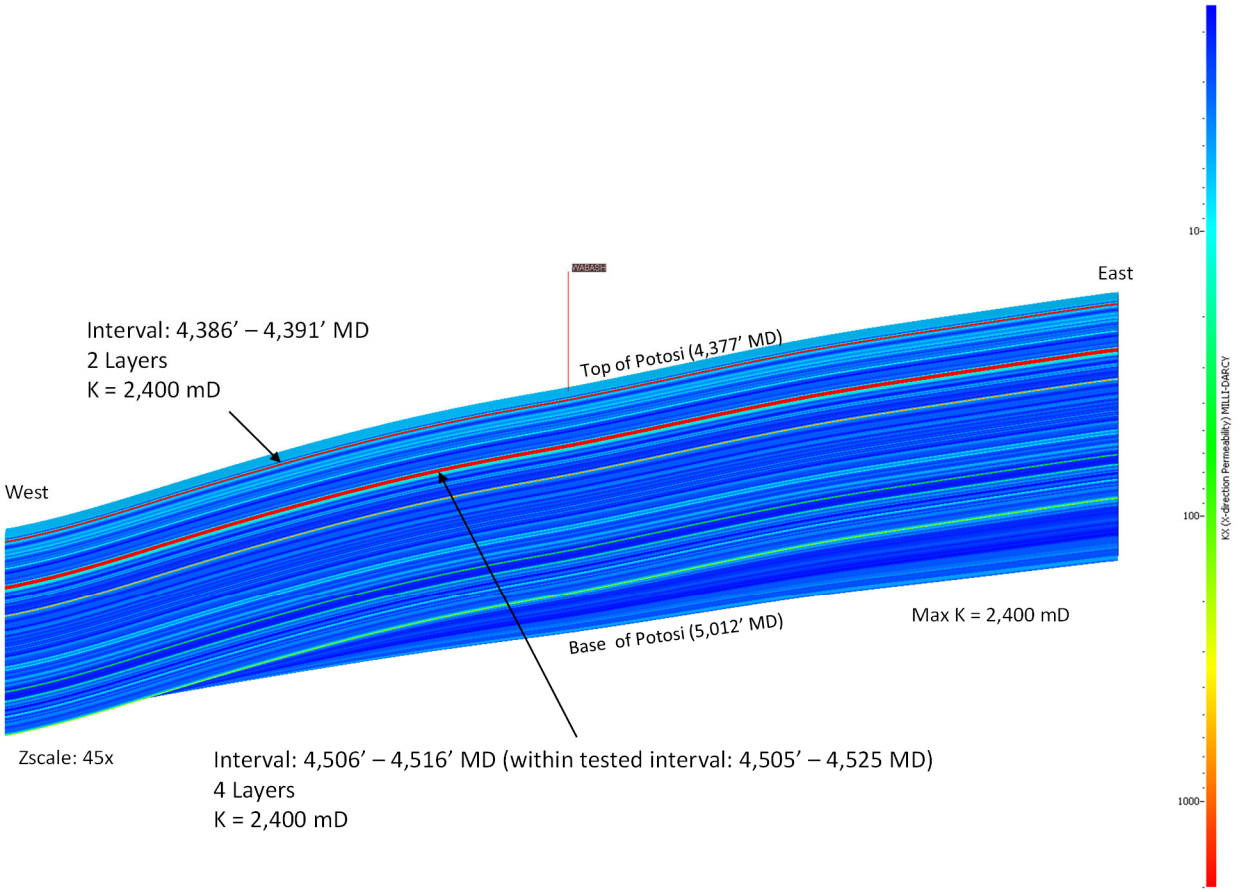

Figure 36. *Cross section through the center of the preliminary Potosi simulation model, showing the horizontal permeability distribution on a log scale.*

Multiple CO_2 injection scenarios were run using the preliminary Potosi simulation model. Six simulation cases are described here. Three perforation intervals were considered, with both a rate constrained and pressure constrained case simulated for each perforation interval. The three perforation intervals are as follows:

- Entire Potosi Interval: 4,377 – 5,012 ft, MD
- Interval : 4,385 – 4,395 ft, MD
- Tested Interval : 4,505 – 4,525 ft, MD

The first interval is the entire Potosi, and the remaining two are vuggy intervals that were either tested or identified on Wabash #1 logs. The rate constrained cases simulate the injection of 1.67 MMTA of CO_2. The pressure constrained cases simulate the injection of CO_2 at the maximum BHP, which is 90% of the measured fracture gradient (0.9 x 0.71 psi/ft). The pressure constrained cases reflect the maximum CO_2 injection rate.

The simulation results are summarized in Table 11. Average CO_2 injection rate and CO_2 plume radius were extracted and tabulated after 6,12, and 30 years of injection. Figure 37 shows the CO_2 injection rate vs. time for the six simulation cases. The simulation results show that there is adequate injectivity to support the injection of 1.67 MMTA of CO_2 into any of the three intervals for at least 30 years. After injecting 1.67 MMTA of CO_2, the plume radius is approximately 2.5 miles, 3.1 miles and 3.8 to 4.7 miles after 6, 12 and 30 years of injection; respectively. When injecting at the max BHP, it is feasible to inject 5 MMTA of CO_2

for 30 years if injecting either across the entire Potosi interval or across the tested interval (4,505 – 4,525 ft, MD). When injecting at the max BHP, the CO_2 plume radius ranges from 3.2 to 4 miles, 4.3 to 5.3 miles and 6.3 to 6.7 miles at 6, 12, and 30 years of injection; respectively.

Figure 38 through Figure 41 show CO_2 plume radii along a cross section through the center of the model at 6, 12, and 30 years for the pressure and rate constrained cases for the two perforation intervals: 1) Entire Potosi and 2) Tested vuggy interval (4,505 – 4,525 ft, MD). The figures show simulation cells having gas saturation values ≥ 1%. Figure 38 and Figure 39 are the pressure constrained CO_2 plumes, and they show similar plume radii at 6, 12, and 30 years for both cases. However, the quantity of CO_2 injected is different. Less CO_2 is injected in the case where only the tested vuggy interval is perforated. Perforating the entire Potosi interval allows for the injection of a total of 37, 72, and 169 MMtonnes of CO_2 at 6, 12 and 30 years; respectively. Whereas, perforating only the tested vuggy interval allows for the injection of a total of 33, 63 and 149 MMtonnes of CO_2 at 6, 12, and 30 years; respectively. Figure 40 and Figure 41 are the rate constrained CO_2 plumes, and they also show similar plume radii at 6, 12, and 30 years between the two cases. The amount of CO_2 injected is the same in these rate constrained cases. A large amount of CO_2 goes into the tested vuggy interval in both perforation cases, and this results in the similar plume radii observed in the results. The amount of CO_2 injected is 10, 20, and 50 MMtonnes at 6, 12, and 30 years; respectively.

Table 11. *Preliminary Potosi model simulation results.*

			6-yrs			12-yrs			30-yrs		
	Case	Perf Interval	Avg Rate (MMTA)	Plume Radius (miles)	CO2 Injected (MMtonnes)	Avg Rate (MMTA)	Plume Radius (miles)	CO2 Injected (MMtonnes)	Avg Rate (MMTA)	Plume Radius (miles)	CO2 Injected (MMtonnes)
Pressure Constrained	Case1P	4,377' - 5,012'	6.21	4.0	37	6.00	5.1	72	5.64	6.6	169
	Case2P	4,385 - 4,395'	3.31	3.2	20	3.24	4.3	39	3.14	6.3	94
	Case3P	4,505' - 4,525'	5.42	4.0	33	5.26	5.2	63	4.97	6.7	149
Rate Constrained	Case1R	4,377' - 5,012'	1.67	2.3	10	1.67	2.9	20	1.67	3.8	50
	Case2R	4,385 - 4,395'		2.5	10		3.2	20		4.7	50
	Case3R	4,505' - 4,525'		2.5	10		3.1	20		4.0	50

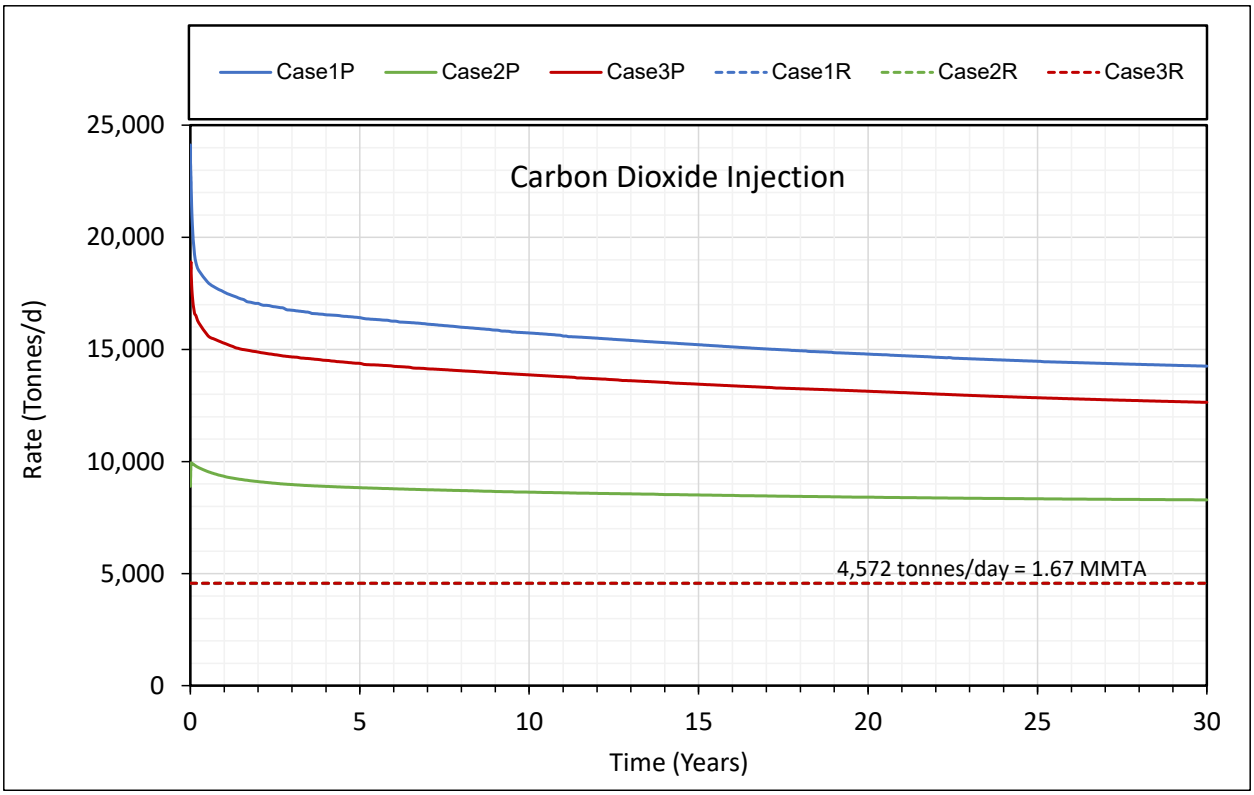

Figure 37. *CO_2 injection rate vs. time for various completion intervals using either rate or max BHP constraints.*

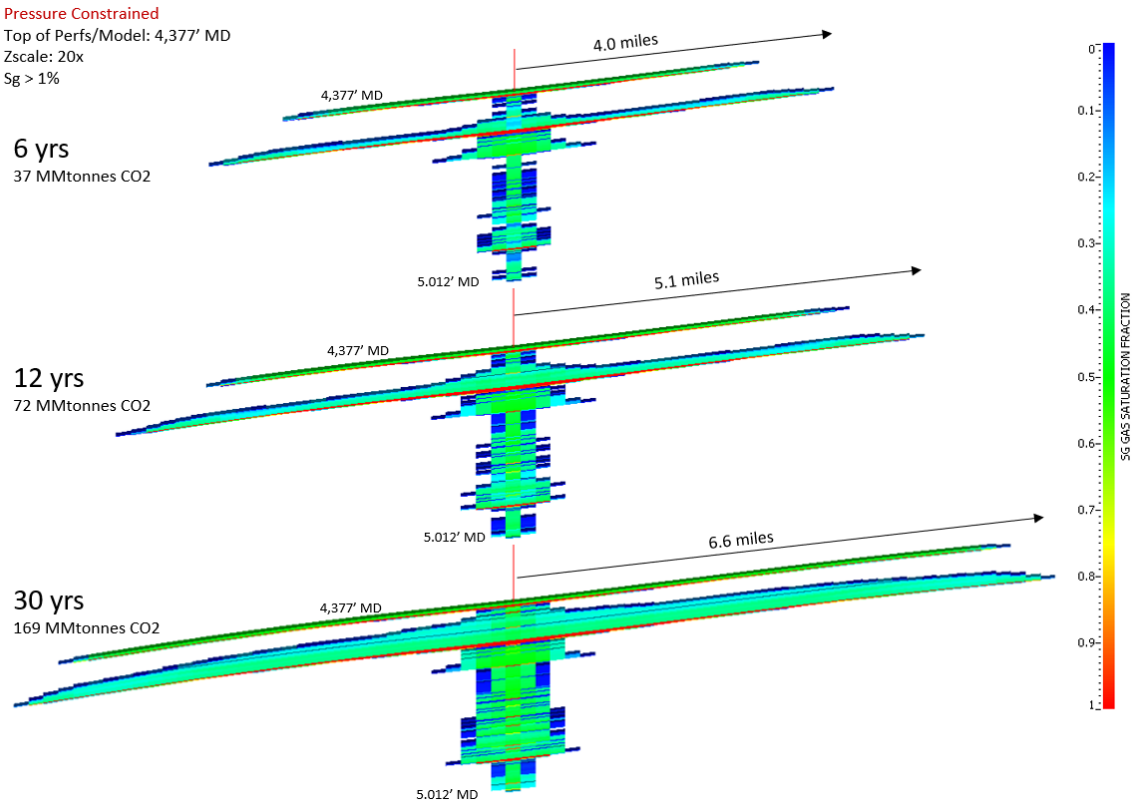

Figure 38. *Case1P: CO_2 plume cross section after 6, 12 and 30 years of injection across the entire Potosi interval at the max BHP. Only cells with gas saturation ≥ 1% are visible.*

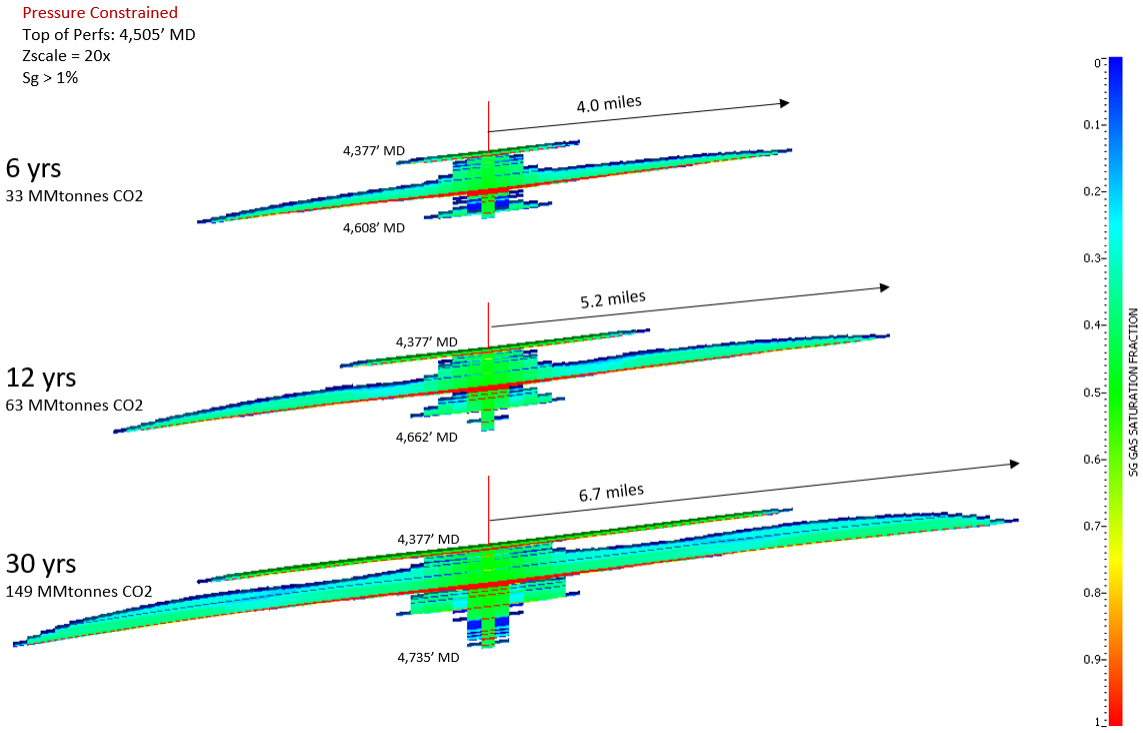

Figure 39. *Case3P: CO_2 plume cross section after 6, 12 and 30 years of injection across the tested vuggy interval (4,505 – 4,525 ft, MD) at the max BHP. Only cells with gas saturation ≥ 1% are visible.*

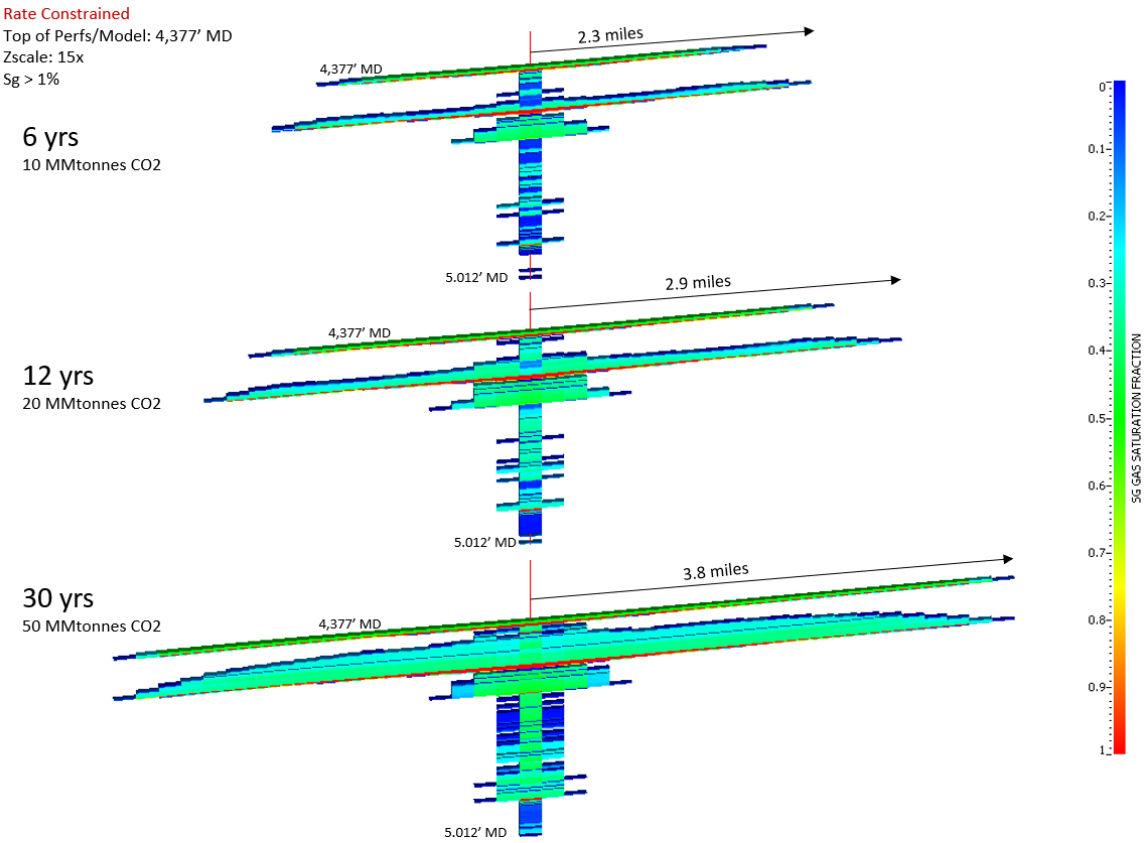

Figure 40. *Case1R: CO_2 plume cross section after 6, 12 and 30 years of injection across the entire Potosi interval at a constant rate of 1.67 MMTA. Only cells with gas saturation ≥ 1% are visible.*

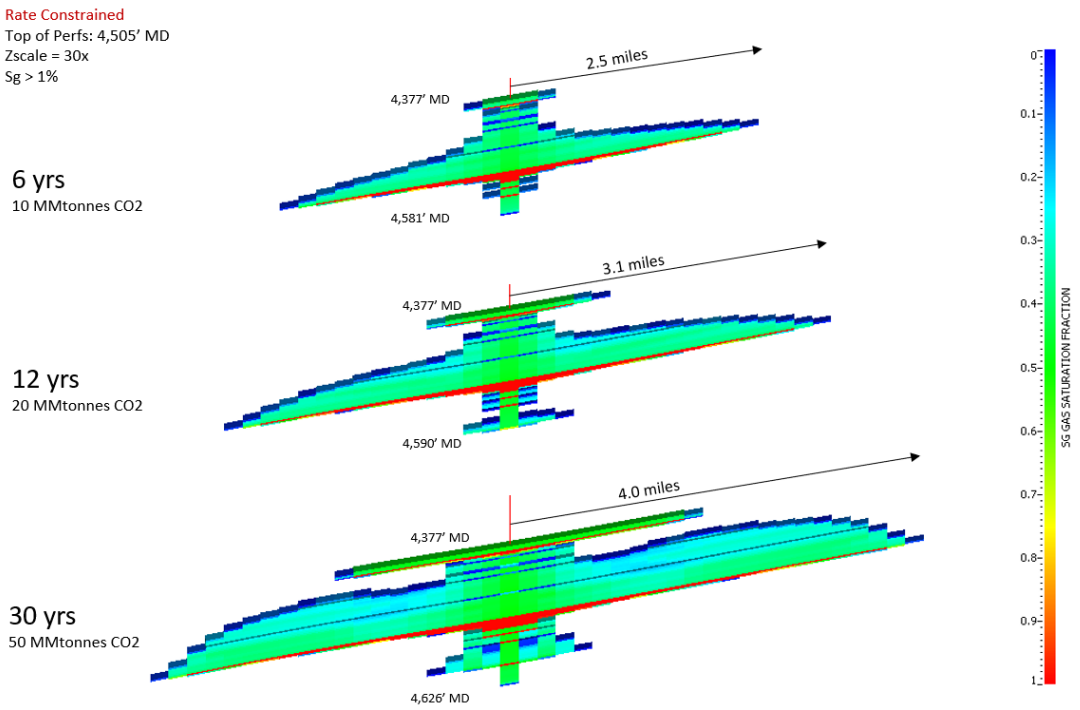

Figure 41. *Case3R: CO_2 plume cross section after 6, 12 and 30 years of injection across the tested vuggy interval at a constant rate of 1.67 MMTA. Only cells with gas saturation ≥ 1% are visible.*

Several additional cases were run on the Preliminary Potosi model to both assess grid size sensitivity and frame an injection concept for a 12 year CO_2 injection project:

- A lateral grid size sensitivity was run to assess the impact of grid size on simulation results
- CO_2 plume size vs. year at a constant injection rate of 1.67 MMTA
- CO_2 plume radius vs. injection rate after 12 years of injection at a constant rate
- CO_2 plume radius at 12 years vs. well spacing for a two well injection case; each well injecting 1/2 of the total rate of 1.67 MMTA (which is 0.835 MMTA per well)

The grid sensitivity study was performed using local grid refinement in an area around the well. The refined area is 12 x 6 miles, and grid sizes of 333 x 333 ft and 200 x 200 ft were simulated; see Figure 42. These grid sizes correspond to 3:1 and 5:1 refinement of each simulation cell within the refined area. The simulation cases were run for a total of 12 years of injection, at a constant rate of 1.67 MMTA. Figure 43 shows the CO_2 plume radius vs. time for the grid sizes investigated. There is a substantial difference in the plume size vs. time for the 333 x 333 ft grid as compared with the base 1000 x 1000 ft grid. The difference in plume size vs. time for 200 x 200 ft vs. 333 x 333 ft grid size is not as large. This is to be expected, as the results should converge to one solution as the grid is refined. The grid size of 333 x 333 ft was chosen as the refined grid size to use for all future simulations of the Potosi model in this report. This decision is based on the small difference in results when the grid is refined to 200 x 200 ft and on numerical efficiency in terms of total number of cells, memory requirements and simulation run time. For example, the runtime for the 200 x 200 ft grid is 3 times longer than the runtime for the 300 x 300 ft grid; for only a marginal improvement of the simulation results.

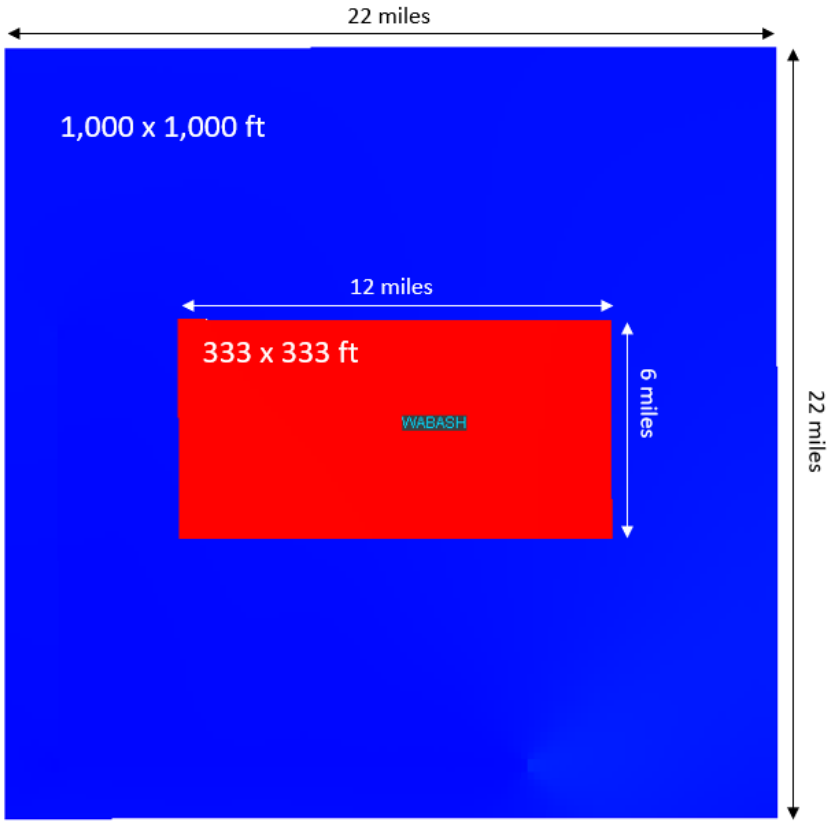

Figure 42. *Local grid refinement area of 12 x 6 miles in the center of the simulation model for grid sensitivity and 2 injection wells scenarios. Refined grid sizes of 333 and 200 ft were considered.*

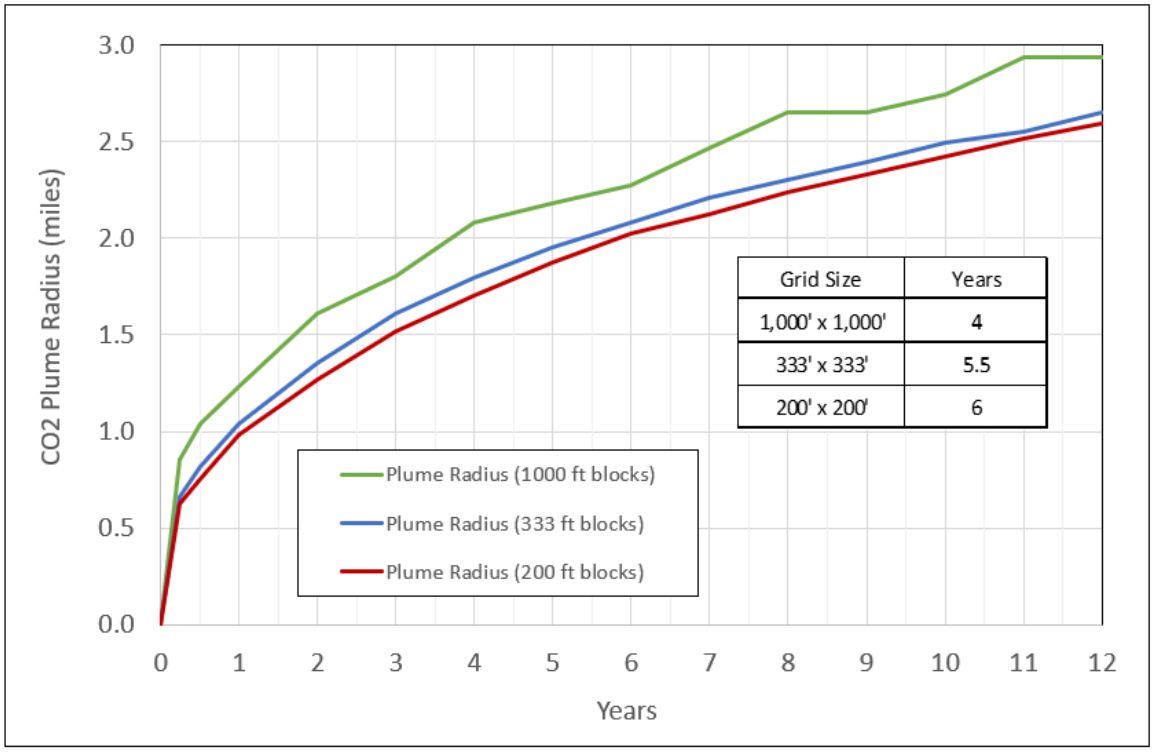

Figure 43. *CO_2 plume size vs. time for three refined grid sizes based on the injection of 1.67 MMTA across the entire Potosi interval.*

A single well simulation with a constant injection rate of 1.67 MMTA for 12 years was performed on the refined grid (see Figure 42), to determine how long it will take to reach a CO_2 plume radius of 2 miles. Figure 44 shows that after 5.5 years of injection at 1.67 MMTA, the plume radius reaches 2 miles.

Single well simulations with different constant injection rates were run for 12 years to determine what CO_2 injection rate would yield a plume radius of 2 miles at 12 years. Figure 45 shows that an injection rate of 0.93 MMTA would yield a CO_2 plume radius of 2 miles after 12 years of injection.

Simulations were run with two injection wells to assess the impact of well spacing on CO_2 plume radius at 12 years. The wells are centered within the 12 x 6 mile refined area of the model as shown in Figure 46. Both wells inject simultaneously, with each well injecting 1/2 of the total rate of 1.67 MMTA (0.835 MMTA per well). Figure 47 shows the CO_2 plume radius after 12 years of injection vs. well spacing. The plume size and shape vs. time is shown in Figure 48. The plume is not perfectly centered around each well. This is due to both reservoir dip and well interference. The reservoir updip direction is to the North-east, and the dip is relatively low at < 0.85 degrees. There are two curves in Figure 47, to reflect that the plume is not centered over each well. One shows the overall plume radius, and the other shows the maximum distance from the well to the edge of the plume. When the wells are close, there is interference between the wells and the plume radius is large. As the well spacing increases, there is less interference between the wells and the plume radius decreases. The plume radius approaches a value of 1.96 miles for well spacings ≥ 4 miles. The distance from the well to the edge of the plume is always slightly larger than the plume radius, but also decreases as well spacing increases. The results indicate that placing two injection wells ≥ 4 miles apart will yield the smallest amount of interference between the wells and produce a CO_2 plume with a radius ~ 2 miles after 12 years of injection at 1.67 MMTA (1/2 in each well simultaneously). The combined area of the two plumes (one around each well) is approximately 7.1 sq miles, for all well spacings considered. The combined area is 17.07, 17.04, 17.07, 17.13, 17.15 and 17.17 sq miles for well spacings of 1, 2, 3, 4, 5 and miles; respectively.

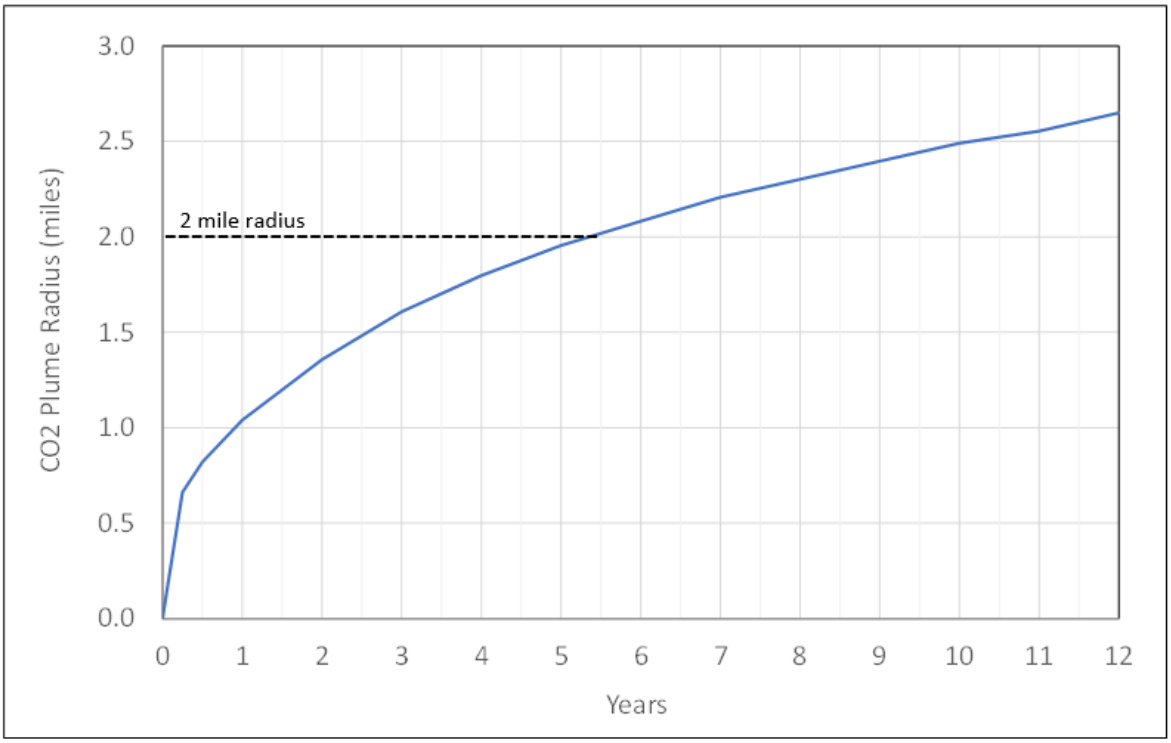

Figure 44. *CO_2 plume radius vs. time for a constant injection rate of 1.67 MMTA, showing that a plume radius of 2 miles is reached after 5.5 years of injection.*

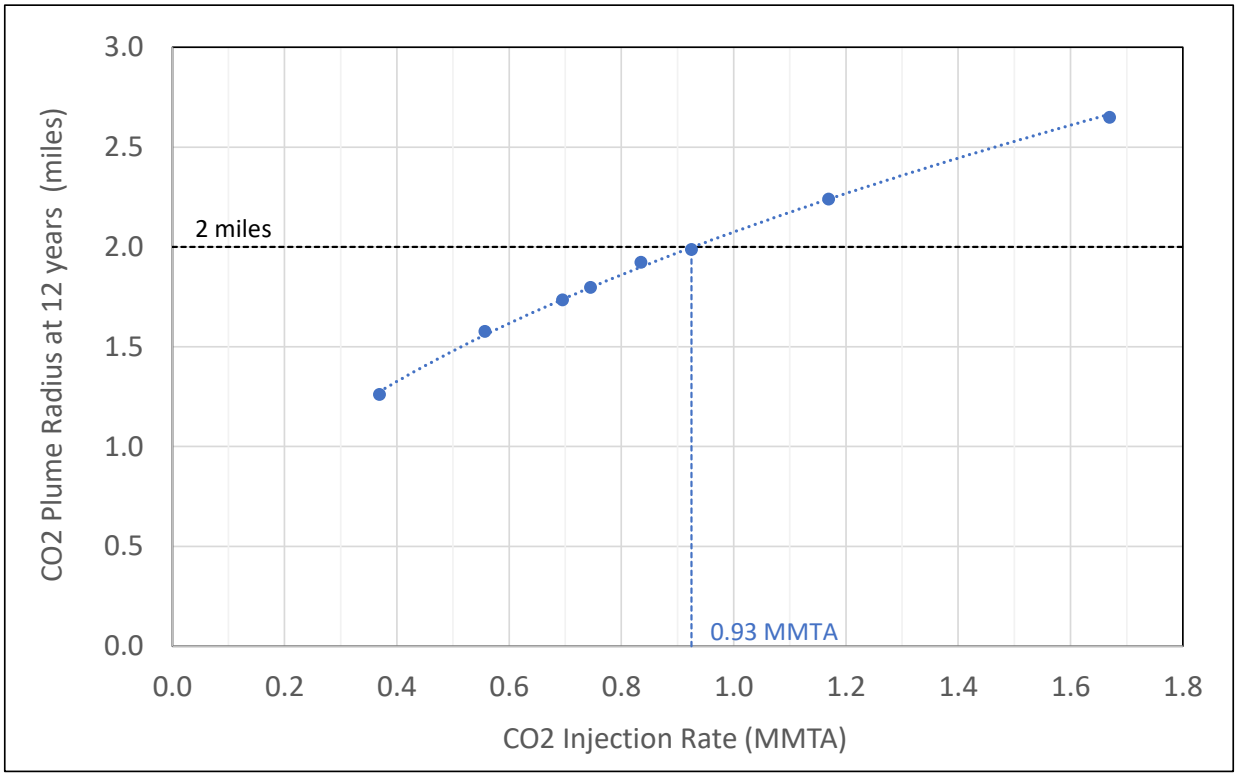

Figure 45. *CO_2 plume radius at 12 years vs. injection rate, showing that an injection rate of 0.93 MMTA would yield a plume radius of 2 miles after 12 years of injection.*

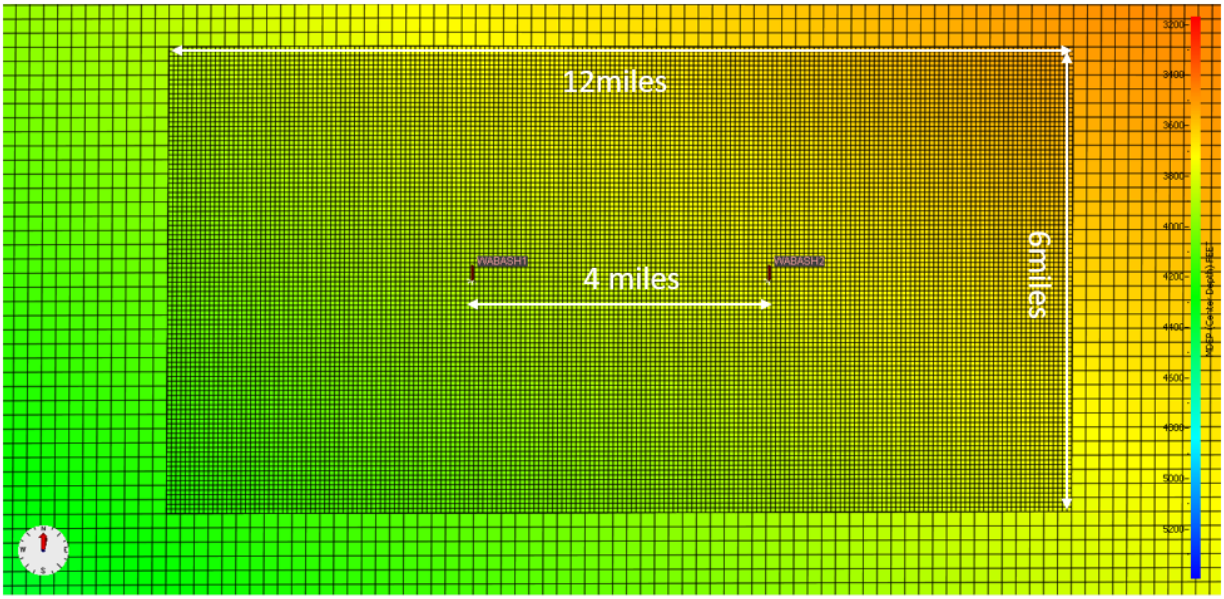

Figure 46. *Example of a 2 well injection case with wells centered within the 12 x 6 mile refined area of the grid. Well spacings of 0.5 to 6 miles were considered. The blocks are colored by depth (ft).*

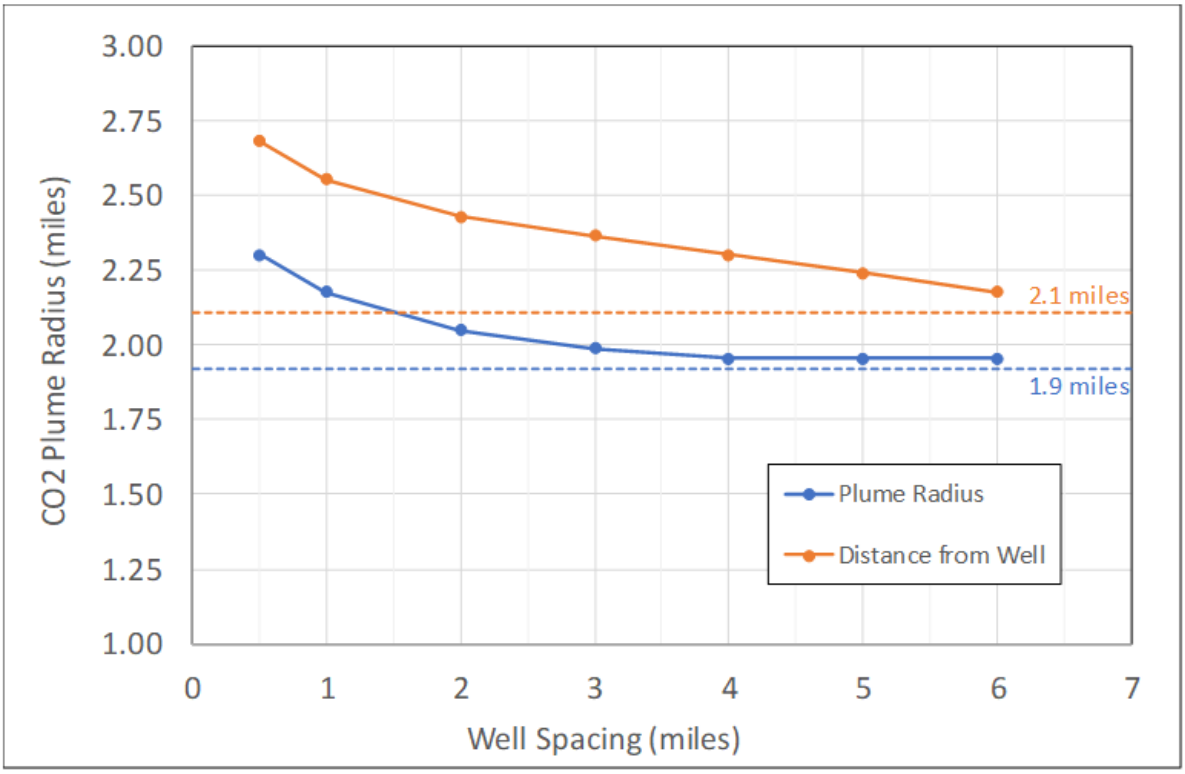

Figure 47. *CO_2 plume radius after 12 years of injection at various well spacings, for a two well injection case with each well simultaneously injecting ½ of the total 1.67 MMTA.*

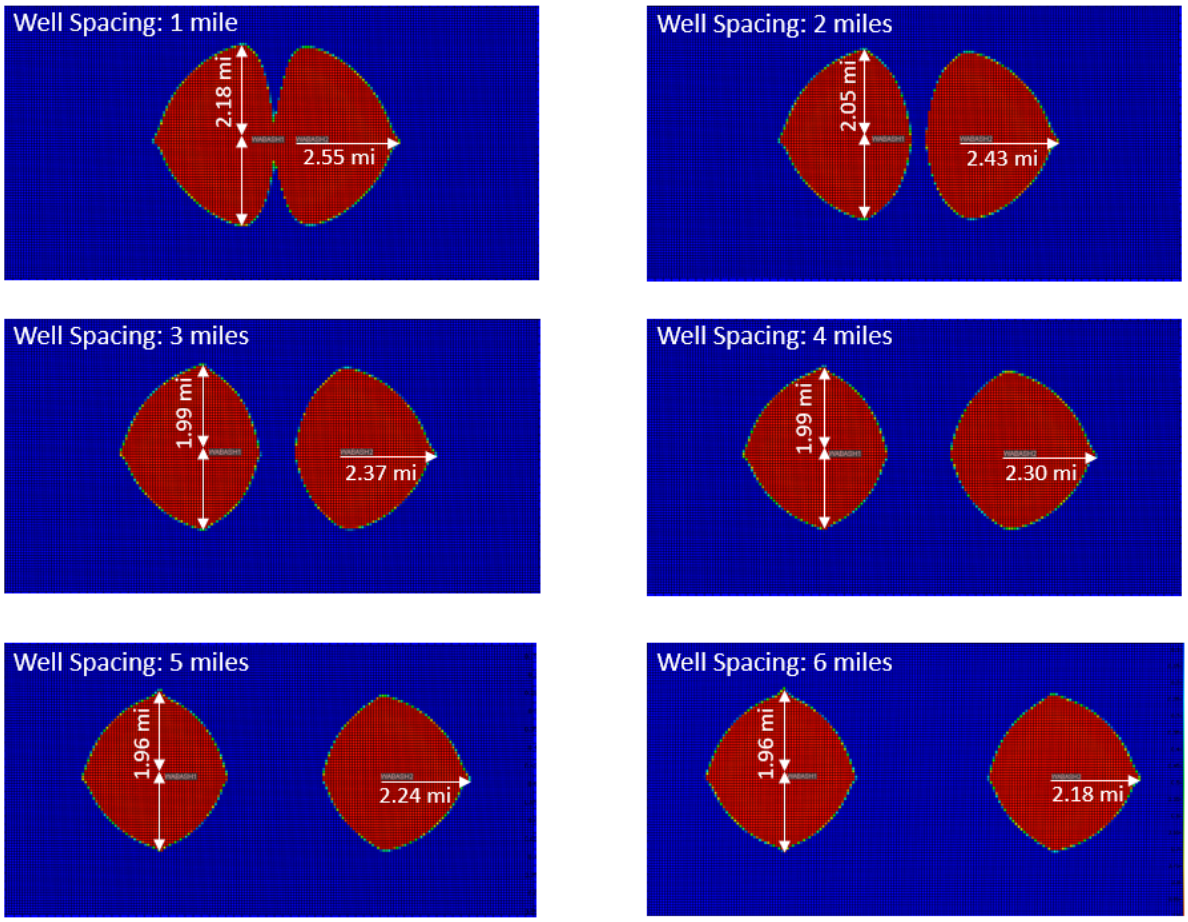

Figure 48. *CO_2 plume after 12 years of injection at various well spacings, for a two well injection case with each well simultaneously injecting ½ of the total 1.67 MMTA.*

3.2.3 Updated Potosi Model: with overburden and underlying formations

The Potosi simulation model was updated to include the overburden as well as underlying formations. The grid cells and properties within the Potosi Dolomite formation are identical to those in the Preliminary simulation model. The updated model includes the Potosi Dolomite, underlying Davis Formation, and the overburden formations (listed in descending order) the Maquoketa Shale (Maquoketa Group), Trenton Limestone, Platteville (Black River) Group, Dutchtown Limestone, St. Peter Sandstone, Shakopee Dolomite, and Oneota Dolomite. The model is a layer cake model, with constant properties within each layer but the properties varying vertically from layer-to-layer. Figure 49 shows a 3-D image of the simulation model showing the included formations.

The simulation model is 22 x 22 miles areally. The model is centered over a pair of proposed injection wells; denoted as North and South. Wabash #1 is included in the model and is located in the Southeastern portion of the model. Figure 50 is a map view of the mid-layer depth for the first layer within the Potosi interval (layer 24), showing the locations of the three wells: North, South and Wabash #1 (Wabash1).

The grid block dimensions are 1000 x 1000 ft areally, and an area of local grid refinement is placed around the wells. The size and location of the refined area changes relative to the injection scenario simulated, but the refined blocks are always 333 x 333 ft areally. The refined area of the grid will be discussed with each case later in this report. There are 241 layers in the model, and the cell thickness varies by layer. Cells within the Potosi Dolomite layers are approximately 3 ft thick, and there are 217 layers within this interval.

The cell thickness in the overburden and underlying formations vary. The number of grid blocks in the x, y and z directions of the unrefined model are 116 x 116 x 241: respectively. There is a total of 3.2 million cells in the unrefined simulation model. After refinement is added around the wells, the total number of cells increases to 7.5 million.

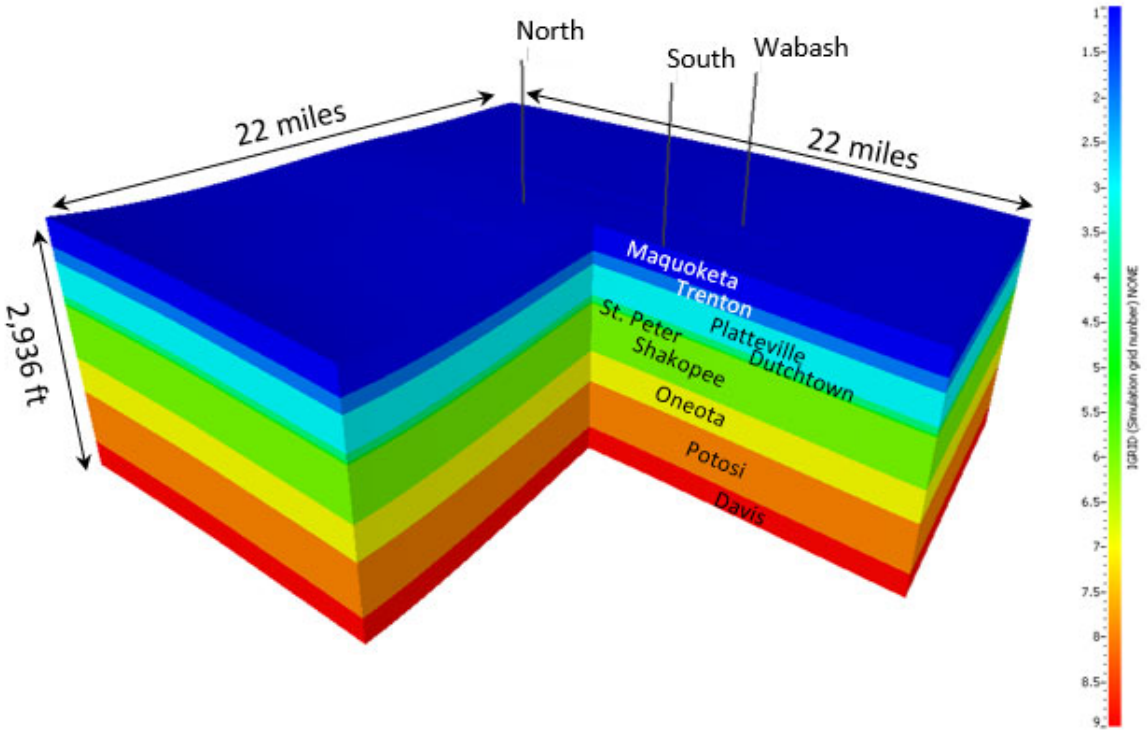

Figure 49. *Updated Potosi simulation model, which contains the underlying Davis and the overlying Oneota, Shakopee, St. Peter, Dutchtown, Platteville, Trenton and Maquoketa formations.*

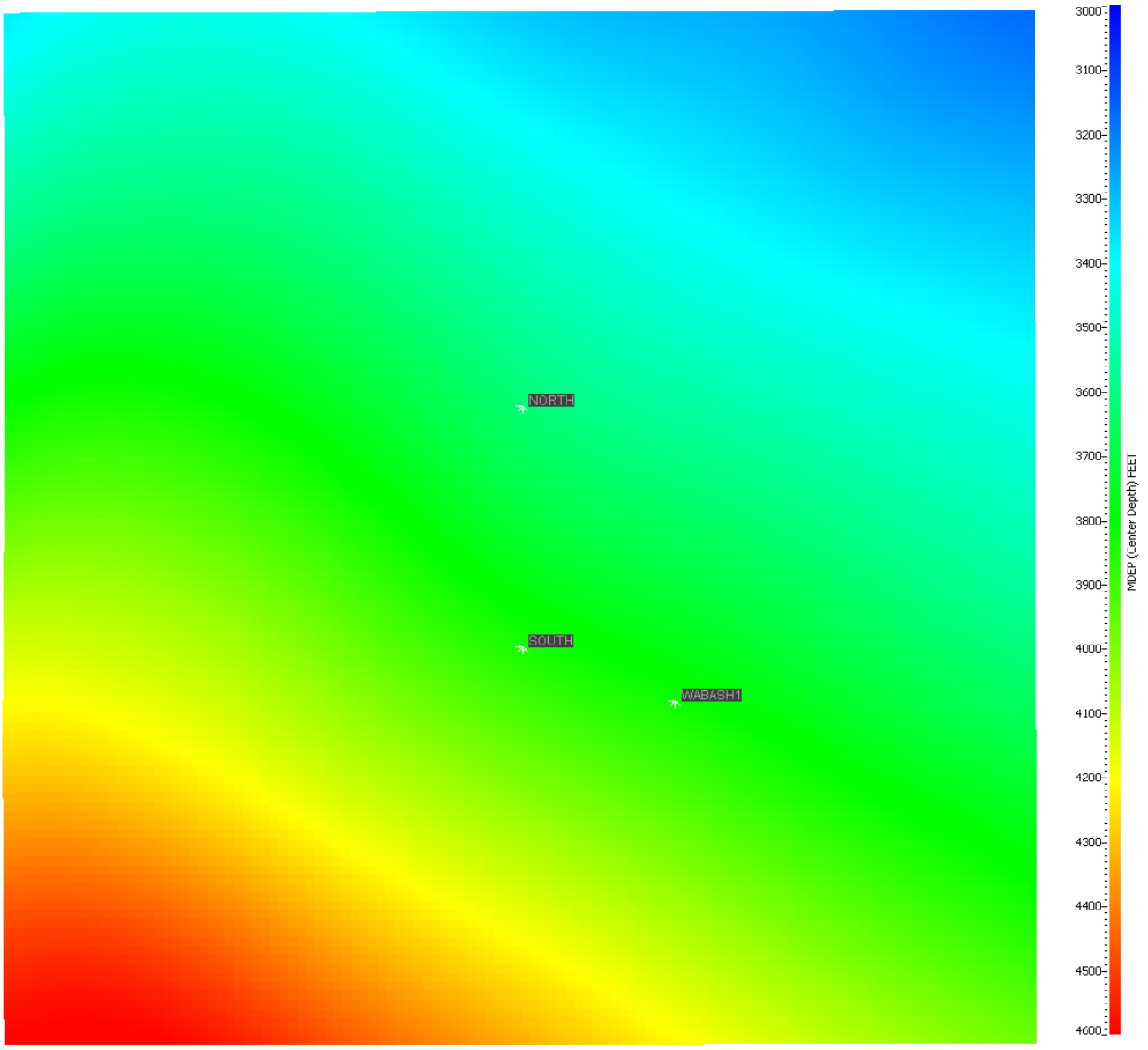

Figure 50. *Map view of the mid-point depth of the first layer in the Potosi (layer 24), showing the location of the potential injection wells: North and South and the location of Wabash #1 (bottom right).*

Porosity and permeability in both the x-direction (k_x) and vertical direction (k_z) were populated within the Petrel™ model. Within *Nexus*®, permeability in the y-direction (Ky) was set to the values of Kx. Figure 51 and Figure 52 shows the horizontal ($k_x = k_y$) permeability distribution along a west-east cross section through the model at Wabash #1 for the overburden and Potosi and Davis formations; respectively. The overburden is shown in a separate figure for viewing clarity. The warmer colors are high permeability, and the cooler colors are low permeability. Figure 51 also shows the vertical layering within the overburden formations. There are 23 layers in the overburden. The total thickness of the overburden is 1,992 ft and the layer thickness varies from 12 to 380 ft. Figure 53 shows the model layer thicknesses on a South-North cross section through the center of the model. Table 12 details the horizontal and vertical permeability within the overburden. Most of the overburden formations are represented by a single layer in the model. However, the Shakopee and Oneota intervals have multiple layers and the permeability values in Table 12 show the range of permeability for these two formations. The permeability drops substantially in the St. Peter and shallower overburden formations, making these formations a good seal for the injection interval (Potosi). The Maquoketa is identified as the primary seal for injection into the Potosi, and simulation results will show that the pressure increase from injection into the Potosi is negligible at the Maquoketa during the

model runs. Figure 52 shows the permeability distribution for the Potosi and the underlying Davis formation. As the properties for the Potosi are the same as in the Preliminary model (see prior discussion on the Potosi properties). The Davis formation is represented by a single layer in the model and has a horizontal permeability of 4 mD and a vertical permeability of 3.4 mD.

The top and bottom surfaces of the model are sealed, no flow boundaries. An infinite-acting aquifer is attached to the edges (lateral) of the model. The infinite-acting aquifer was calibrated prior to running CO_2 injection scenarios. The fracture gradient was measured from Step Rate Tests that were performed on the Potosi formation at Wabash #1. The measured fracture gradient is 0.71 psi/ft. In the simulation model, the maximum bottom-hole-pressure (BHP) is constrained by 90% of the fracture gradient to prevent fracturing the rock during CO_2 injection. The maximum BHP constraint is applied at the top of the perforation interval. The perforated interval for all simulations is the entire Potosi interval, and this interval was selected because it yields the smallest plume radius.

The reservoir rock is an aquifer, with a water saturation of 100%. *Nexus*® requires a gas-water contact and an initial pressure at a reference depth to initialize the simulation model. The simulation model is initialized with a gas-water contact placed just above the top of the model and an initial pressure at datum depth of 1,954 psia at 3,938 ft, TVDss (4,500 ft, MD). Again, the pressure at this depth was measured during the well tests in Wabash #1.

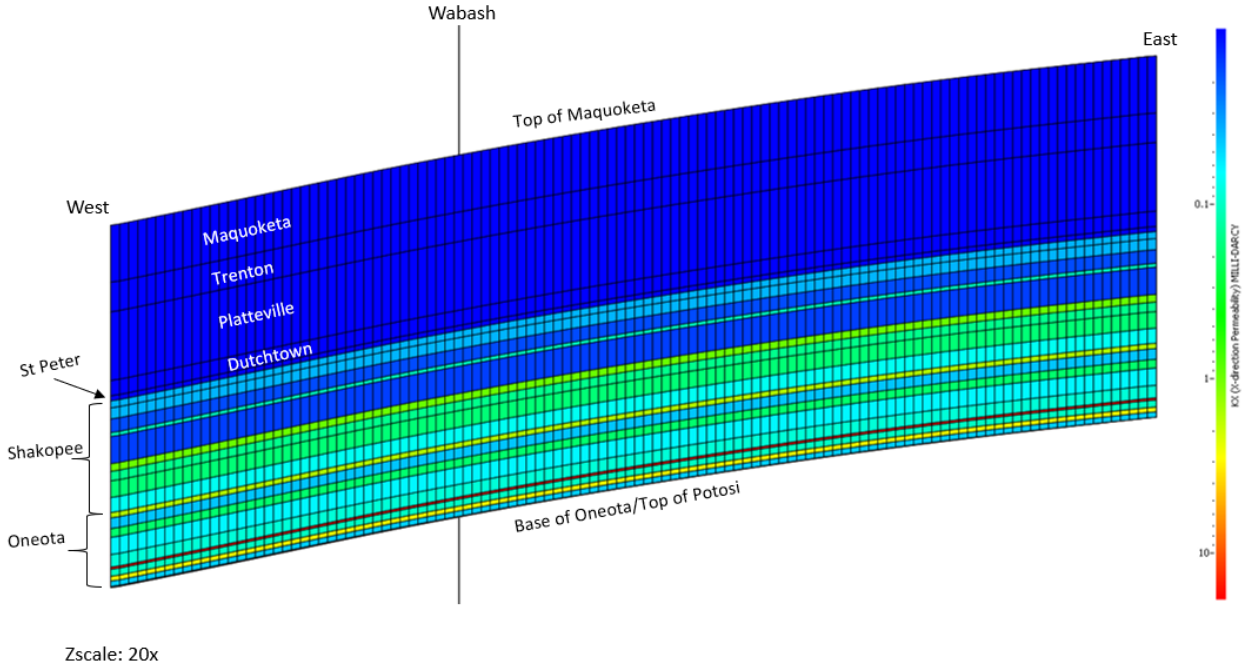

Figure 51. *West-east cross section through the model at the Wabash location showing the horizontal permeability in the overlying formations: Oneota, Shakopee, St. Peter, Dutchtown, Platteville, Trenton and Maquoketa.*

Table 12. *Horizontal and vertical permeability in the overburden formations.*

Zone	Permeability (mD)	
	Kx	Kz
Maquoketa	1.0E-04	8.5E-05
Trenton	3.0E-06	2.0E-06
Platteville	5.0E-06	4.0E-06
Duchtown	8.4E-05	7.1E-05
St. Peter	4.0E-03	3.0E-03
Shakopee	0.015 - 0.878	0.013 - 0.747
Oneota	0.038 - 19.2	0.033 - 16.3

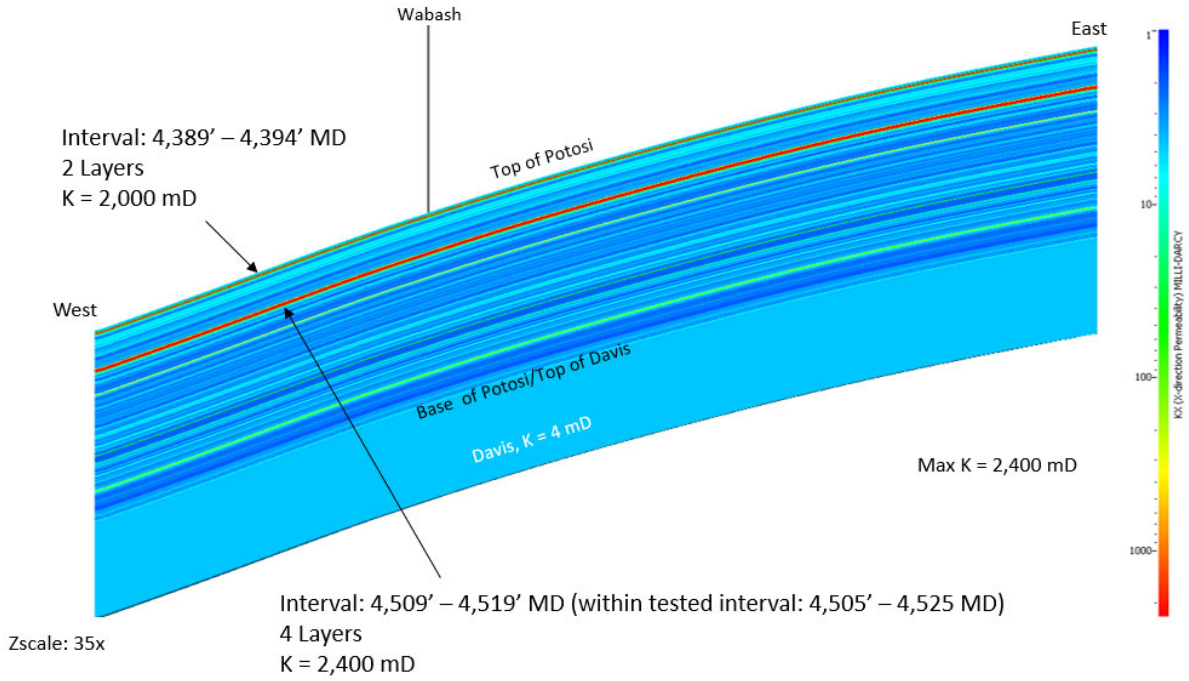

Figure 52. *West-east cross section through the model at Wabash #1 showing the horizontal permeability in the Potosi Dolomite and the underlying Davis Formation.*

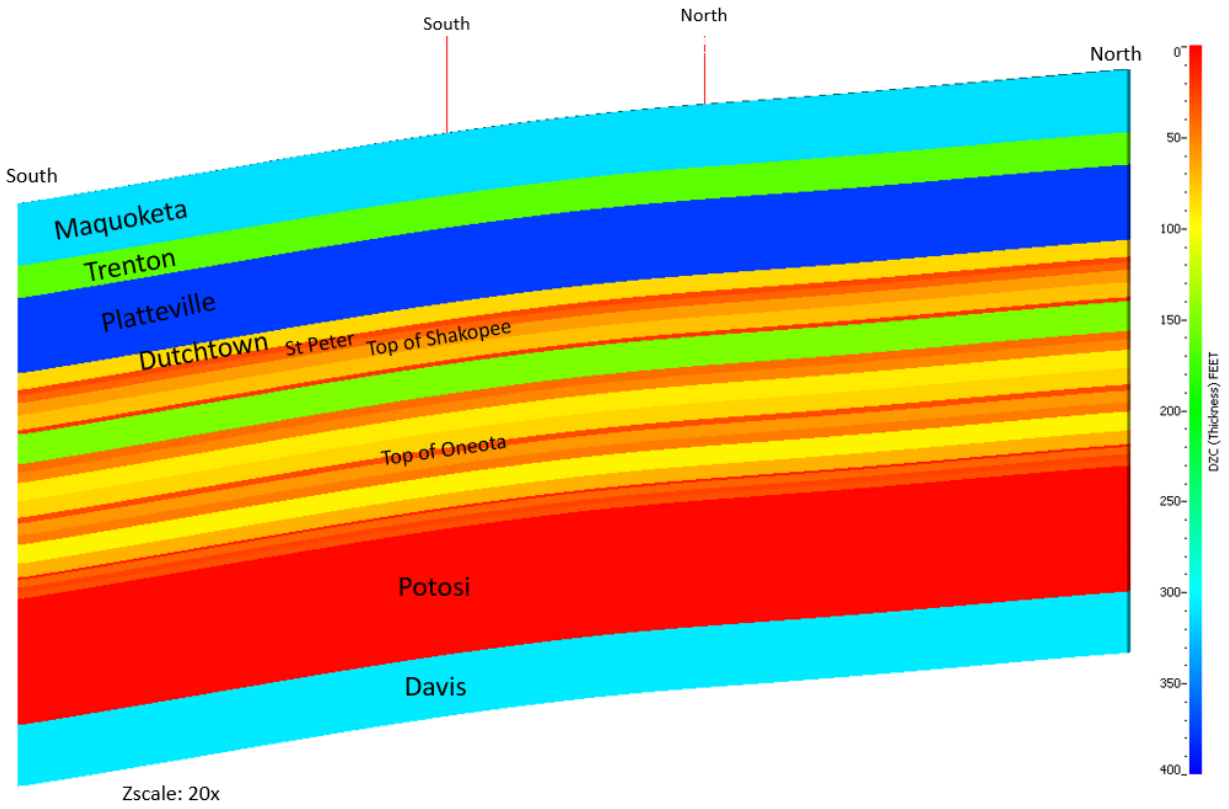

Figure 53. *South-North cross section through the center of the model showing the simulation layer thicknesses.*

3.2.4 Updated Potosi Model: Simulation Results

The next few sections discuss the simulation of several injection scenarios. Each simulation includes an injection period of either 12 or 30 years, followed by a 50 year post-injection observation period. The injection scenarios are as follows:

- Two well injection of 1.67 MMTA of CO_2 for 30 years
- Two well injection of 1.67 MMTA of CO_2 for 12 years
- Single well injection of 1.67 MMTA of CO_2 into Wabash #1 for 30 years
- Single well injection of 1.67 MMTA of CO_2 into Wabash #1 for 12 years

3.2.4.1 Two well injection of 1.67 MMTA of CO_2 for 30 years

This simulation scenario is a two well injection of 1.67 MMTA of CO_2 for 30 years. CO_2 is injected in both North and South simultaneously for 30 years, followed by a 50 year post injection observation period. Each well injects 0.835 MMTA, which is ½ of the total injection rate. The total volume of CO_2 injected after 30 years is 50 MMtonnes. The injection wells are 5 miles apart and there is a 12 x 6 mile refined grid region around the two injection wells, as shown in Figure 54.

Figure 55 shows the CO_2 plume after 30 years of injection at the layer having the greatest plume extent, layer 67 within the Potosi interval at the top of the tested vuggy interval. The plume shows some impact of well interference and of reservoir dip. Largest dimensions of the plume are denoted on the plumes. The North plume extends the furthest, 3 miles to the North. Both plumes extend about 2.6 to 2.7 miles to the east. Figure 56 contains a South-North cross section through the injection wells and shows the CO_2 plume after 30 years of injection. Only simulation cells having gas saturation values $\geq$ 1% are visible. The asymmetric lateral shape of the plume shows the impact of well interference and reservoir dip. The vertical

scale has been exaggerated 30 times so the reservoir dip looks much larger than in reality. The majority of the CO_2 has entered the two highest-perm vuggy intervals within the Potosi. The plume has also migrated vertically and has entered the 2 bottom layers of the overlying Oneota formation.

Figure 57 shows a South-North cross section through the injection wells and the change in pressure (ΔP) after 30 years of injection. The highest increase in pressure is at the well locations and is approximately 180 psi. It is important to note that the pressure change only reaches the Dutchtown formation. The formations overlying the Dutchtown see a negligible increase in pressure due to 30 years of injection. Figure 58 contains maps of pressure increase (ΔP) after 30 years of injection at several layers within the model. These maps also illustrate that the pressure change stops at the Dutchtown formation.

Figure 59 contains plots of BHP and ΔP (= BHP at 30 years – initial pressure) vs. time for the two injection wells. The BHP at South is higher than the BHP at North due to reservoir dip. South is deeper than North by approximately 225 ft. The BHP at both wells increases by approximately 200 psi after 30 years of injection. After injection stops, the BHP shows a rapid initial drop and then slowly decreases over time towards the initial pressure. Fifty years after injection stopped, the BHP is within 20 psi of initial pressure. The maximum BHP for both wells after 30 years of injection (2,014 psia and 2,110 psia for North and South; respectively) is significantly below the maximum BHP (90% of fracture pressure), which is 2,672 psia and 2,816 psia for North and South; respectively.

Figure 60 and Figure 61 show map views of the CO_2 plume within the Potosi, at layer 67 (which is the top of the tested vuggy interval) vs. time. Dimensions are denoted on both the North and South plumes. The plume shape starts to show the influence of interference between the wells after 3 years of injection, as evident by the difference in plume size and shape of the North and South plumes. Although injection stops at 30 years, the largest plume size appears at 31 years, which is 1 year into the post injection period. Simulation results were output on a yearly basis, so the plume may have reached the maximum lateral extend anytime between the end of injection and 1 year into the post injection period. The plume stabilizes laterally after 31 years and does not expand laterally during the remainder of the 50 year post injection observation period. However, vertical migration of the plume within the Potosi and into the bottom two layers of the overlying Oneota continues throughout the 50 year post injection observation period.

Figure 62 through Figure 64 contain South-North cross sections through the injection wells and show a cross section of the CO_2 plume vs. time. Only grid cells having gas saturation ≥ 1% are visible. The top of the CO_2 plume only enters the two bottom layers of the overlying Oneota. No CO_2 enters any overburden formations above the Oneota. Some vertical migration of the plume within the Potosi and into the lower Oneota is observed during the 30 year injection period, but substantial vertical migration of the plume within the Potosi is observed during the 50 year post injection observation period.

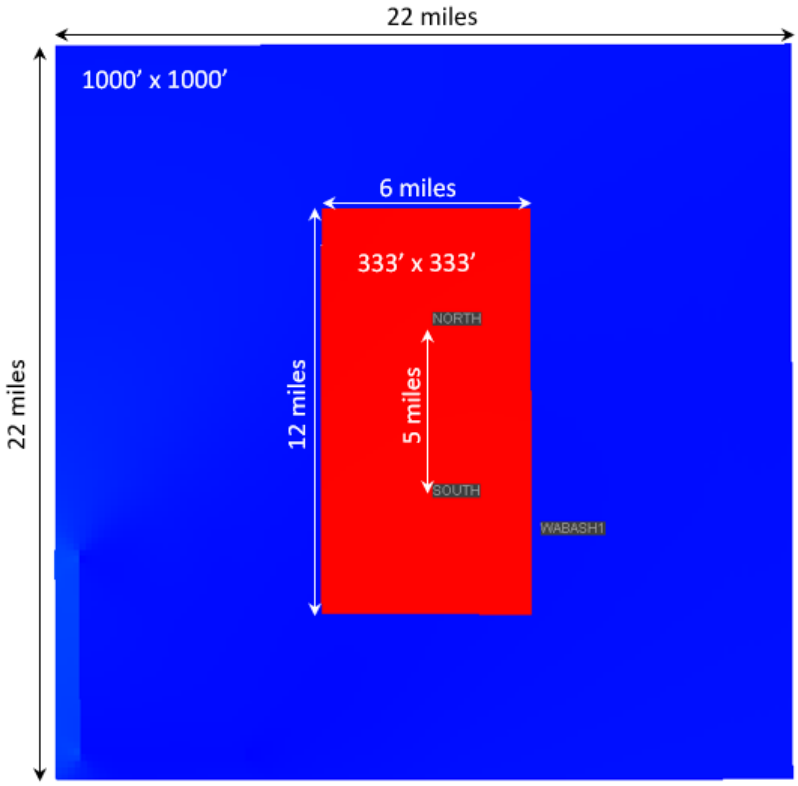

Figure 54. *Map view showing the two injection wells, North and South, that are 5 miles apart and centered within a 12 x 6 mile refined grid region.*

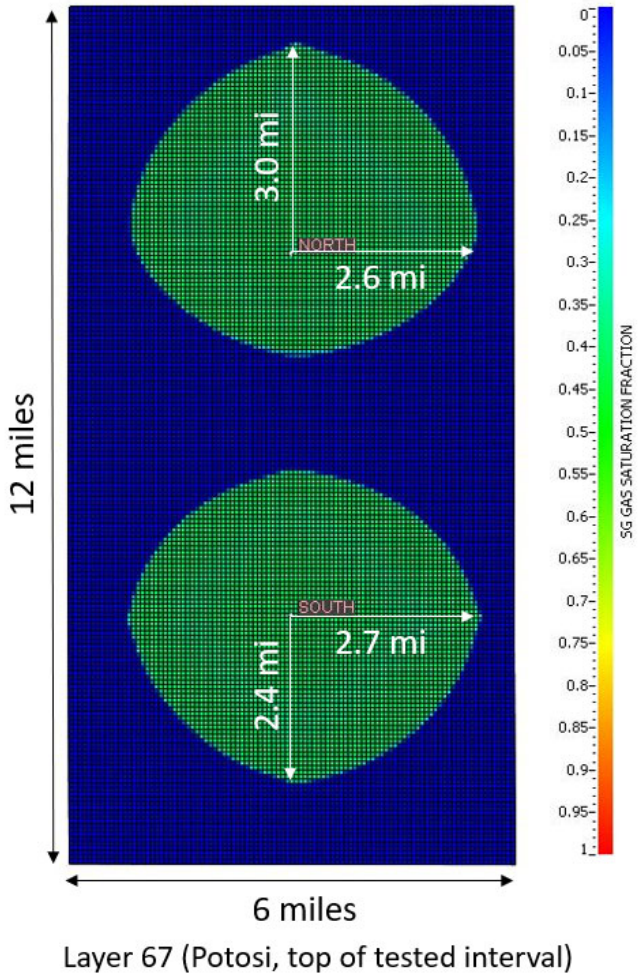

Figure 55. *Map view of the CO_2 plume after 30 years of injection at the simulation layer showing the largest plume extent (layer 67, within the Potosi).*

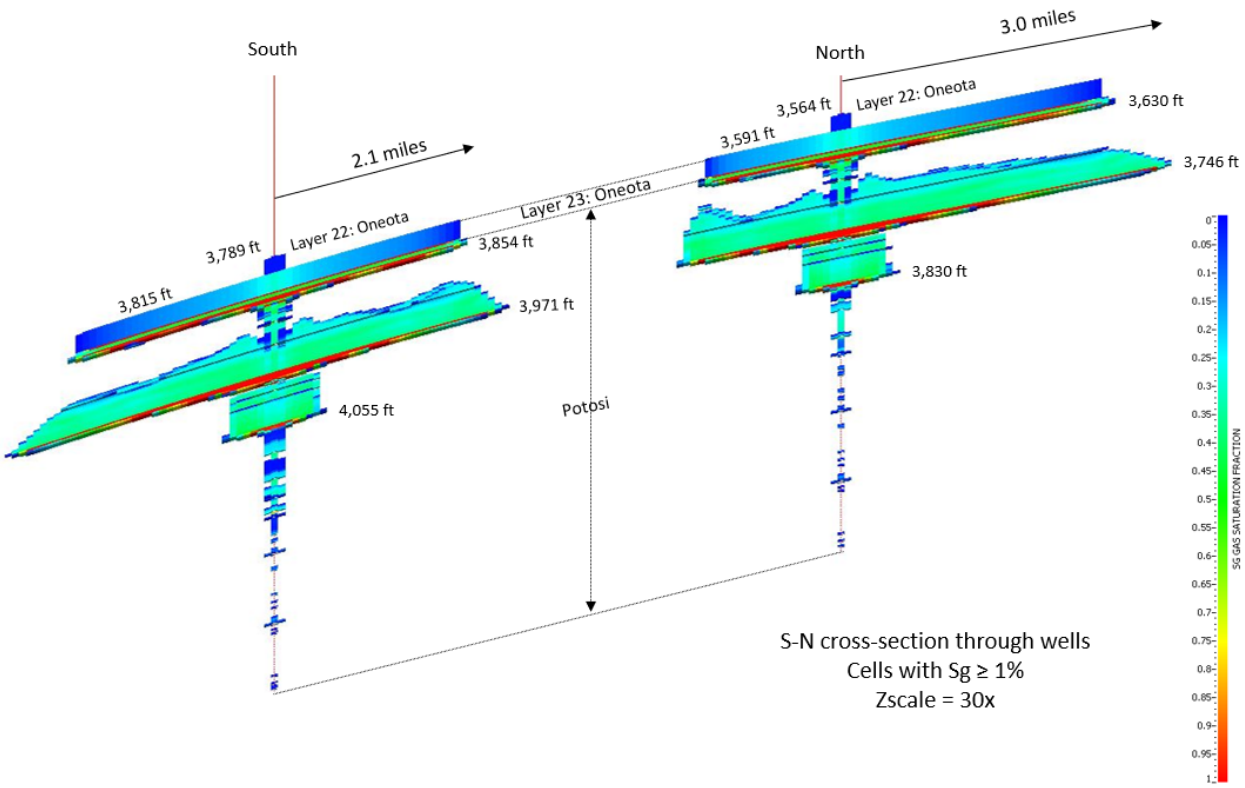

Figure 56. *South-North cross section through the injection wells, showing a cross section of the CO_2 plume after 30 years of injection. Only cells with gas saturation ≥ 1% are visible.*

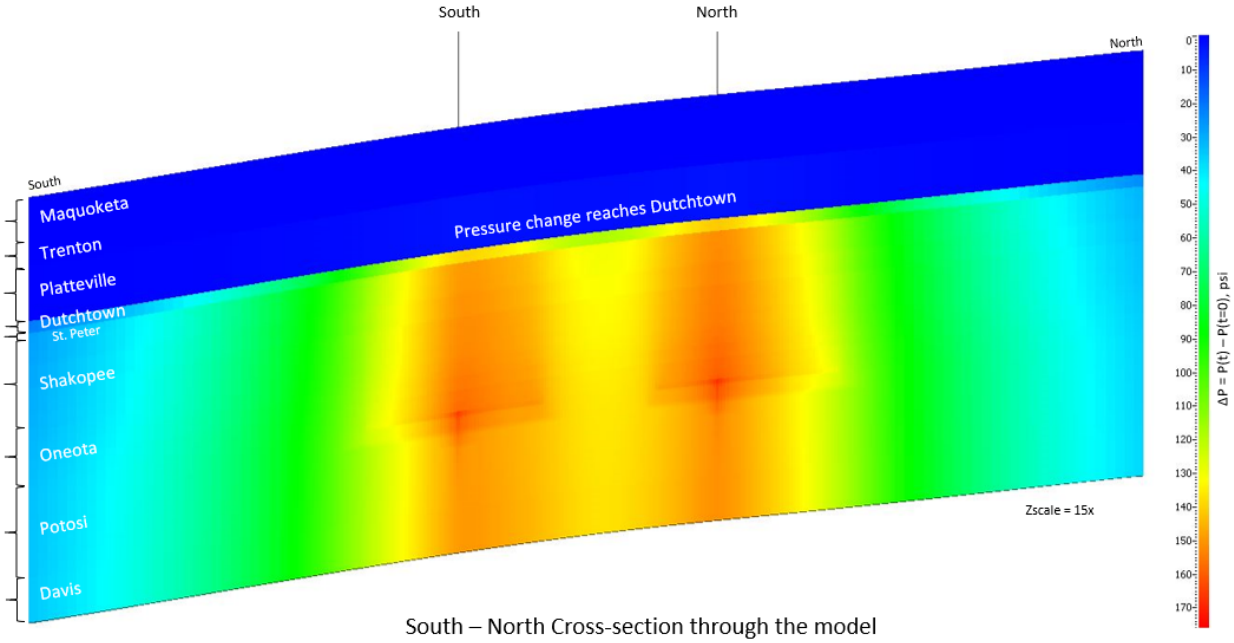

Figure 57. *South-North cross section through the wells showing the change in pressure (ΔP) after 30 years of injection.*

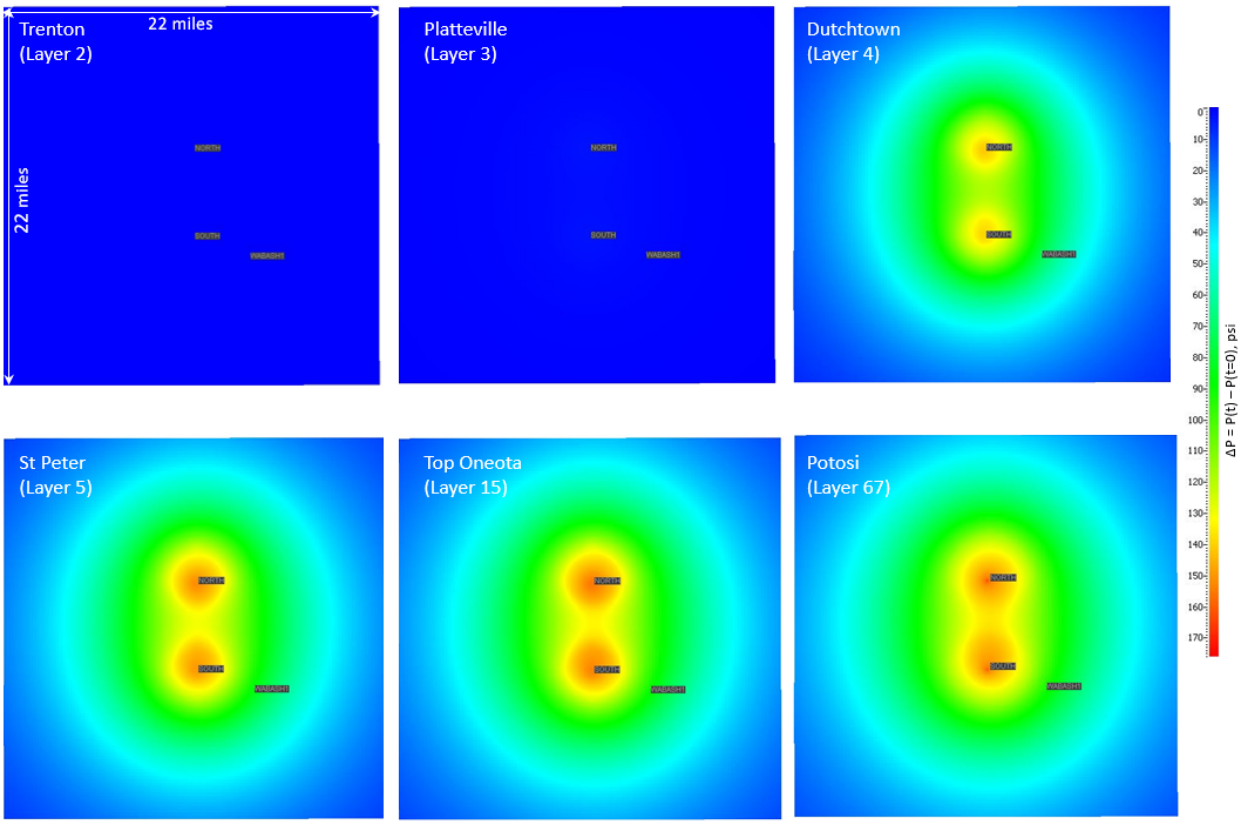

Figure 58. *ΔP maps, showing the change in pressure after 30 years of injection for several overburden formations and the Potosi (layer 67).*

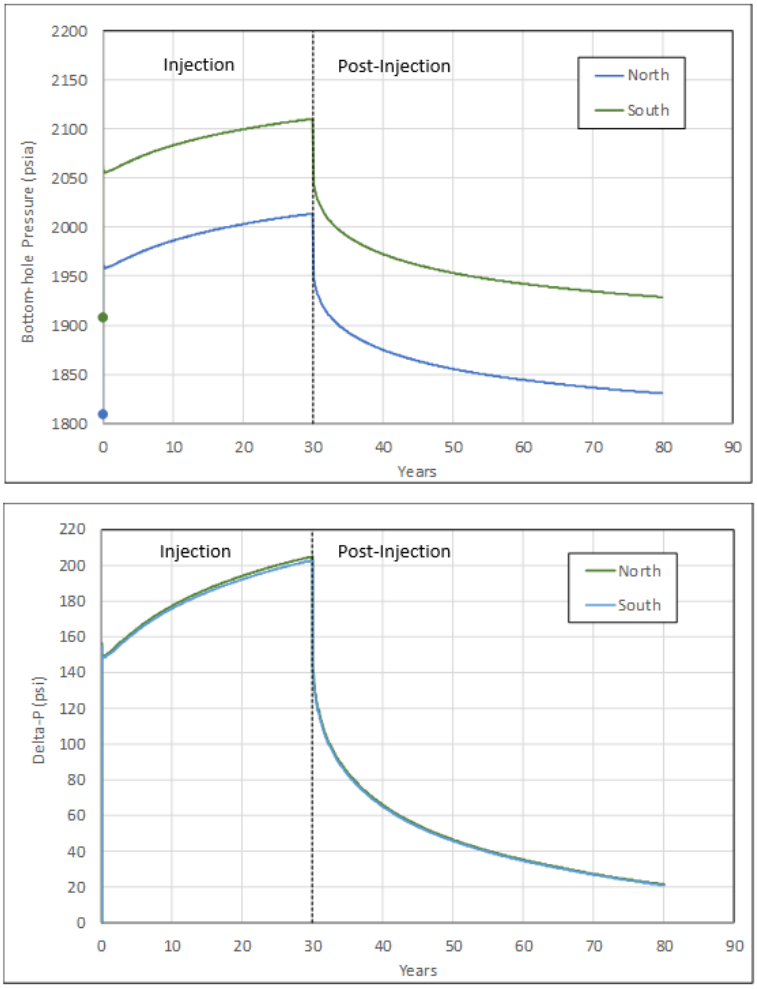

Figure 59. *Well BHP and pressure change (ΔP) vs. time for North and South during the 30 year injection period and the 50 year post injection observation period.*

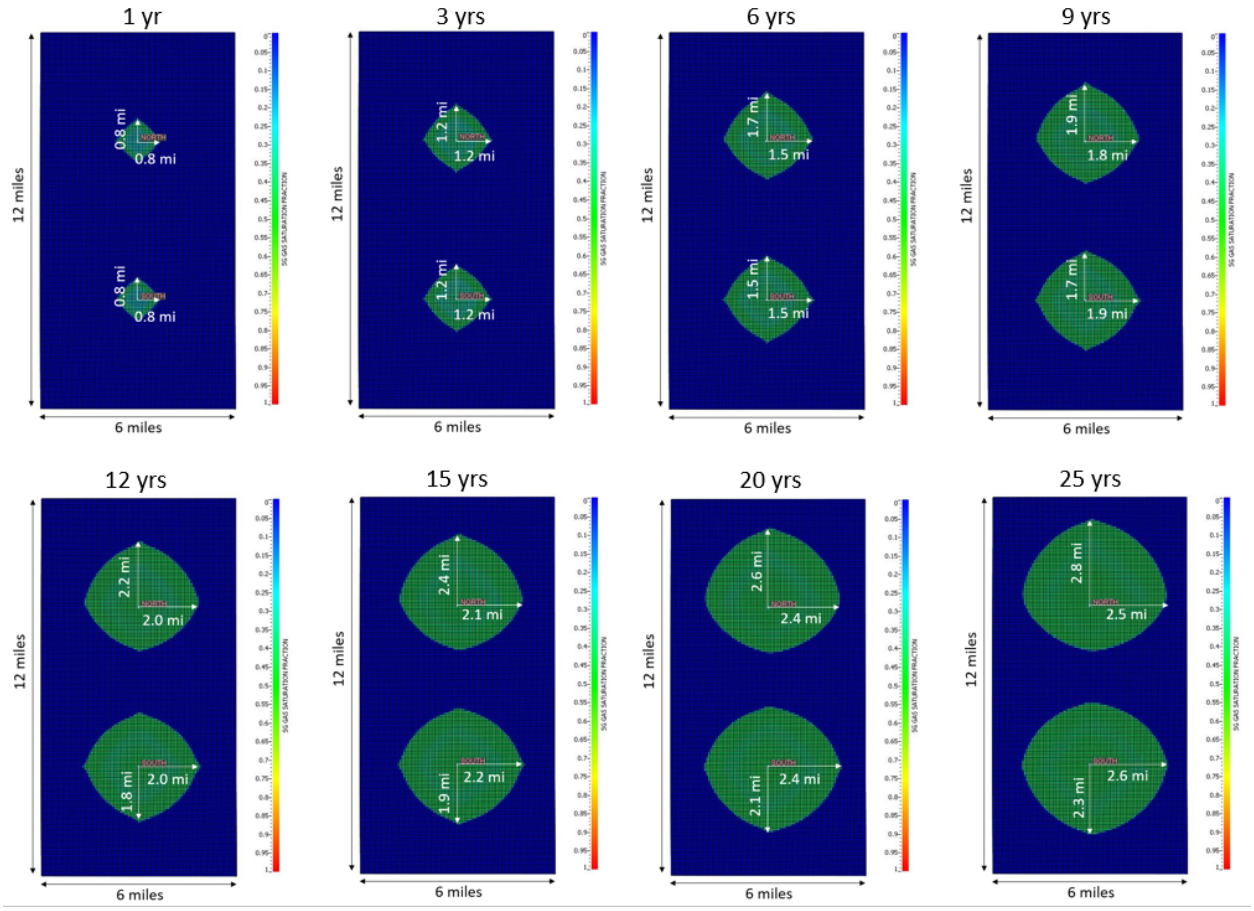

Figure 60. *Map view of the CO_2 plume vs. time at the simulation layer showing the largest plume extent (layer 67, within the Potosi) at 1, 3, 6, 9, 12, 15, 20 and 25 years.*

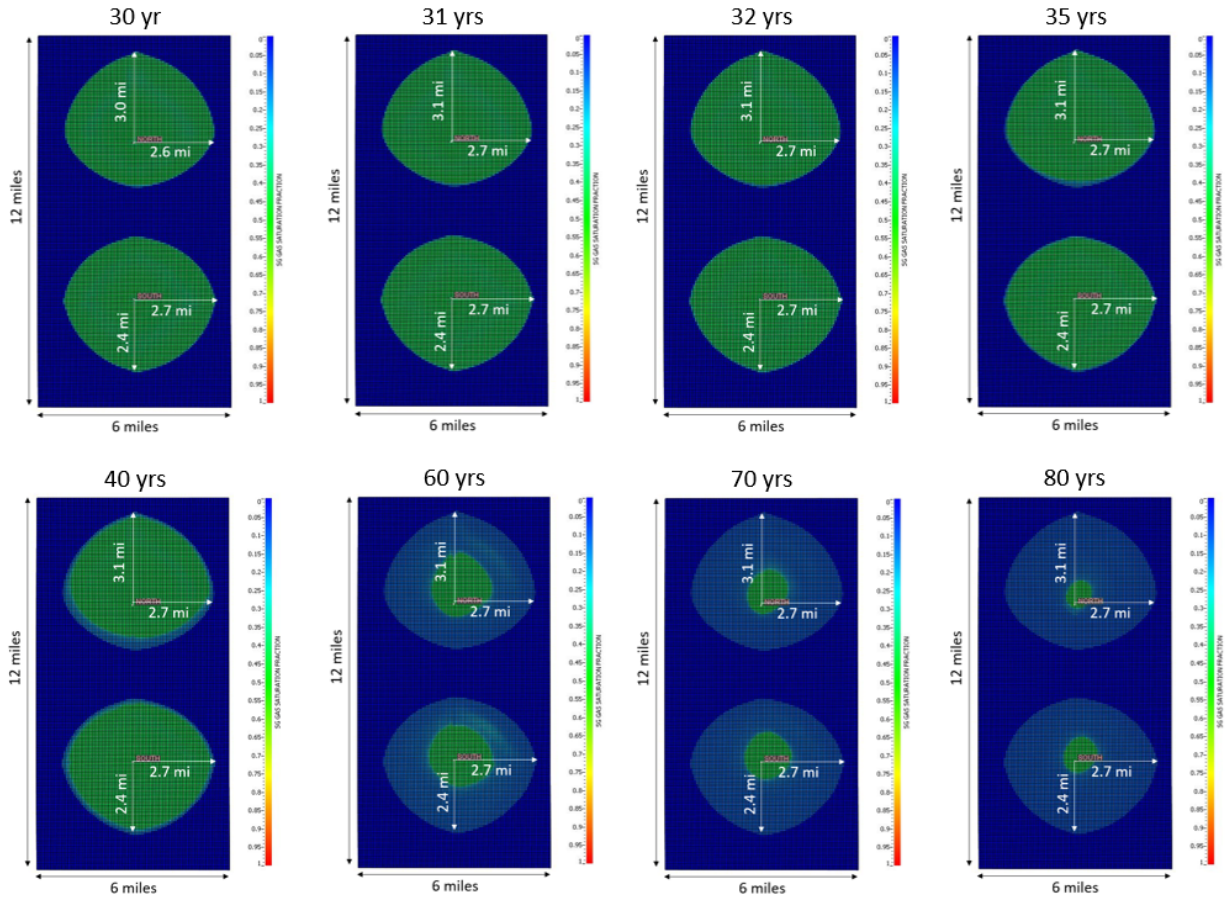

Figure 61. *Map view of the CO_2 plume vs. time at the simulation layer showing the largest plume extent (layer 67, within the Potosi) at 30, 31, 32, 35, 40, 60, 70 and 80 years.*

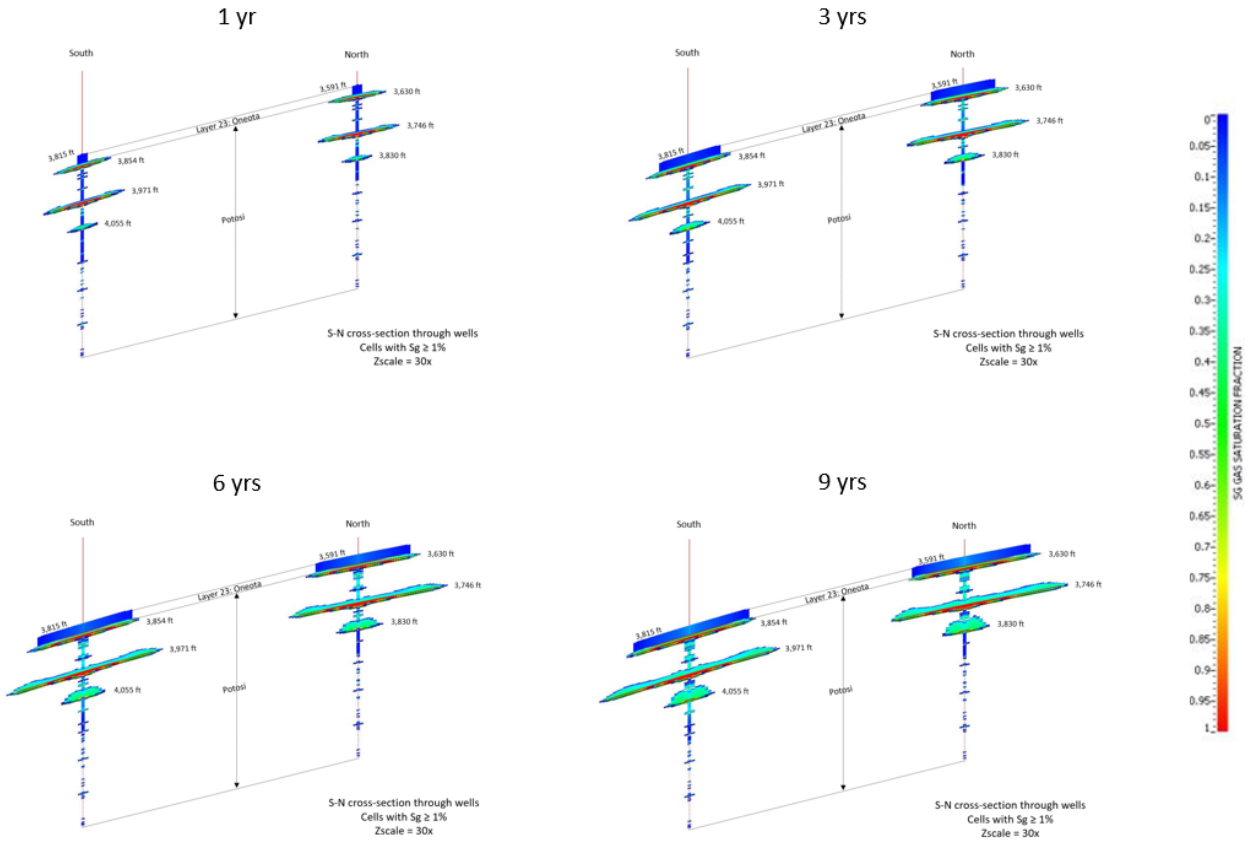

Figure 62. *South-North cross section through the injection wells, showing the CO_2 plume vs. time at 1, 3, 6 and 9 years. Only cells with gas saturation ≥ 1% are visible.*

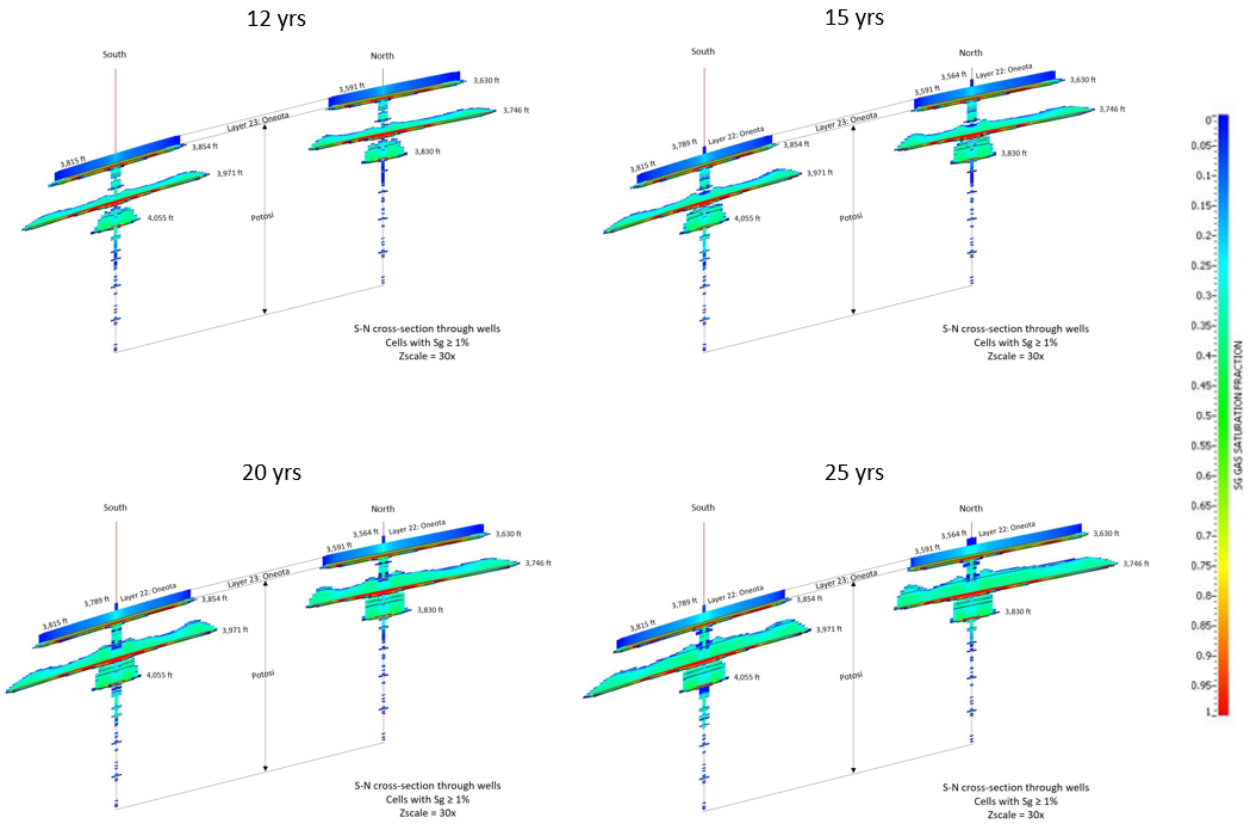

Figure 63. *South-North cross section through the injection wells, showing the CO_2 plume vs. time at 12, 15, 20 and 25 years. Only cells with gas saturation ≥ 1% are visible.*

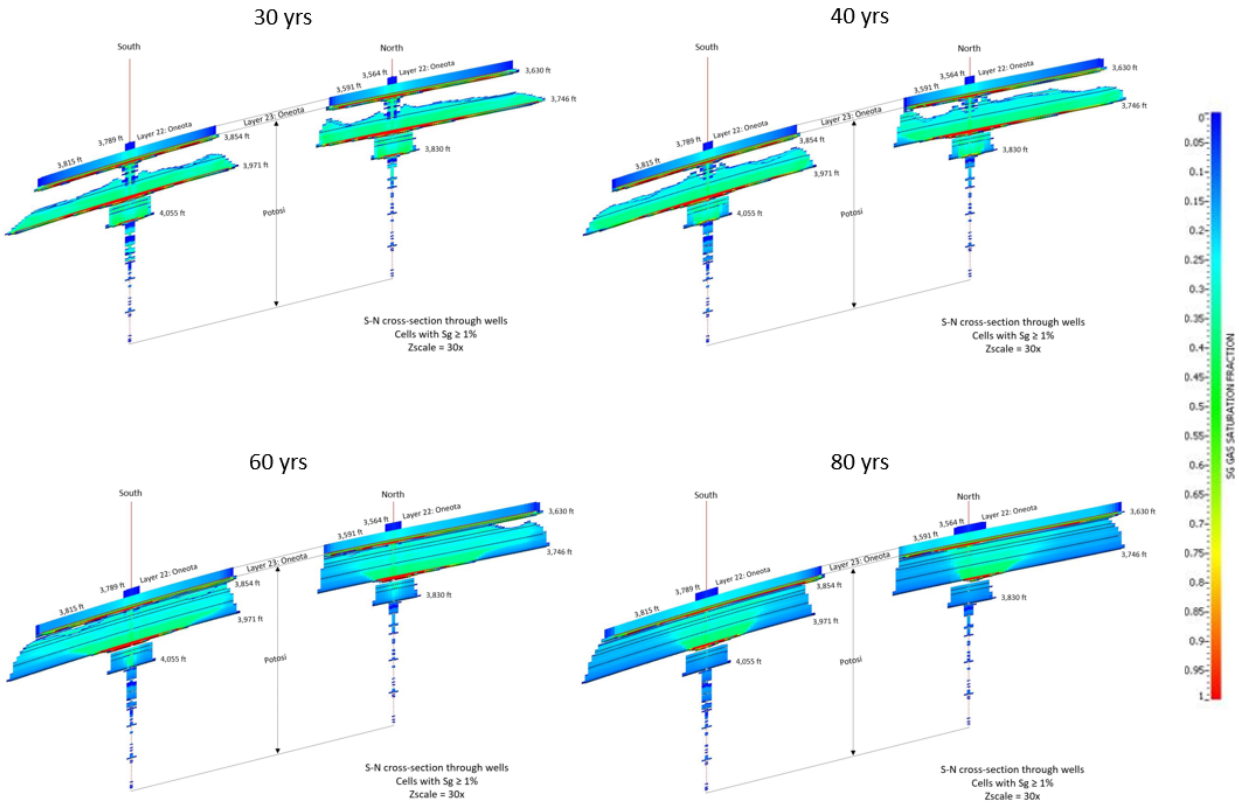

Figure 64. *South-North cross section through the injection wells after 30 years of injection, showing the CO_2 plume vs. time at 30, 40, 60 and 80 years. Only cells with gas saturation ≥ 1% are visible.*

3.2.4.2 Two well injection of 1.67 MMTA of CO_2 for 12 years

This simulation scenario is a two well injection of 1.67 MMTA of CO_2 for 12 years. CO_2 is injected in both North and South simultaneously for 12 years, followed by a 50 year post injection observation period. Each well injects 0.835 MMTA, which is ½ of the total injection rate. The total volume of CO_2 injected after 12 years is 20 MMtonnes. The injection wells are 5 miles apart and there is a 12 x 6 mile refined grid region around the two injection wells, identical to the 30 year injection case described in the previous section (see Figure 54).

Figure 65 shows the CO_2 plume after 12 years of injection at the layer having the greatest plume extent, layer 67 within the Potosi interval at the top of the tested vuggy interval. The plume shows some impact of well interference and of reservoir dip. Largest dimensions of the plume are denoted on the plumes. The North plume extends the furthest, 2.2 miles to the North. Both plumes extend 2 miles to the east. Figure 66 contains a South-North cross section through the injection wells and shows the CO_2 plume after 12 years of injection. Only simulation cells having gas saturation values ≥ 1% are visible. The asymmetric lateral shape of the plume shows the impact of well interference and reservoir dip. The vertical scale has been exaggerated 30 times, as a result, the reservoir dip looks much larger than in reality. The majority of the CO_2 has entered the two highest-perm vuggy intervals within the Potosi. The plume has also migrated vertically into the bottom layer of the overlying Oneota formation.

Figure 67 contains a South-North cross section through the injection wells and shows the change in pressure (ΔP) after 12 years of injection. The highest increase in pressure is at the well locations and is approximately 150 psi. It is important to note that the pressure change only reaches the Dutchtown formation. The formations overlying the Dutchtown see a negligible increase in pressure due to 12 years of injection. Figure

68 contains maps of pressure increase (ΔP) after 12 years of injection at several layers within the model. These maps also illustrate that the pressure change stops at the Dutchtown formation.

Figure 69 contains plots of BHP and ΔP (= BHP at 12 years – initial pressure) vs. time for the two injection wells. The BHP at South is higher than the BHP at North due to reservoir dip. South is deeper than North by approximately 225 ft. The BHP at both wells increases by approximately 180 psi after 12 years of injection. After injection stops at 12 years, the BHP shows a rapid initial drop and then slowly decreases over time towards the initial pressure. Fifty years after injection stopped, the BHP is within 10 psi of initial pressure. The maximum BHP for both wells after 12 years of injection (1,900 psia and 2,087 psia for North and South, respectively) is significantly below the maximum BHP (90% of fracture pressure), which is 2,672 psia and 2,816 psia for North and South; respectively.

Figure 70 and

Figure *71* show map views of the CO_2 plume within the Potosi, at layer 67 (which is the top of the tested vuggy interval) vs. time. Dimensions are denoted on both the North and South plumes. The plume shape starts to show the influence of interference between the wells after 3 years of injection, as evident by the difference in plume size and shape of the North and South plumes. Injection stops at 12 years, and the plume reaches its greatest lateral extent at the end of injection. The plume stabilizes laterally after 12 years and does not expand laterally during the remainder of the 50 year post injection observation period. However, vertical migration of the plume within the Potosi and into the bottom two layers of the overlying Oneota continues throughout the 50 year post injection observation period.

Figure 72 through Figure 74 contain South-North cross sections through the injection wells and show a cross section of the CO_2 plume vs. time. Only simulation cells having gas saturation ≥ 1% are visible. The top of the CO_2 plume only enters the two bottom layers of the overlying Oneota. No CO_2 enters any overburden formations above the Oneota. Some vertical migration of the plume within the Potosi and into the lower Oneota is observed during the 12 year injection period, but substantial vertical migration of the plume within the Potosi is observed during the 50 year post injection observation period.

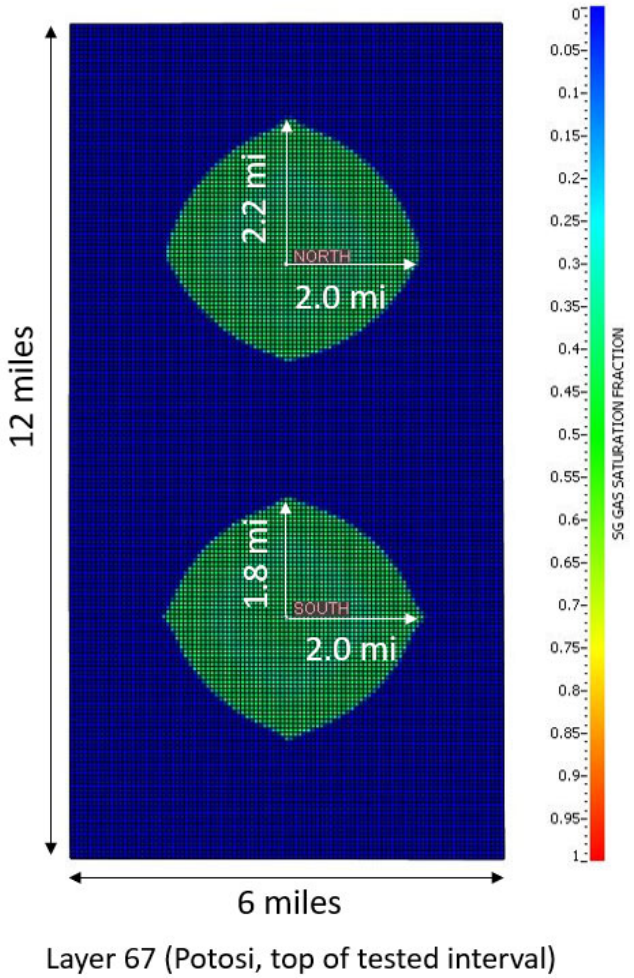

Figure 65. *Map view of the CO_2 plume after 12 years of injection at the simulation layer showing the largest plume extent (layer 67, within the Potosi).*

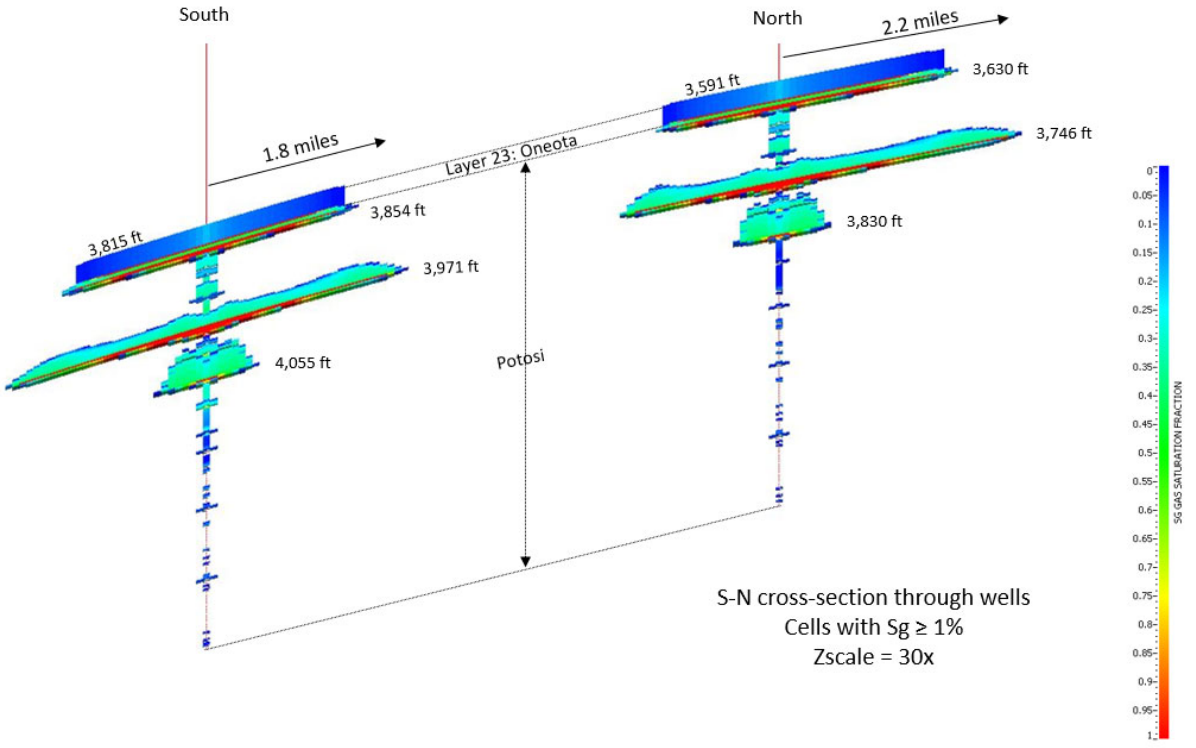

Figure 66. *South-North cross section through the injection wells, showing the CO_2 plume after 12 years of injection. Only cells with gas saturation ≥ 1% are visible.*

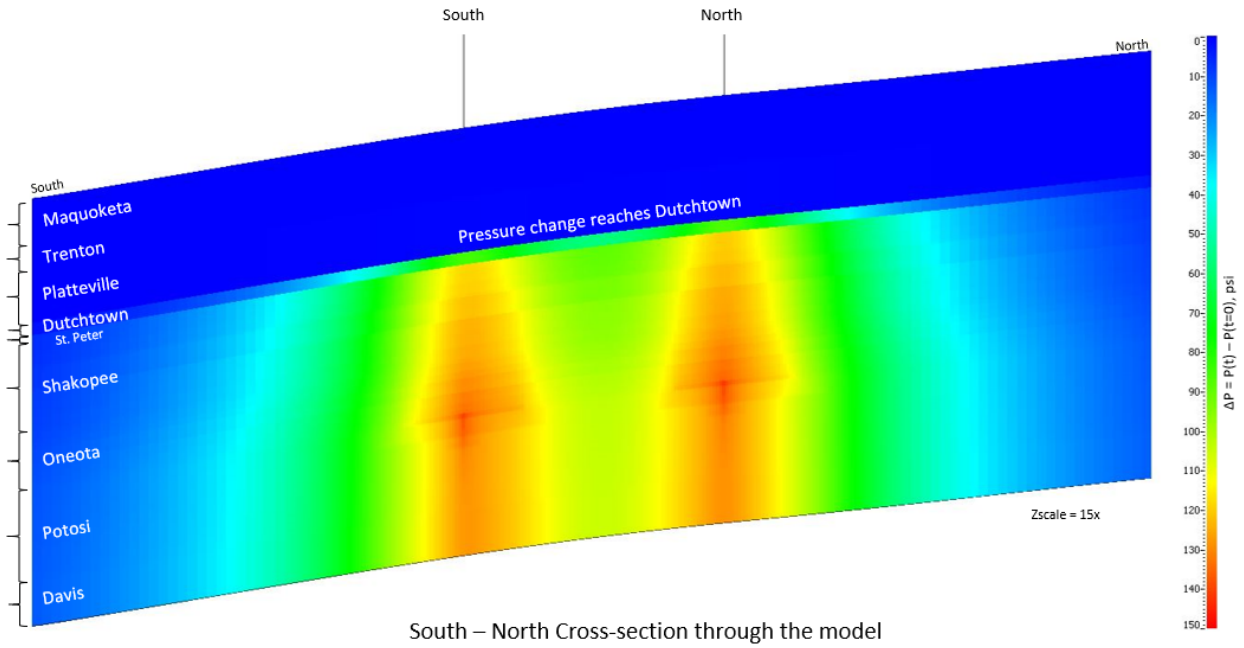

Figure 67. *South-North cross section through the wells showing the change in pressure (ΔP) after 12 years of injection.*

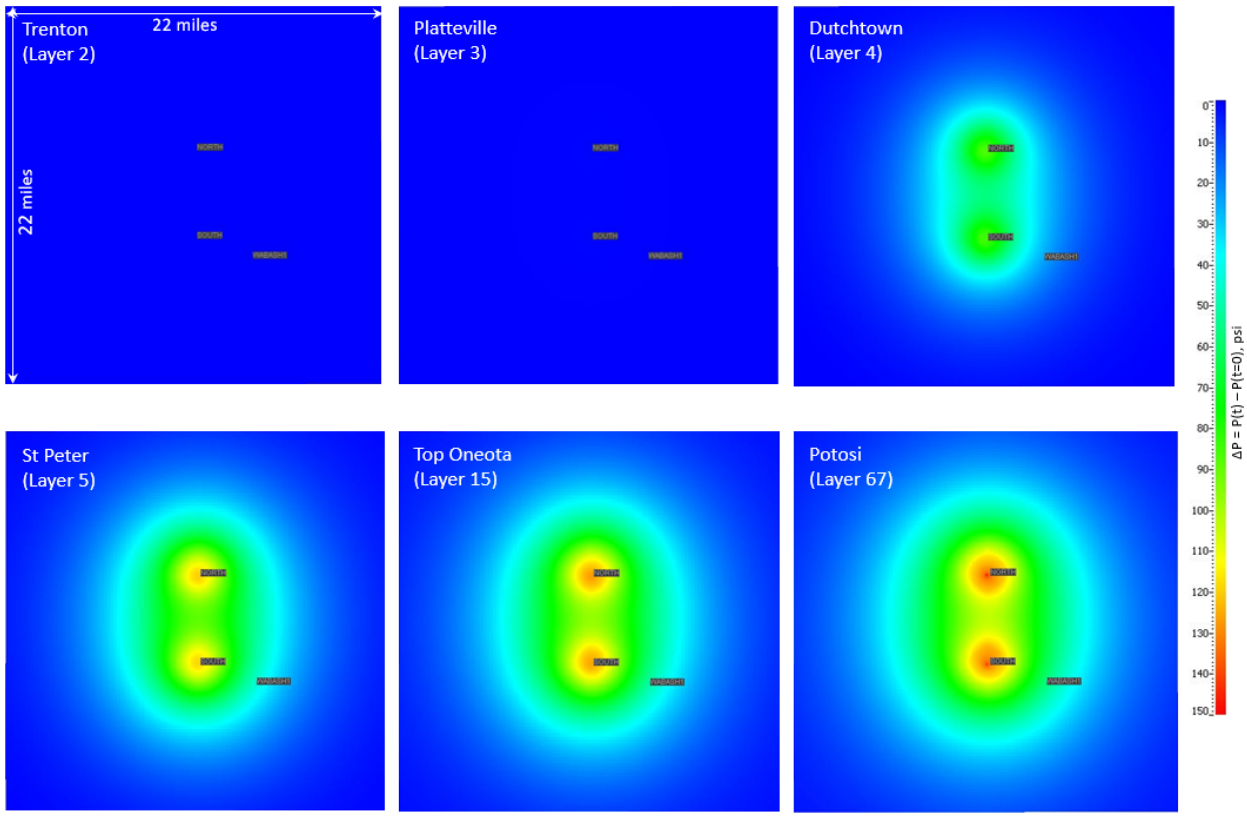

Figure 68. *ΔP maps, showing the change in pressure after 12 years of injection for several overburden formations and the Potosi (layer 67).*

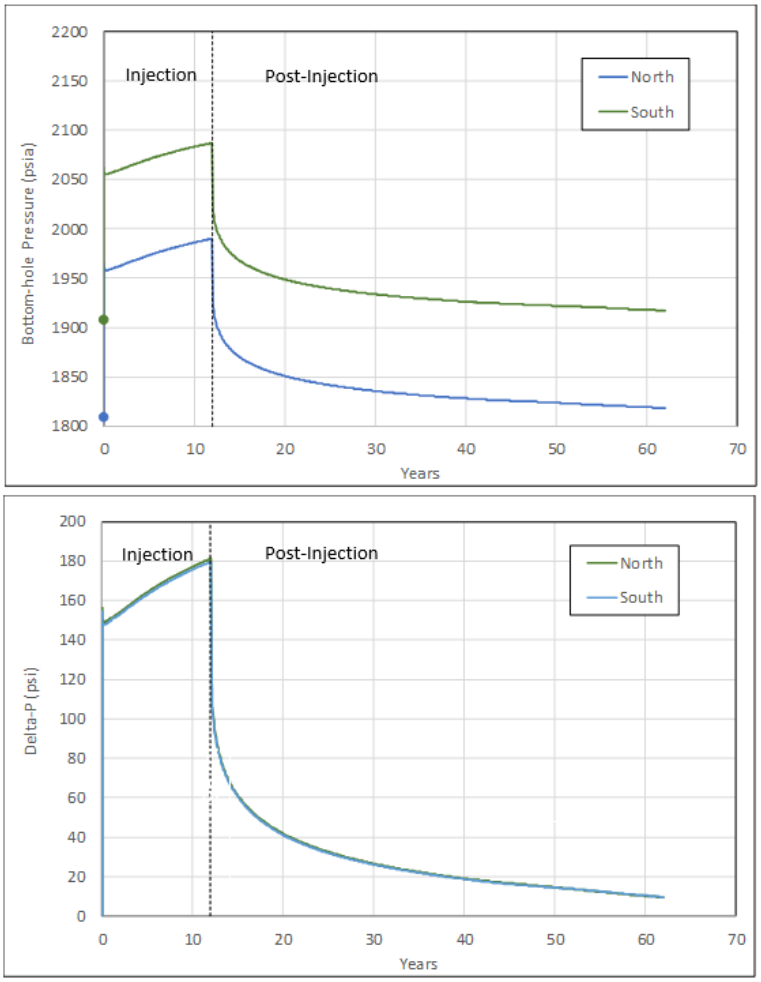

Figure 69. *Well BHP and pressure change (ΔP) vs. time for North and South during the 12 year injection period and the 50 year post injection observation period.*

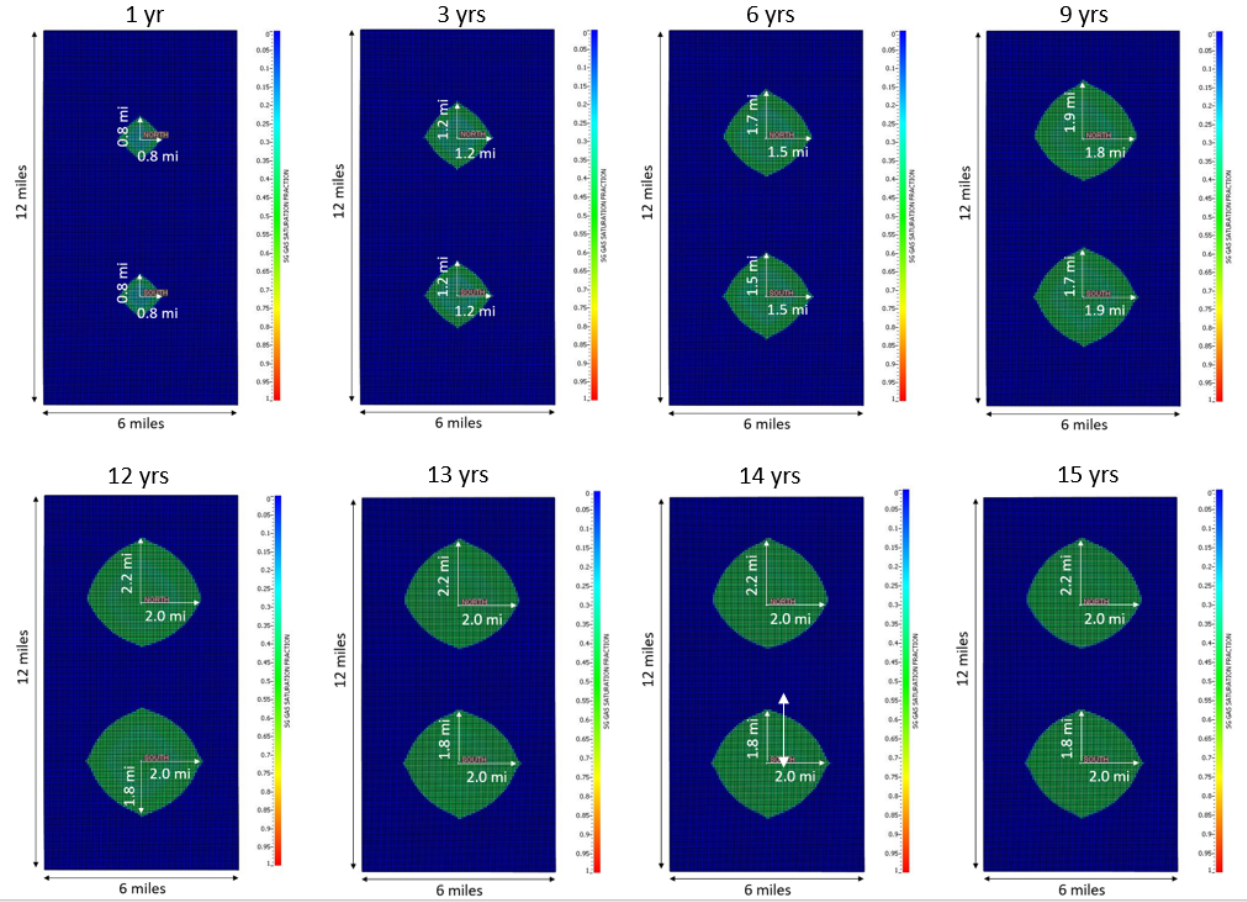

Figure 70. *Map view of the CO_2 plume vs. time at the simulation layer showing the largest plume extent (layer 67, within the Potosi) at 1, 3, 6, 9, 12, 13, 14 and 15 years.*

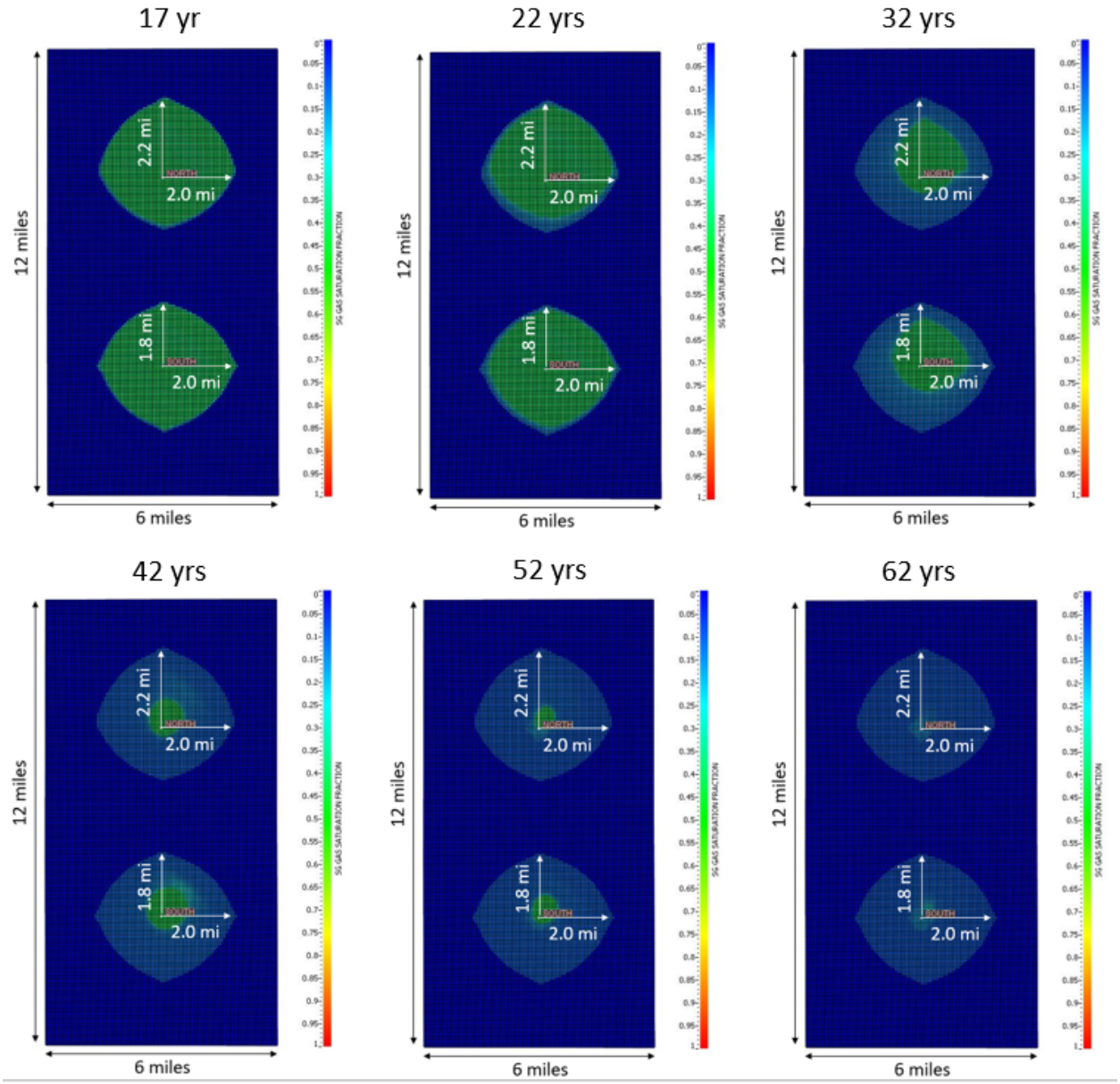

Figure 71. *Map view of the CO_2 plume vs. time at the simulation layer showing the largest plume extent (layer 67, within the Potosi) at 17, 22, 32, 42, 52 and 62 years.*

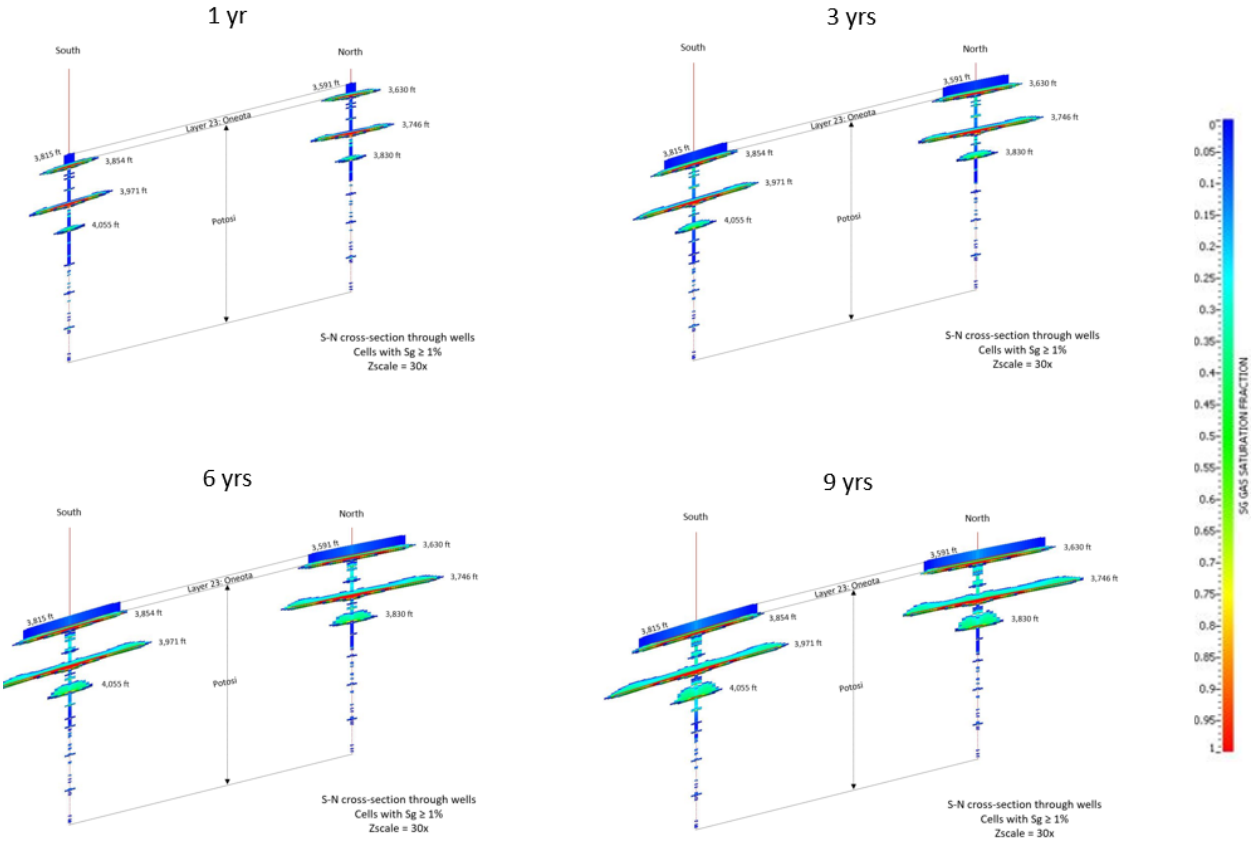

Figure 72. *South-North cross section through the injection wells, showing the CO_2 plume vs. time at 1, 3, 6 and 9 years. Only cells with gas saturation ≥ 1% are visible.*

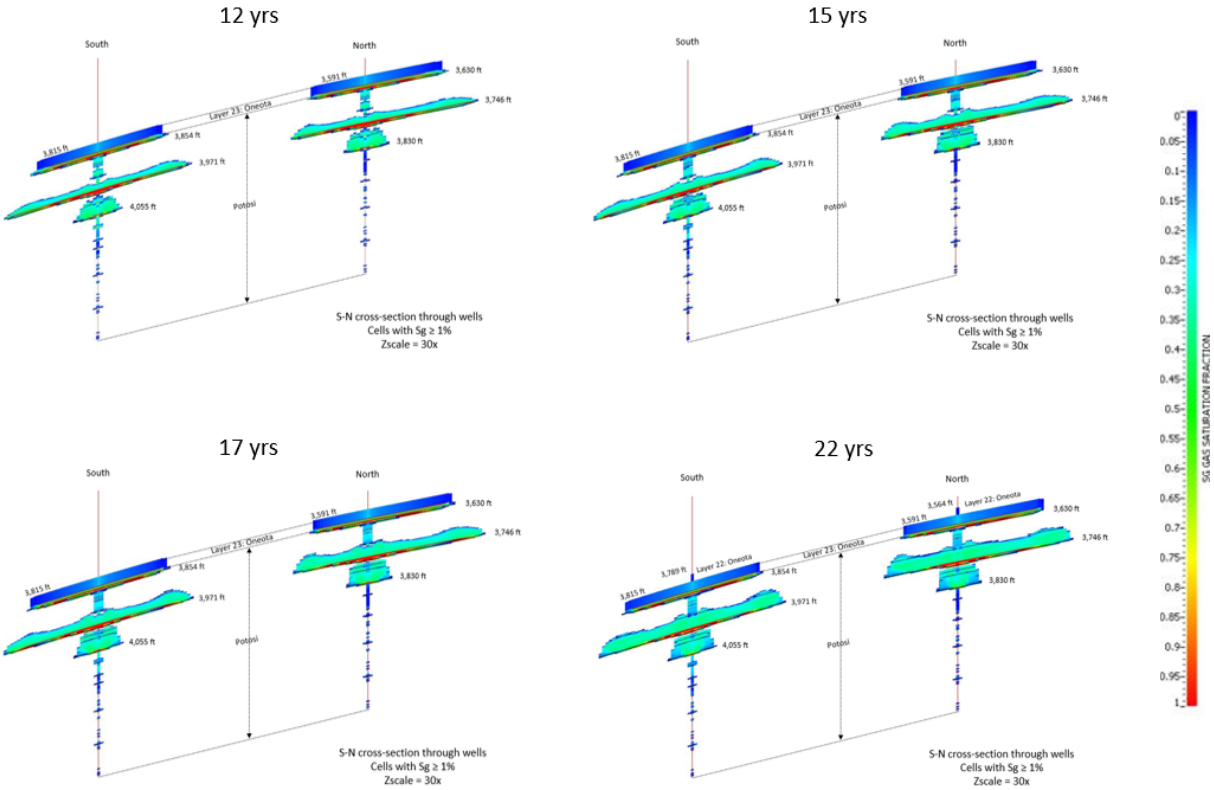

Figure 73. *South-North cross section through the injection wells, showing the CO_2 plume vs. time at 12, 15, 17 and 22 years. Only cells with gas saturation ≥ 1% are visible.*

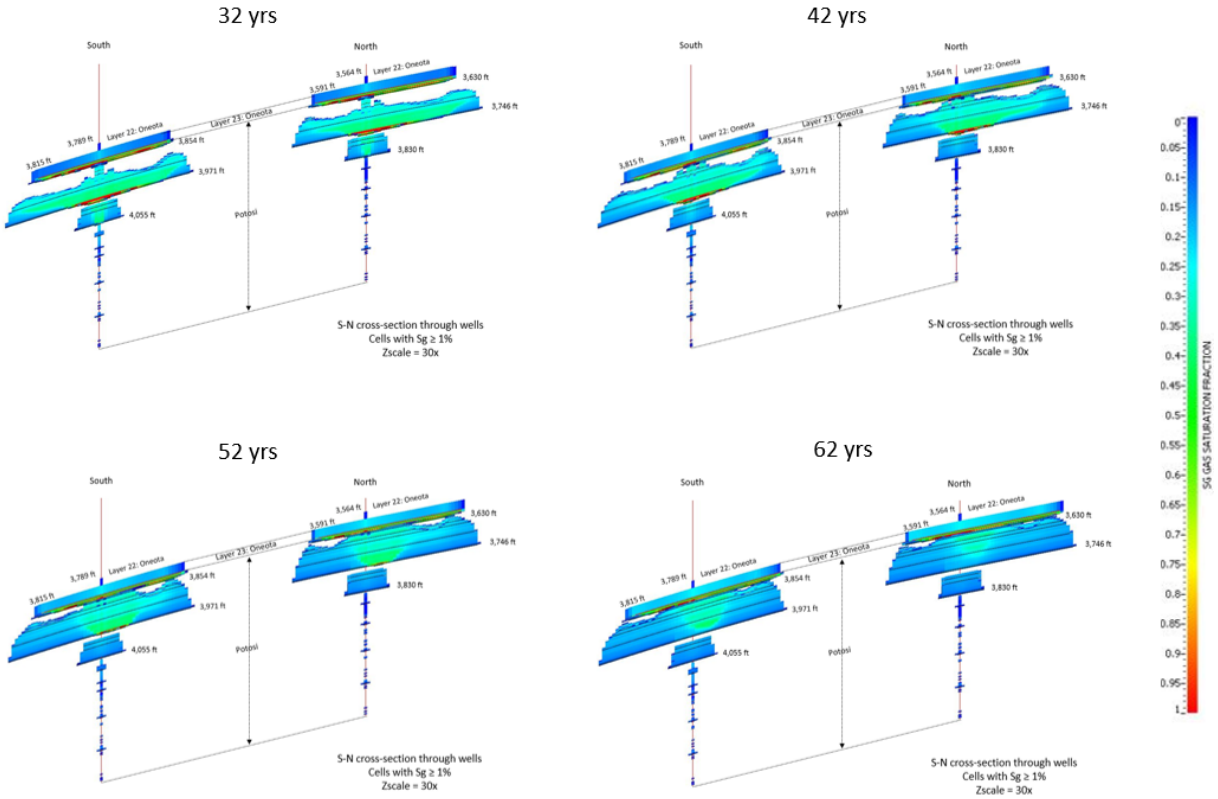

Figure 74. *South-North cross section through the injection wells, showing the CO_2 plume vs. time at 32, 42, 52 and 62 years. Only cells with gas saturation ≥ 1% are visible.*

3.2.4.3 Single well injection of 1.67 MMTA of CO_2 into Wabash #1 for 30 years

This simulation scenario is a single well injecting 1.67 MMTA of CO_2 for 30 years. CO_2 is injected in Wabash #1 (Wabash1) for 30 years, followed by a 50 year post injection observation period. The total volume of CO_2 injected after 30 years is 50 MMtonnes. There is an 8.5 x 8.5 mile refined grid region around the injection well, as shown in Figure 75.

Figure 76 shows the CO_2 plume after 30 years of injection at the layer having the greatest plume extent, layer 67 within the Potosi interval at the top of the tested vuggy interval. The largest dimensions of the plume are denoted. The plume extends furthest to the North and to the east of Wabash #1 at 3.8 and 3.6 miles; respectively. Figure 77 contains a South-North cross section through Wabash #1, and shows the CO_2 plume after 30 years of injection. Only simulation cells having gas saturation values ≥ 1% are visible. The asymmetric lateral shape of the plume shows the impact of reservoir dip. The vertical scale has been exaggerated 20 times, as a result, the reservoir dip looks much larger than in reality. The majority of the CO_2 has entered the two highest-perm vuggy intervals within the Potosi. The plume has migrated vertically and has entered the three bottom layers of the overlying Oneota formation; though a majority of the CO_2 in the Oneota is located in the bottommost layer of the Oneota.

Figure 78 contains a South-North cross section through Wabash #1, and shows the change in pressure (ΔP) after 30 years of injection. The highest increase in pressure is at the well location and is approximately 230 psi. It is important to note that the pressure change only reaches the Dutchtown formation. The formations overlying the Dutchtown see a negligible increase in pressure due to 30 years of injection.

Figure 79 contains maps of pressure increase (ΔP) after 30 years of injection at several layers within the model. These maps also illustrate that the pressure change stops at the Dutchtown formation.

Figure 80 contains plots of BHP and ΔP (= BHP at 30 years – initial pressure) vs. time for Wabash #1. The BHP increases by approximately 282 psi after 30 years of injection. After injection stops at 30 years, the BHP shows a rapid initial drop and then slowly decreases over time towards the initial pressure. Fifty years after injection stopped, the BHP is within 20 psi of initial pressure. The maximum BHP, after 30 years of injection, is significantly below the maximum BHP (90% of fracture pressure), which is 2,804 psia.

Figure 81 and Figure 82 show map views of the CO_2 plume within the Potosi, at layer 67 (which is the top of the tested vuggy interval) vs. time. Dimensions are denoted on the CO_2 plumes. Injection stops at 30 years, and the plume reaches its greatest lateral extent at the end of injection. The plume stabilizes laterally after 30 years and does not expand laterally during the remainder of the 50 year post injection observation period. However, vertical migration of the plume within the Potosi and into the bottom three layers of the overlying Oneota continues throughout the 50 year post injection observation period.

Figure 83 through Figure 85 contain South-North cross sections through Wabash #1, and show a cross section of the CO_2 plume vs. time. Only simulation cells having gas saturation ≥ 1% are visible. The top of the CO_2 plume only enters the three bottom layers of the overlying Oneota. No CO_2 enters any overburden formations above the Oneota. Some vertical migration of the plume within the Potosi and into the lower Oneota is observed during the 30 year injection period, but substantial vertical migration of the plume within the Potosi and the lower Oneota is observed during the 50 year post injection observation period.

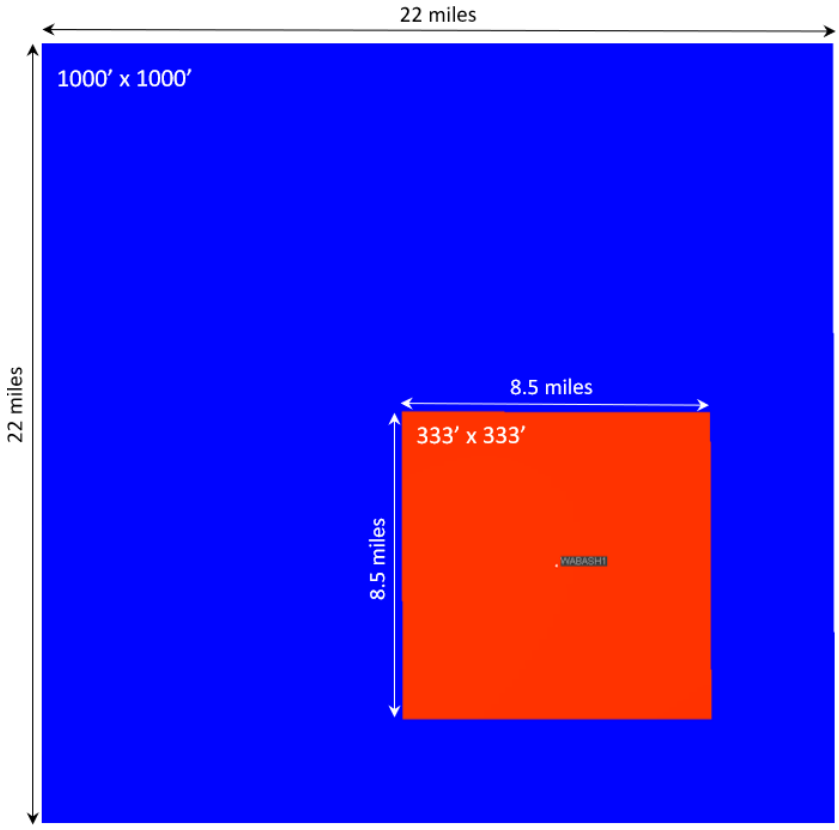

Figure 75. *Map view showing location of Wabash1, which is centered within an 8.5 x 8.5 mile refined grid region.*

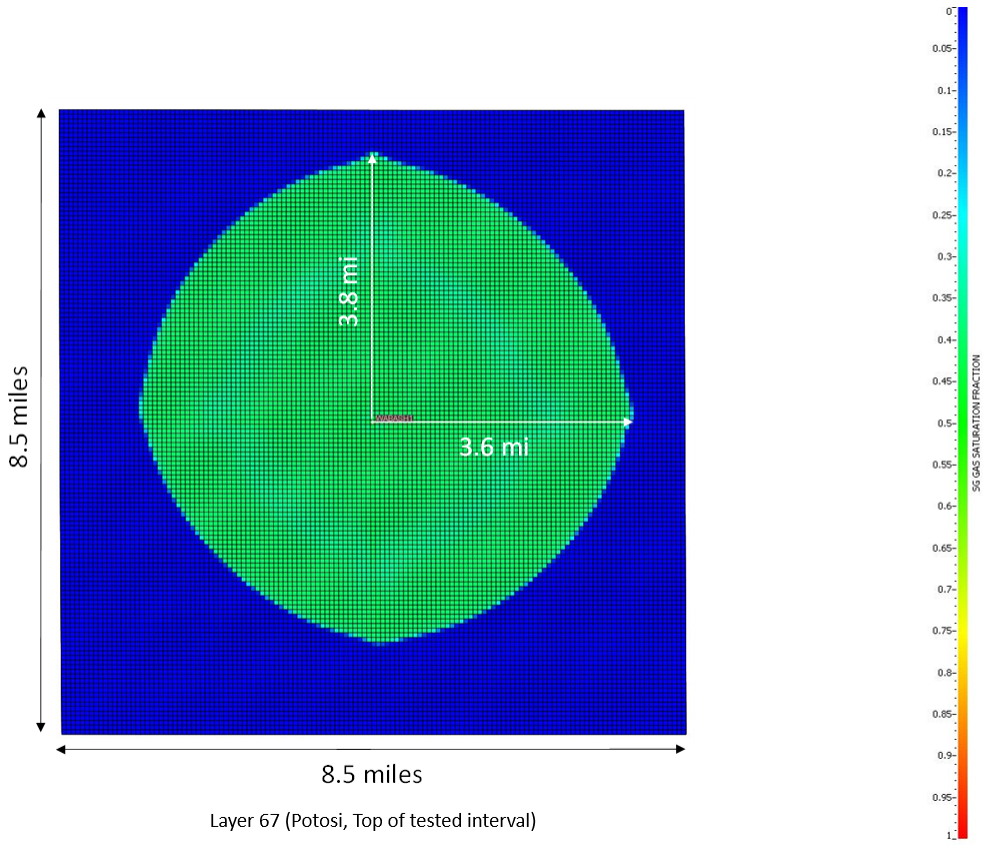

Figure 76. *Map view of the CO_2 plume after 30 years of injection at the simulation layer showing the largest plume extent (layer 67, within the Potosi).*

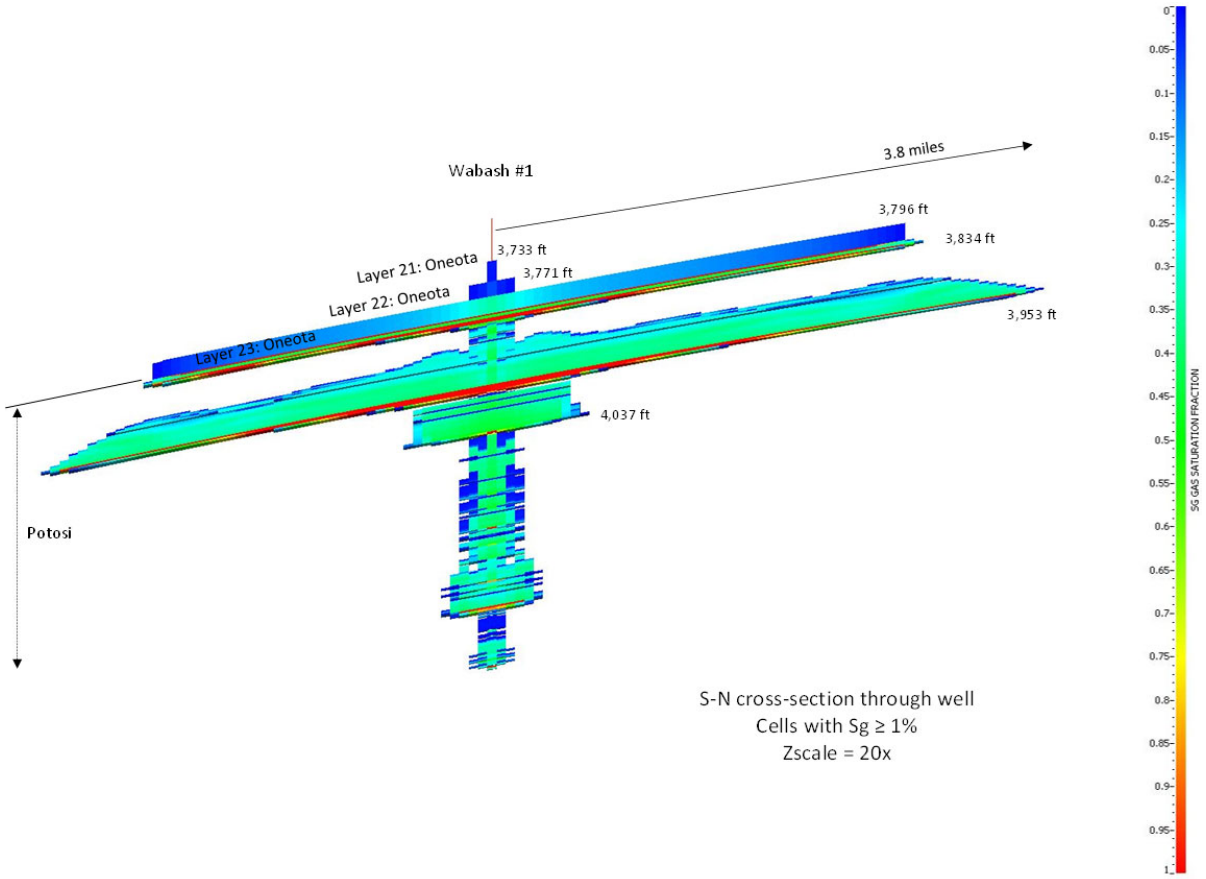

Figure 77. *South-North cross section through Wabash #1, showing the CO_2 plume after 30 years of injection. Only cells with gas saturation ≥ 1% are visible.*

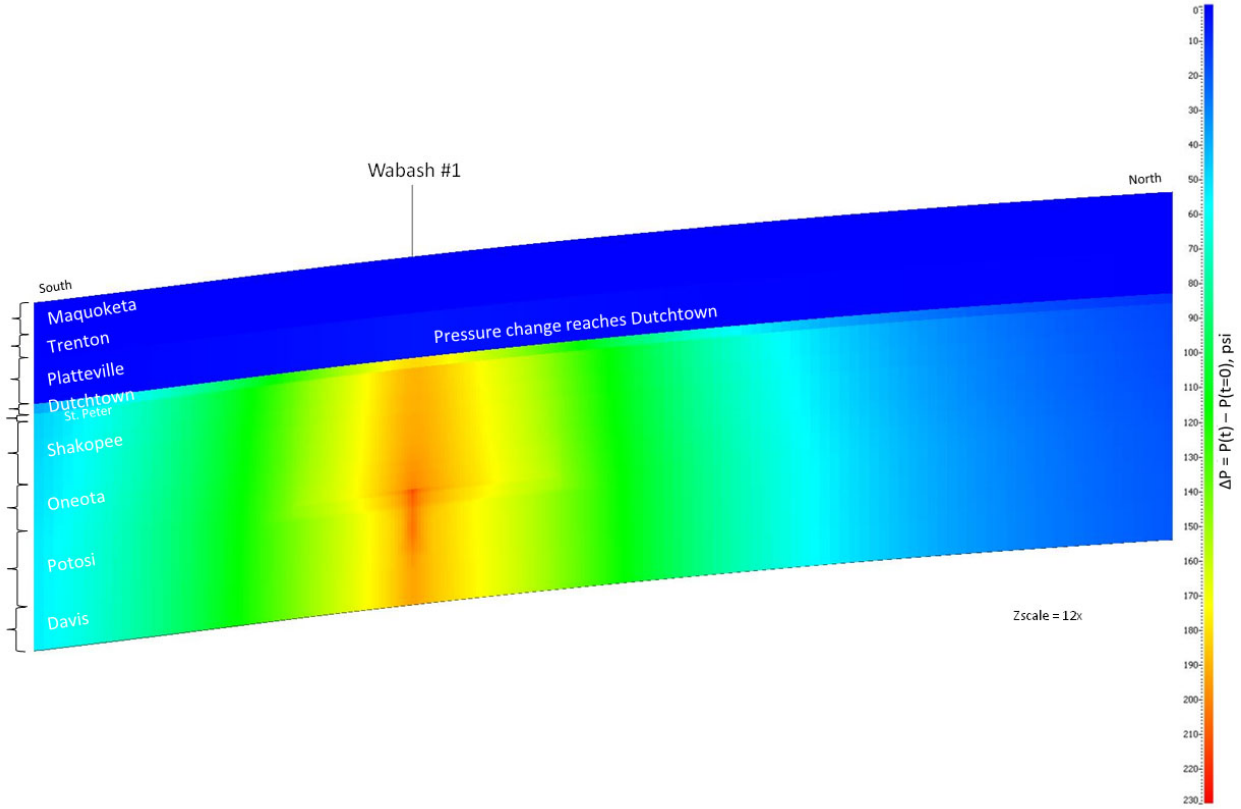

Figure 78. *South-North cross section through Wabash #1 showing the change in pressure (ΔP) after 30 years of injection.*

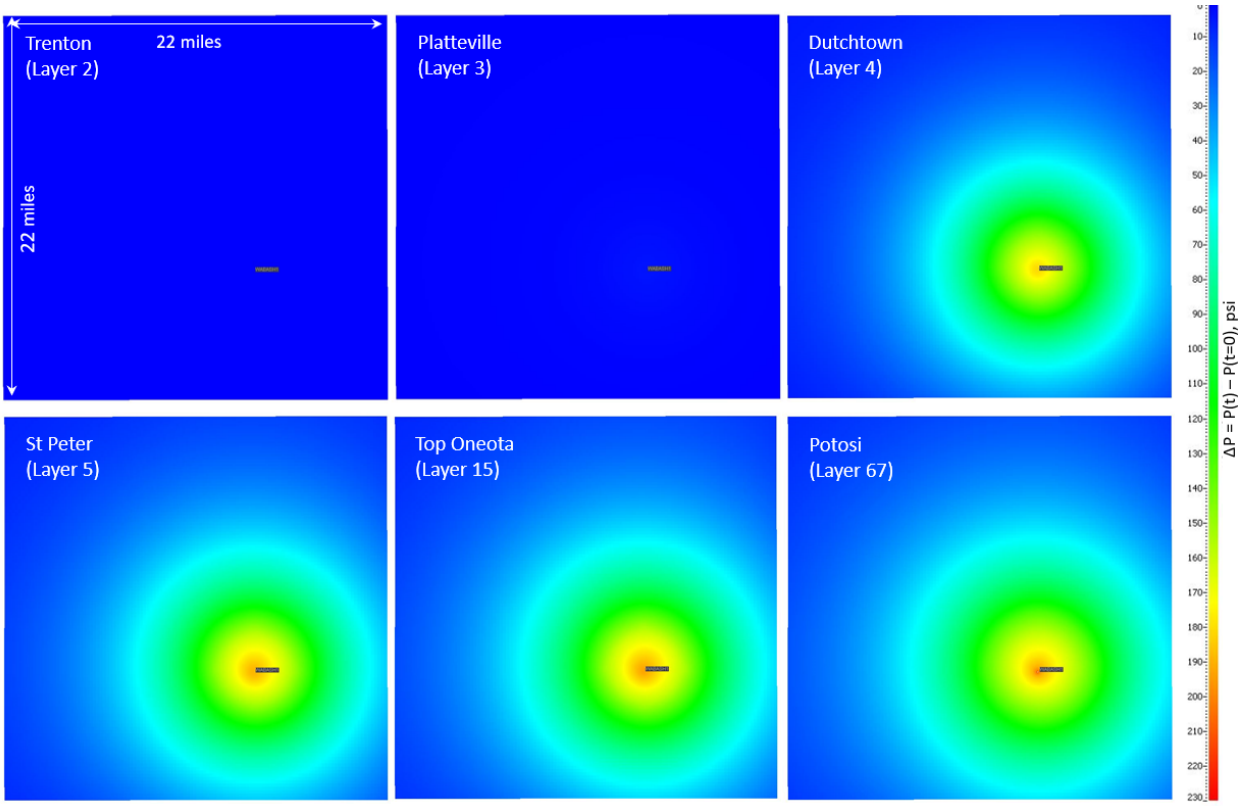

Figure 79. *ΔP maps, showing the change in pressure after 12 years of injection for several overburden formations and the Potosi (layer 67).*

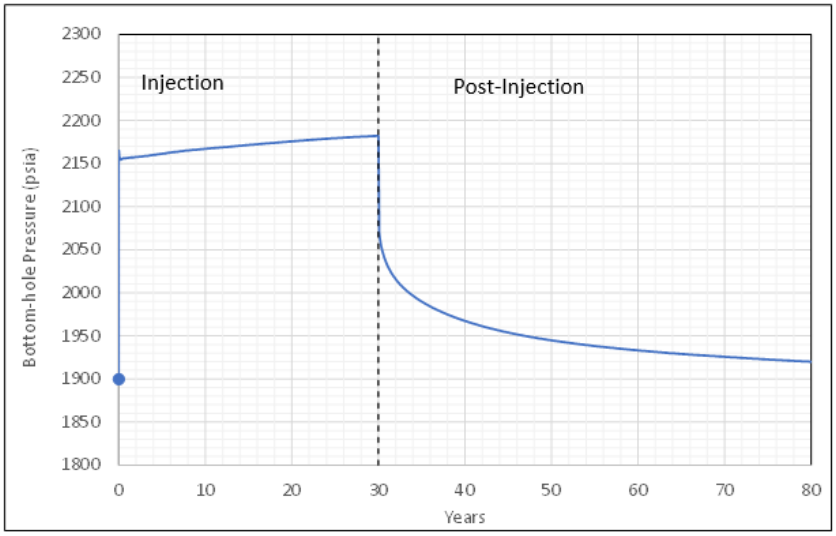

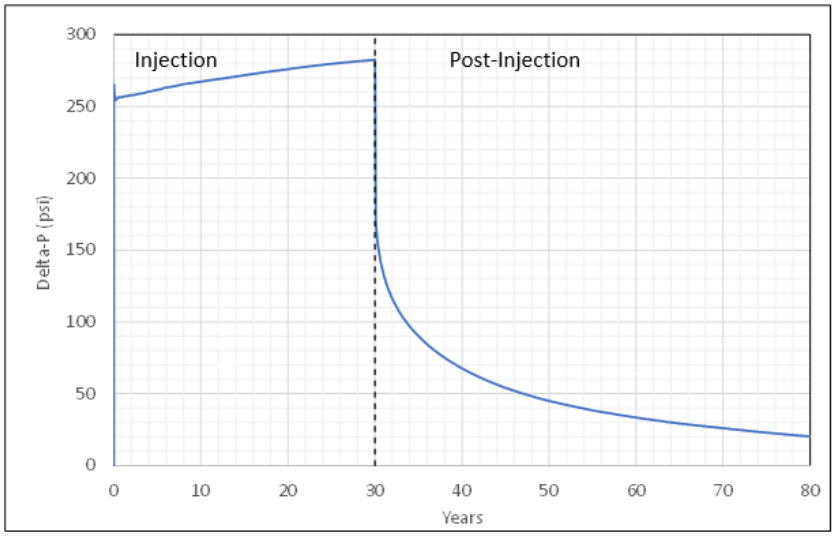

Figure 80. *Well BHP and pressure change (ΔP) vs. time for Wabash #1 during the 30 year injection period and the 50 year post injection observation period.*

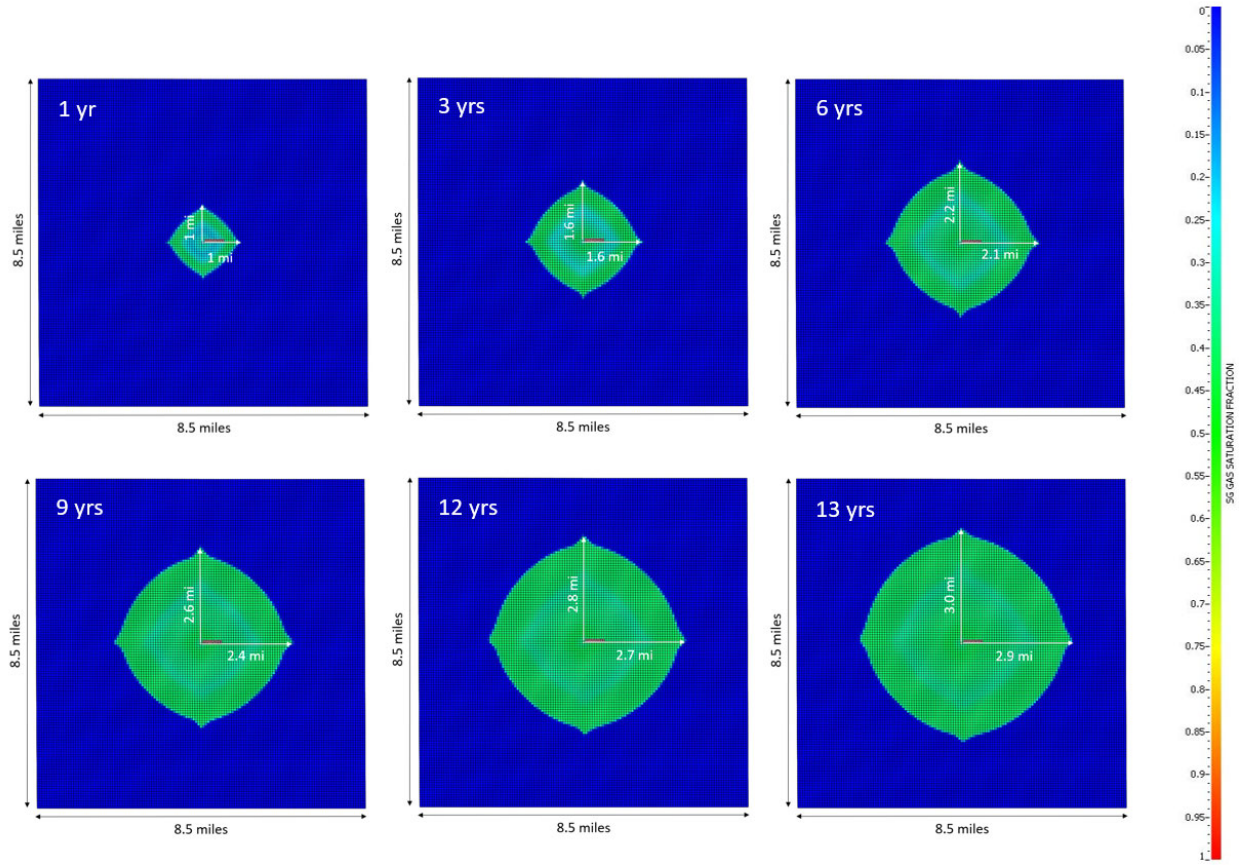

Figure 81. *Map view of the CO2 plume vs. time at the simulation layer showing the largest plume extent (layer 67, within the Potosi) at 1, 3, 6, 9, 12 and 13 years.*

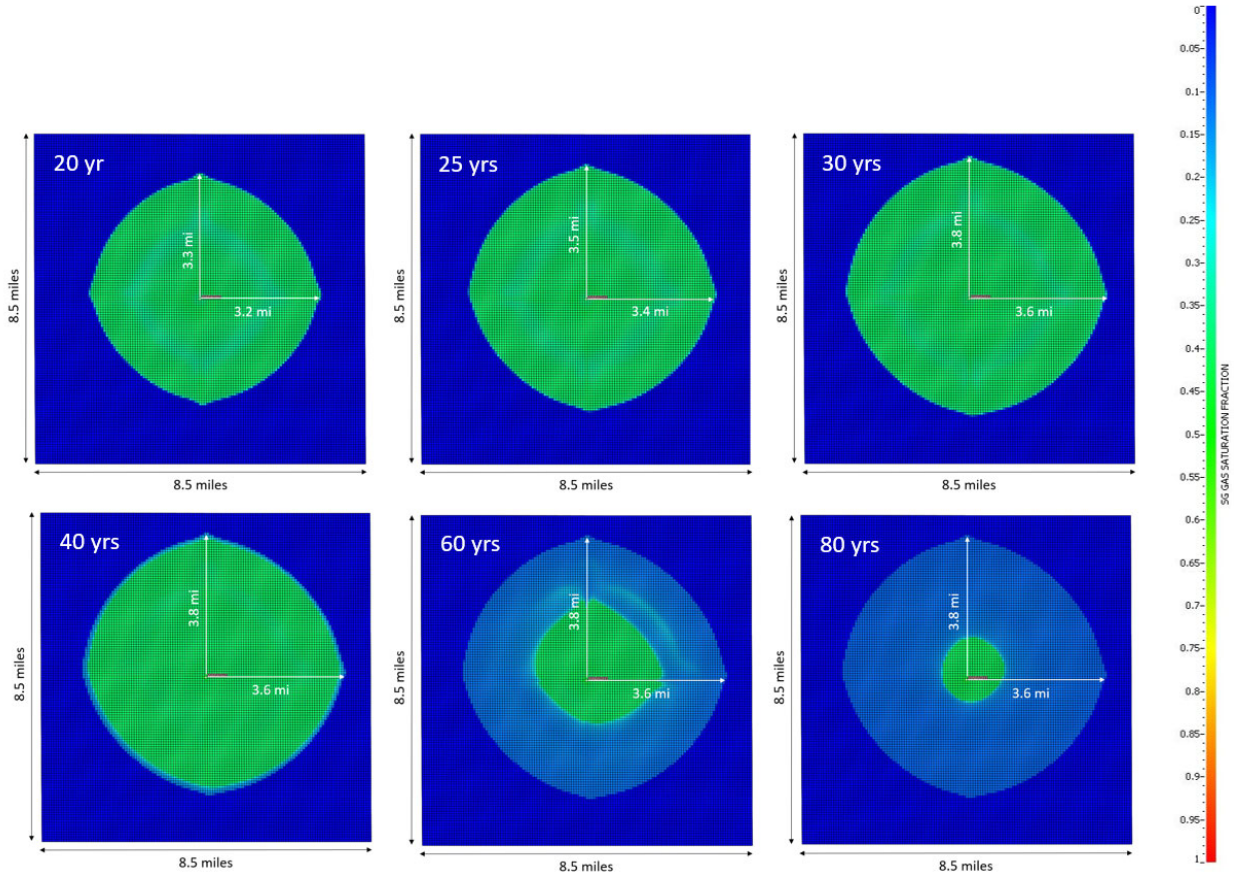

Figure 82. *Map view of the CO2 plume vs. time at the simulation layer showing the largest plume extent (layer 67, within the Potosi) at 20, 25, 30, 40, 60 and 80 years.*

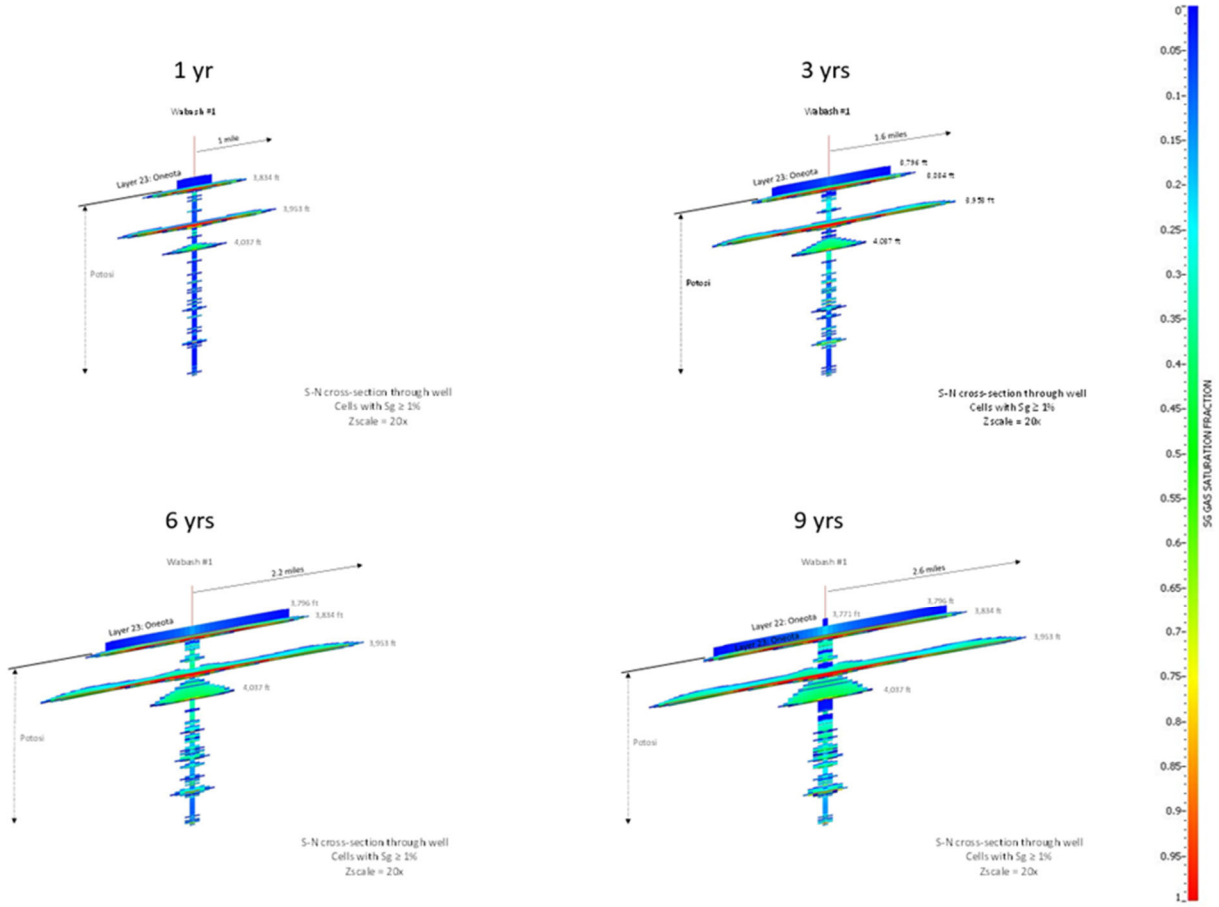

Figure 83. *South-North cross section through Wabash #1, showing the CO2 plume vs. time at 1, 3, 6 and 9 years. Only cells with gas saturation ≥ 1% are visible.*

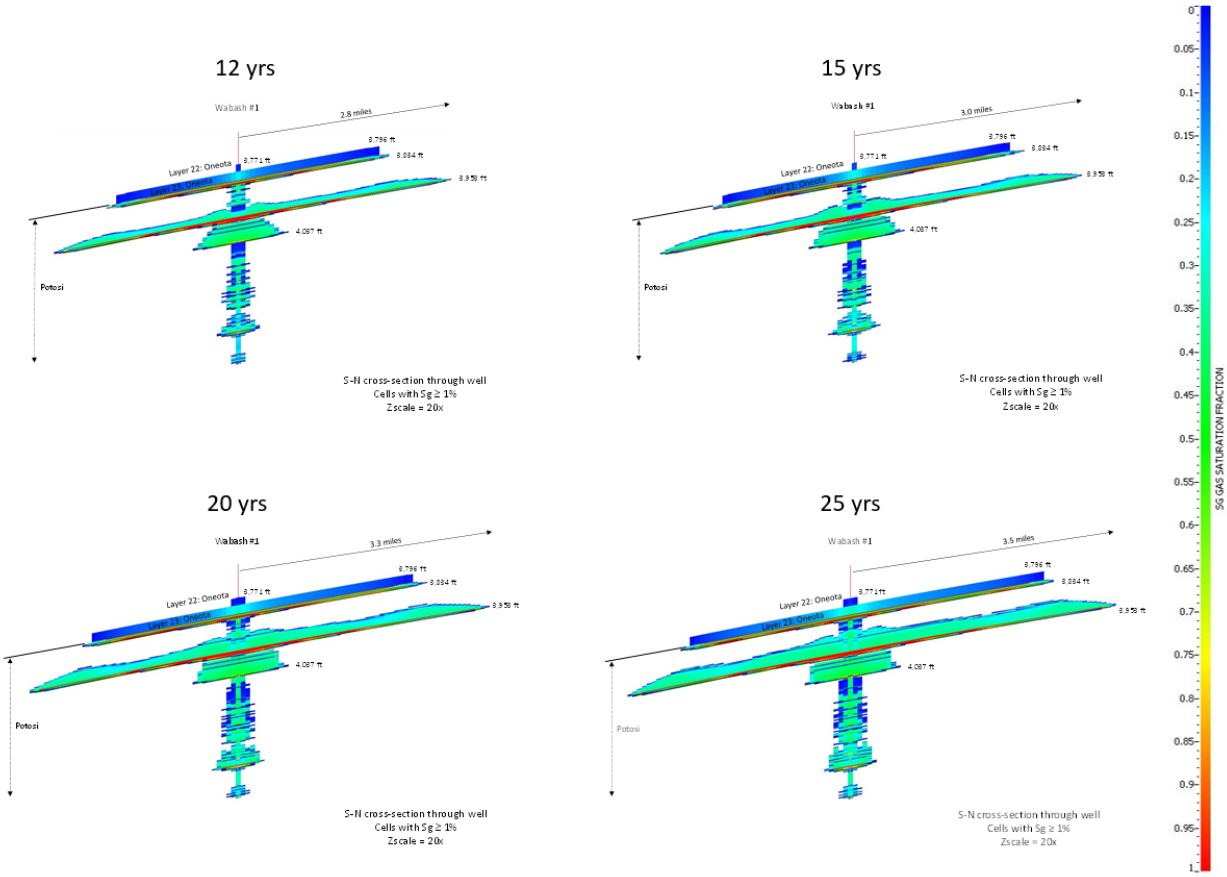

Figure 84. *South-North cross section through Wabash #1, showing the CO2 plume vs. time at 12, 15, 20 and 25 years. Only cells with gas saturation ≥ 1% are visible.*

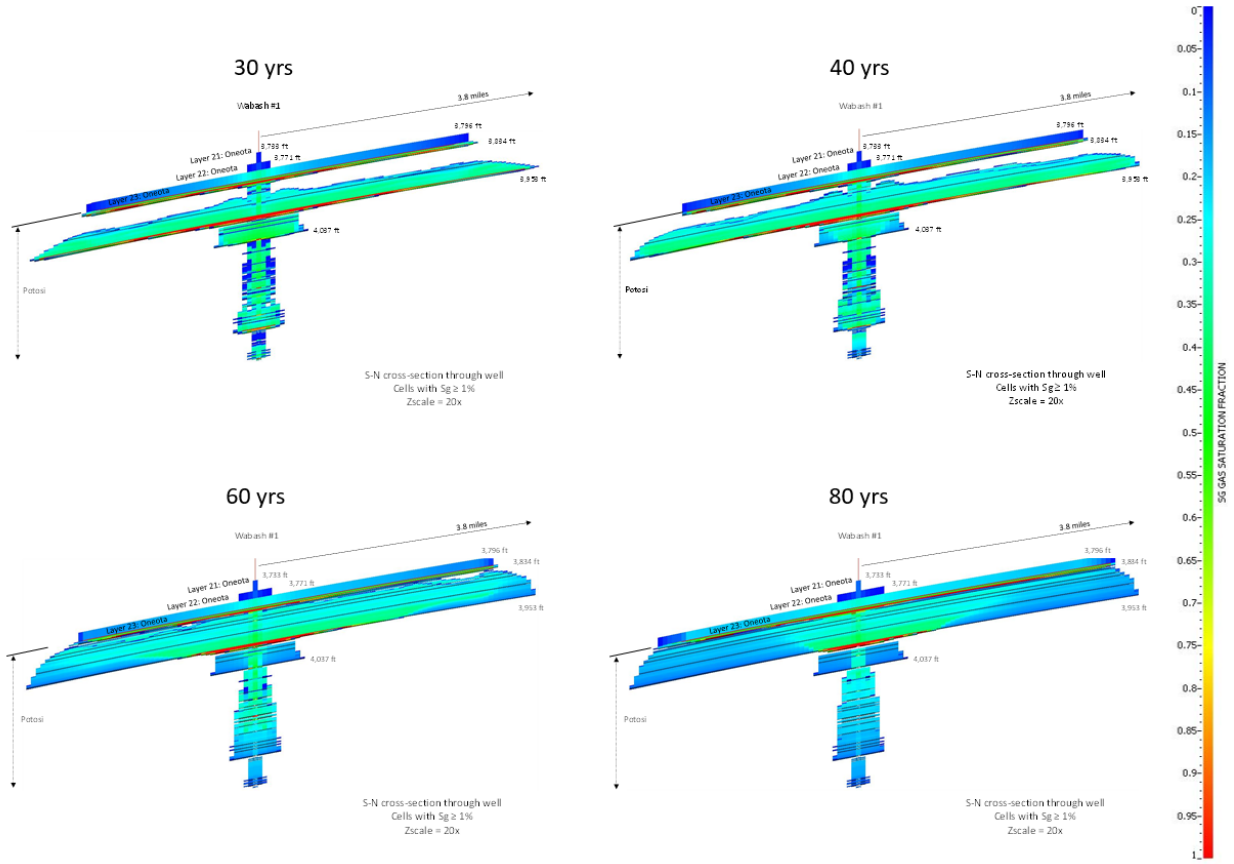

***Figure 85**. South-North cross section through Wabash #1, showing the CO2 plume vs. time at 30, 40, 60 and 80 years. Only cells with gas saturation ≥ 1% are visible.*

3.2.4.4 Single well injection of 1.67 MMTA of CO_2 into Wabash #1 for 12 years

This simulation scenario is a single well injecting 1.67 MMTA of CO_2 for 12 years. CO_2 is injected in Wabash #1 (Wabash1) for 12 years, followed by a 50 year post injection observation period. The total volume of CO_2 injected after 12 years is 20 MMtonnes. The well location and 8.5 x 8.5 mile refined grid region are identical to the 30 year injection case described in the previous section (see Figure 75).

Figure 86 shows the CO_2 plume after 12 years of injection at the layer having the greatest plume extent, layer 67 within the Potosi interval at the top of the tested vuggy interval. The largest dimensions of the plume are denoted. The plume extends furthest to the North and to the east of Wabash #1 at 2.2 and 2.1 miles; respectively. Figure 87 contains a South-North cross section through Wabash #1, and shows the CO_2 plume after 12 years of injection. Only simulation cells having gas saturation values ≥ 1% are visible. The asymmetric lateral shape of the plume shows the impact of reservoir dip. The vertical scale has been exaggerated 15x so the reservoir dip looks much larger than in reality. The majority of the CO_2 has entered the two highest-perm vuggy intervals within the Potosi. The plume has migrated vertically and has entered the bottom layer of the overlying Oneota formation.

Figure 88 contains a South-North cross section through Wabash #1, and shows the change in pressure (ΔP) after 12 years of injection. The highest increase in pressure is at the well location and is approximately 215 psi. It is important to note that the pressure change only reaches the Dutchtown formation. The formations overlying the Dutchtown see a negligible increase in pressure due to 12 years of injection. **Error! Reference source not found.** contains maps of pressure change (ΔP) after 12 years of injection at several layers within the model. These maps also illustrate that the pressure change stops at the Dutchtown formation.

Figure 90 contains plots of BHP and ΔP (= BHP at 30 years – initial pressure) vs. time for Wabash #1. The BHP increases by approximately 269 psi after 12 years of injection. After injection stops at 12 years, the BHP shows a rapid initial drop and then slowly decreases over time towards the initial pressure. Fifty years after injection stopped, the BHP is within 10 psi of initial pressure. The maximum BHP, after 30 years of injection, is significantly below the maximum BHP (90% of fracture pressure), which is 2,804 psia.

Figure 91 and Figure 92 show map views of the CO_2 plume within the Potosi, at layer 67 (which is the top of the tested vuggy interval) vs. time. Dimensions are denoted on the CO_2 plume. Although injection stops at 12 years, the largest plume size appears at 13 years, which is 1 year into the post injection period. Simulation results were output on a yearly basis, so the plume may have reached the maximum lateral extend anytime between the end of injection and 1 year into the post injection period. The plume stabilizes laterally after 13 years and does not expand laterally during the remainder of the 50 year post injection observation period. However, vertical migration of the plume within the Potosi and into the bottom two layers of the overlying Oneota continues throughout the 50 year post injection observation period.

Figure 93 through Figure 95 contain South-North cross sections through Wabash #1, and show a cross section of the CO_2 plume vs. time. Only simulation cells having gas saturation ≥ 1% are visible. The top of the CO_2 plume only enters the two bottom layers of the overlying Oneota. No CO_2 enters any overburden formations above the Oneota. Some vertical migration of the plume within the Potosi and into the lower Oneota is observed during the 30 year injection period, but substantial vertical migration of the plume within the Potosi and the lower Oneota is observed during the 50 year post injection observation period.

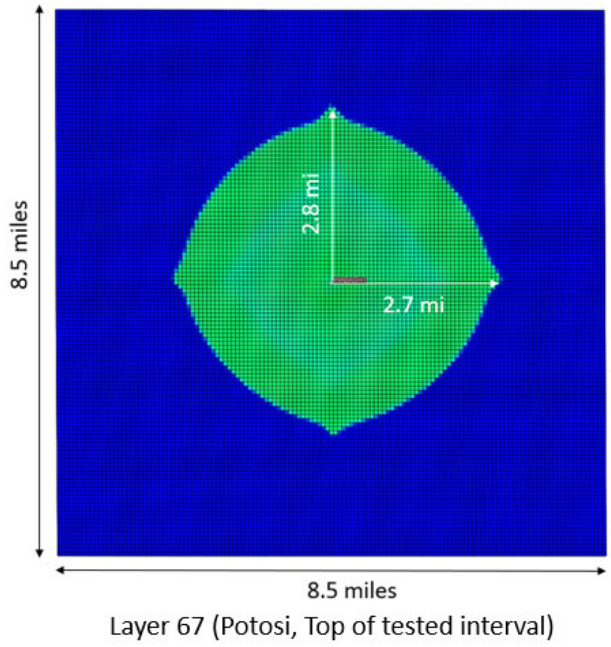

Figure 86. *Map view of the CO_2 plume after 12 years of injection at the simulation layer showing the largest plume extent (layer 67, within the Potosi).*

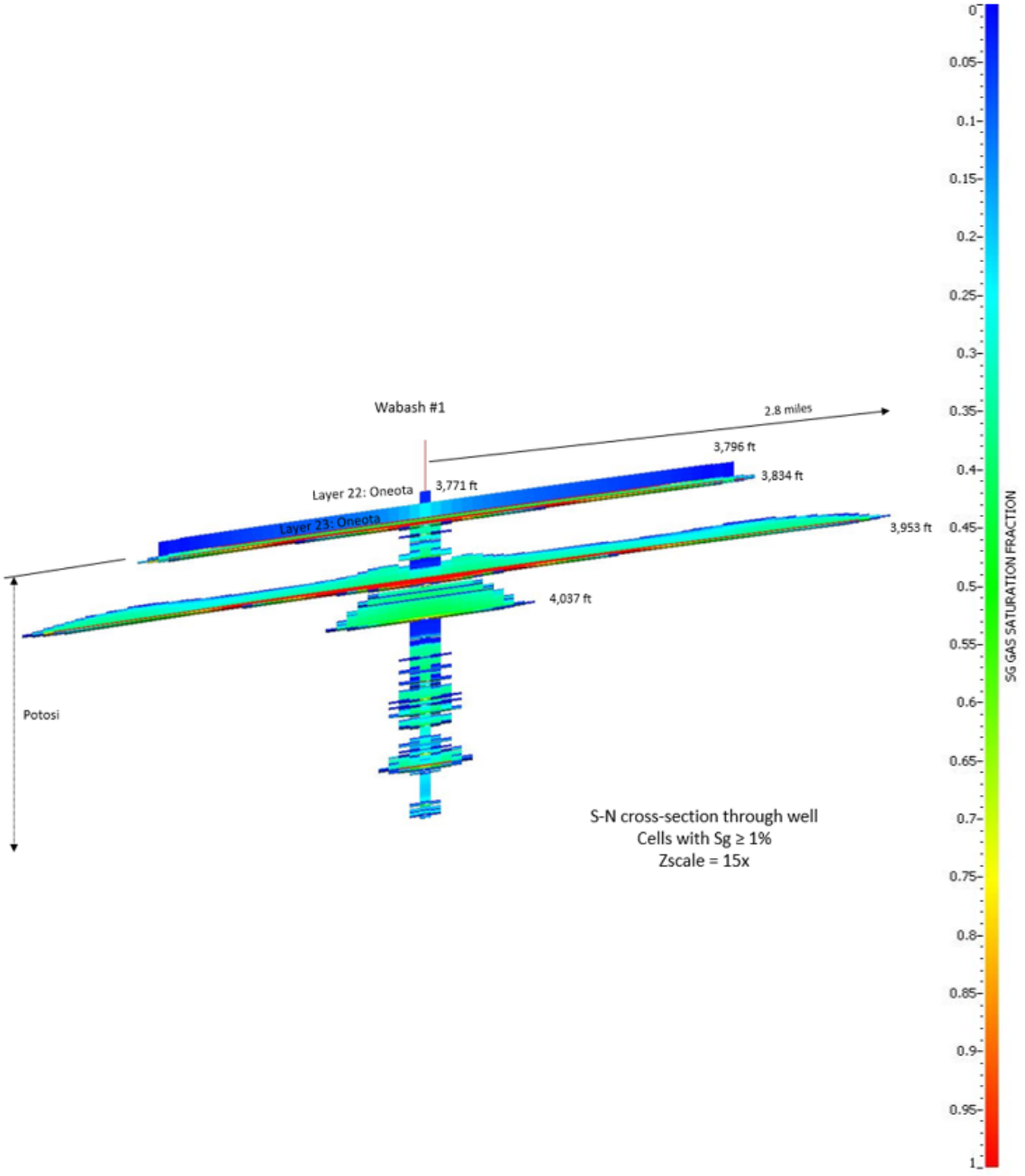

Figure 87*. South-North cross section through Wabash #1, showing the CO2 plume after 12 years of injection. Only cells with gas saturation ≥ 1% are visible.*

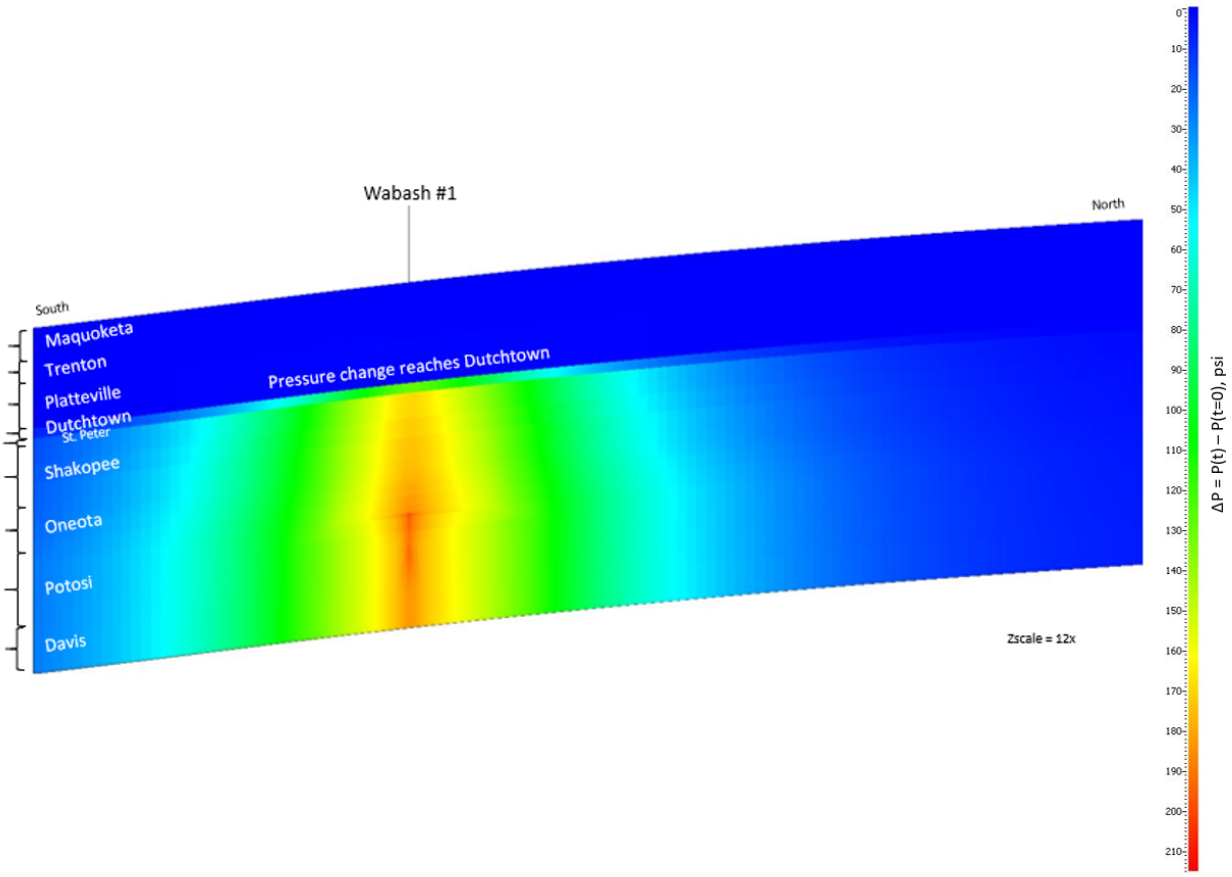

Figure 88. *South-North cross section through Wabash #1 showing the change in pressure (ΔP) after 12 years of injection.*

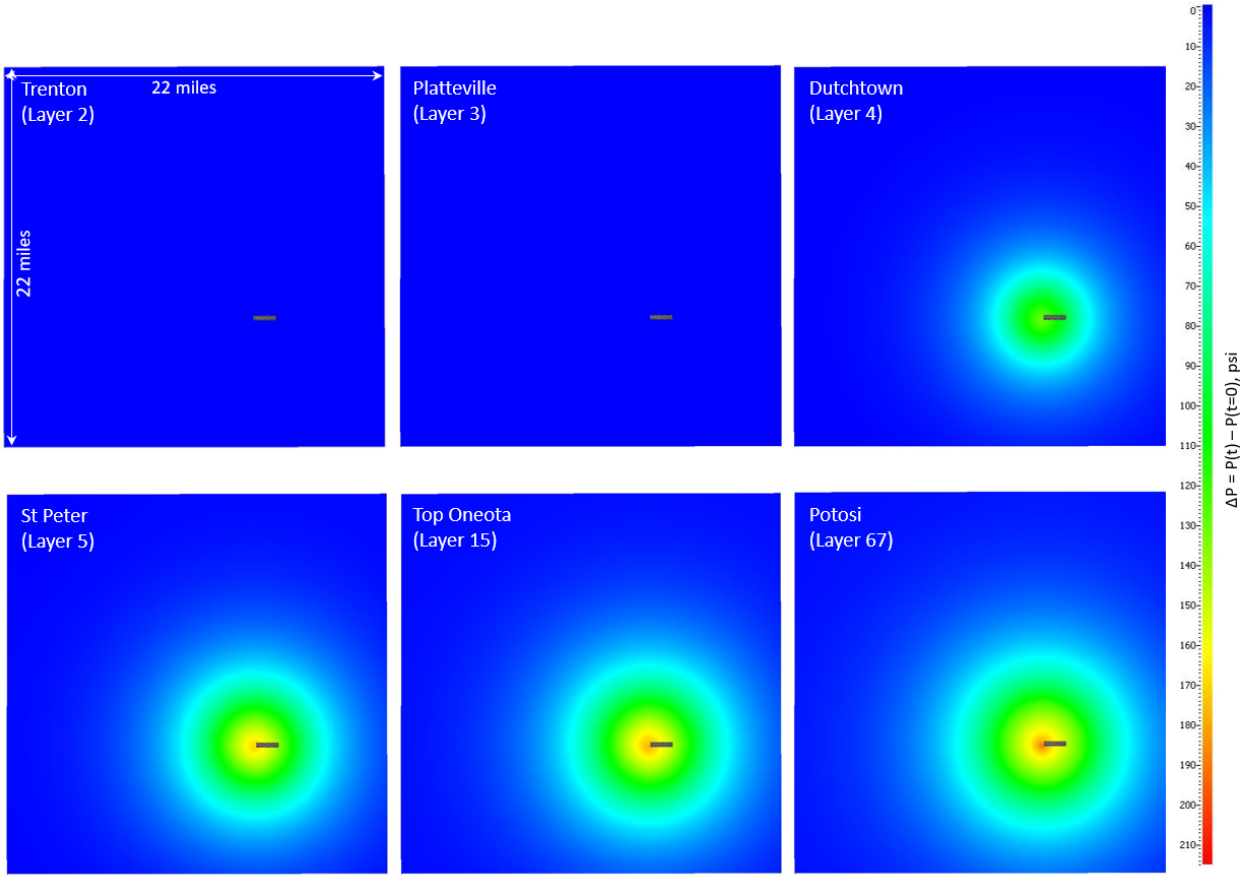

Figure 89. *ΔP maps, showing the change in pressure after 12 years of injection for several overburden formations and the Potosi (layer 67).*

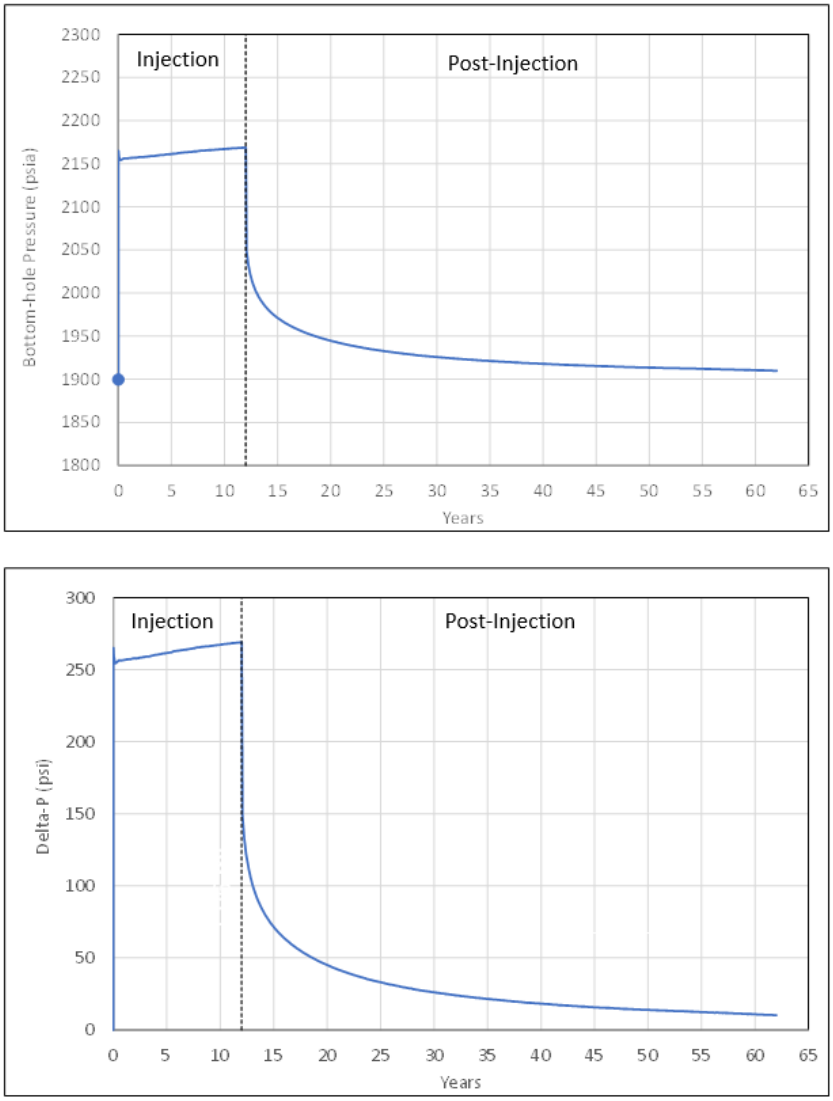

Figure 90. *Well BHP and pressure change (ΔP) vs. time for Wabash #1 during the 12 year injection period and the 50 year post injection observation period.*

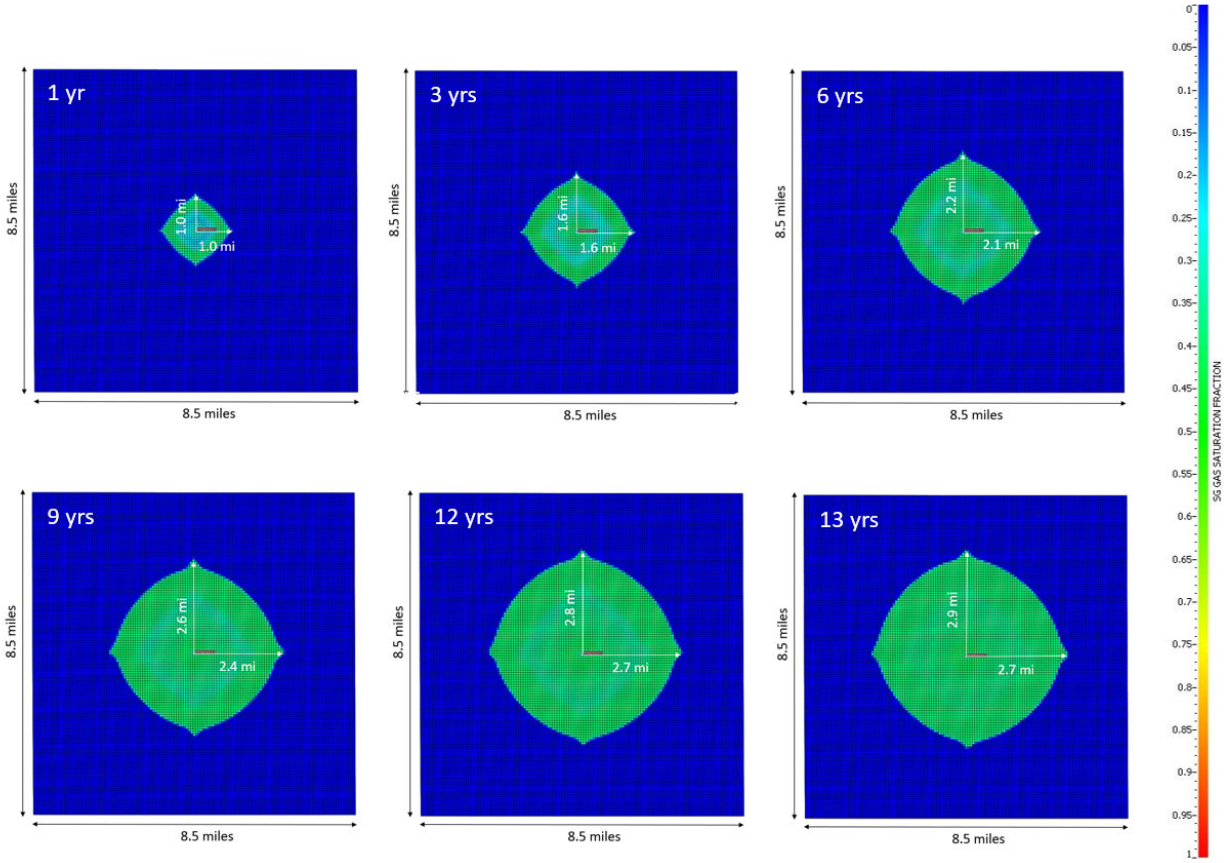

Figure 91. *Map view of the CO_2 plume vs. time at the simulation layer showing the largest plume extent (layer 67, within the Potosi) at 1, 3, 6, 9, 12 and 13 years.*

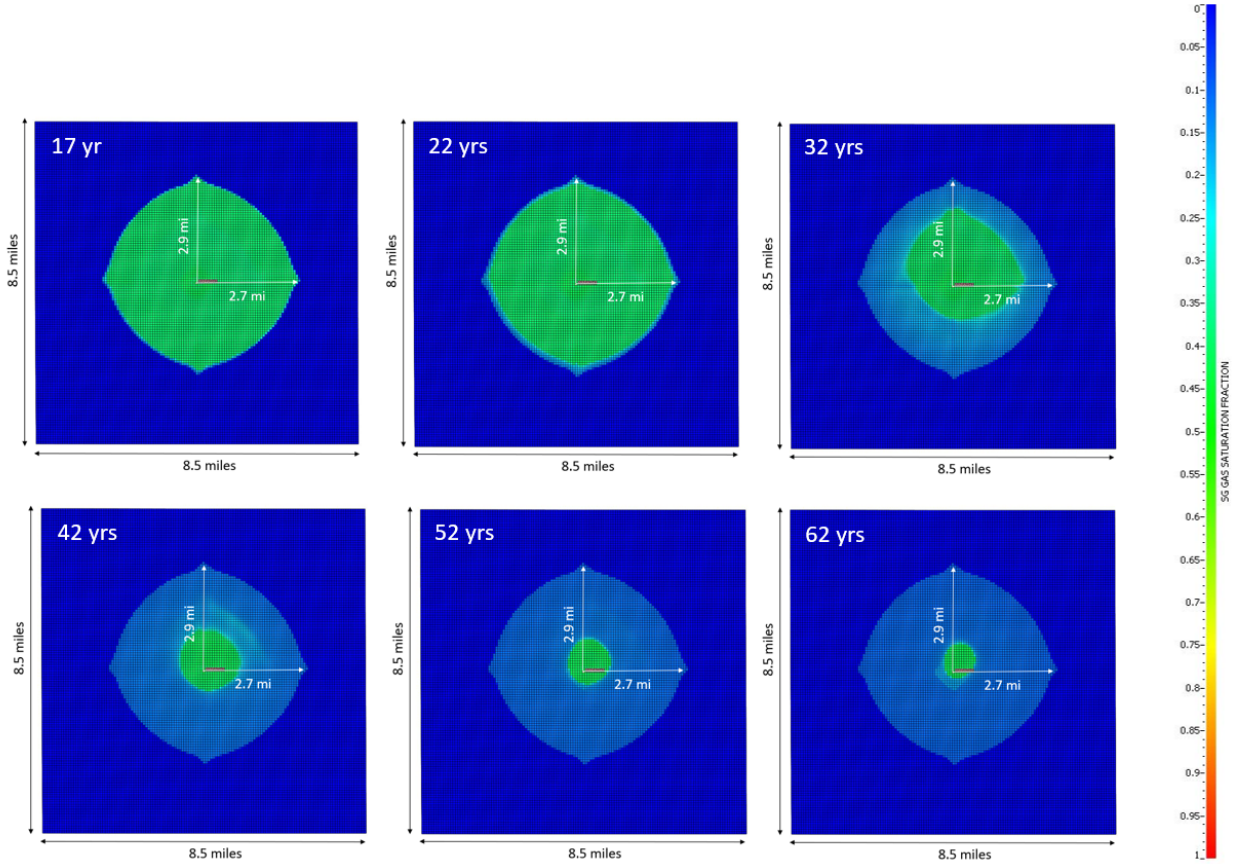

Figure 92. *Map view of the CO2 plume vs. time at the simulation layer showing the largest plume extent (layer 67, within the Potosi) at 17, 22, 32, 42, 52 and 62 years.*

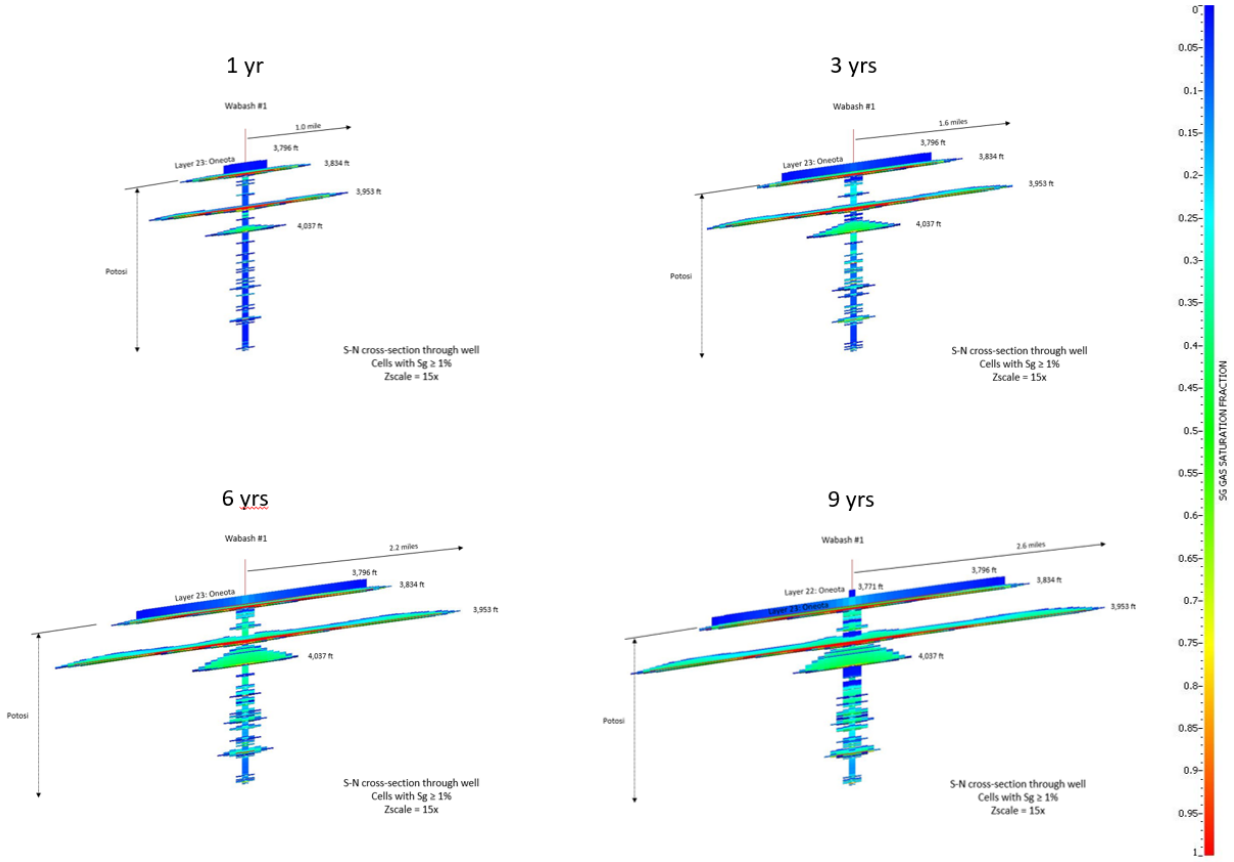

Figure 93. *South-North cross section through Wabash #1, showing the CO_2 plume vs. time at 1, 3, 6 and 9 years. Only cells with gas saturation ≥ 1% are visible.*

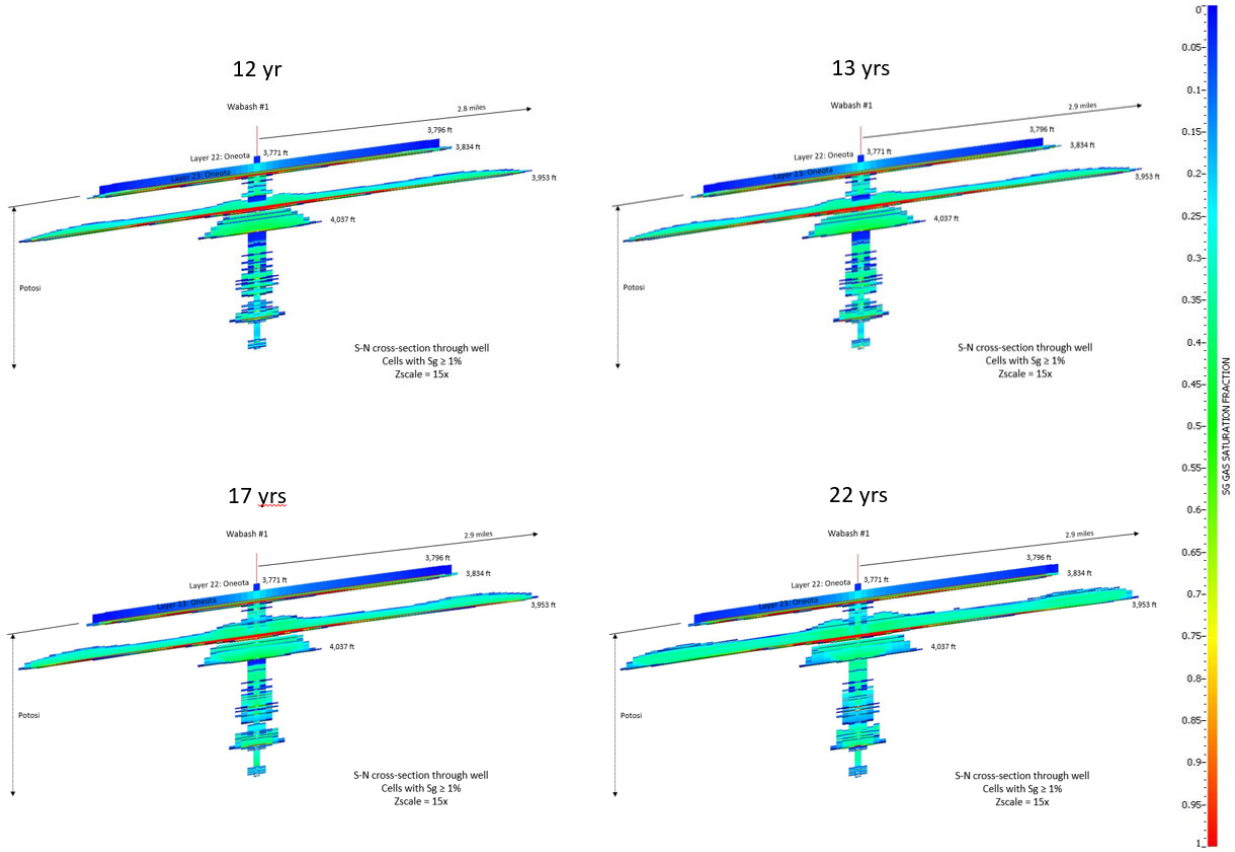

Figure 94. *South-North cross section through Wabash #1, showing the CO2 plume vs. time at 12, 13, 17 and 22 years. Only cells with gas saturation ≥ 1% are visible.*

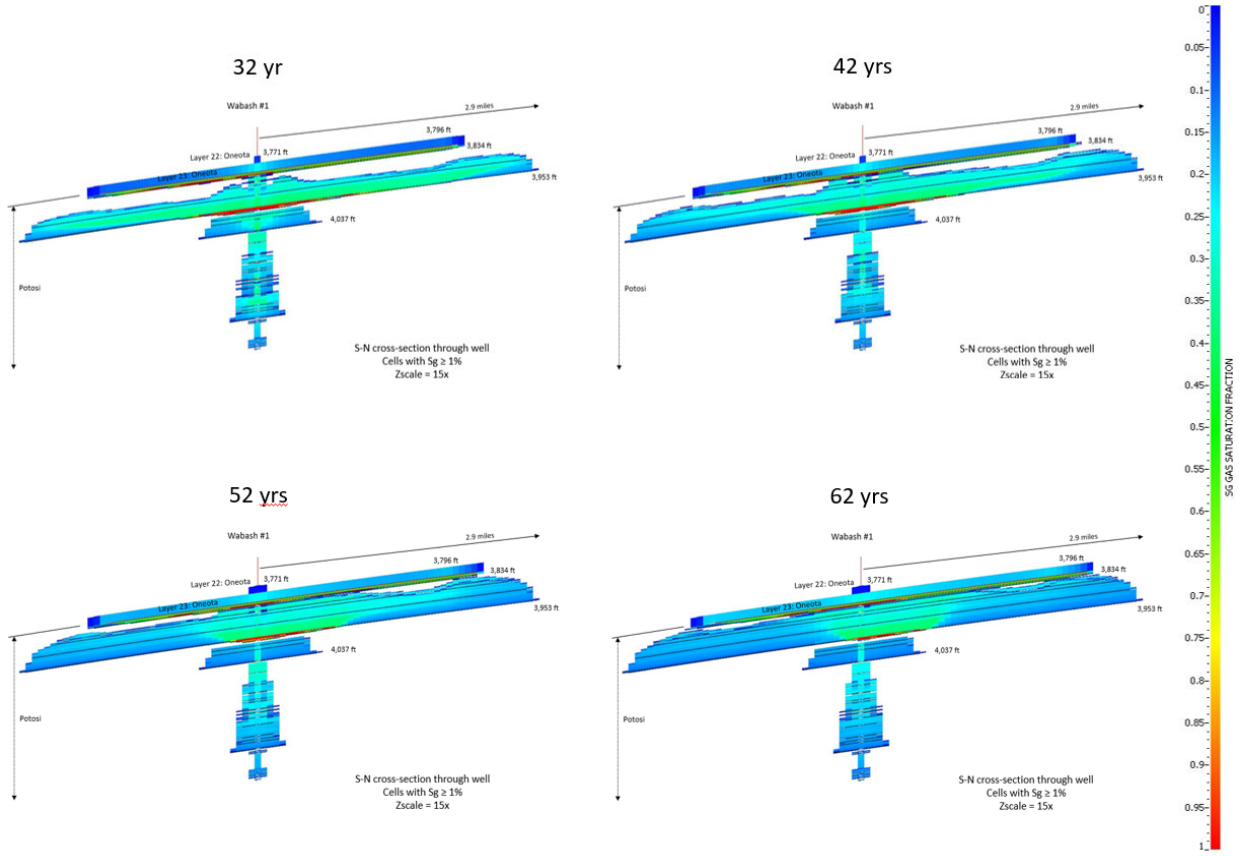

Figure 95. *South-North cross section through Wabash #1, showing the CO_2 plume vs. time at 32, 42, 52 and 62 years. Only cells with gas saturation ≥ 1% are visible.*

3.2.4.5 Estimation of Area of Review (AoR) for Two Well Injection Case

A hypothetical Area of Review (AoR) estimation was performed for the simulation scenario of a two-well combined injection of 1.67 MMTA of CO_2 for 12 years. This case was described in an earlier section and is considered to be feasible for storing 20 million tonnes (1.67 MMTA) of industrially-sourced carbon dioxide (CO_2) in a commercial-scale geological storage complex in the Wabash CarbonSAFE study area.

As indicated in the USEPA's Geologic Sequestration Data Tool (GSDT), "The boundaries of the AoR are based on simulated predictions of the extent of the separate-phase (i.e., supercritical, liquid, or gaseous) plume and pressure front" (USEPA, 2013). Model results were used to calculate the extent of the CO_2 plumes and pressure front, and those results were used to delineate the maximum AoR extent.

The two modeled injection wells are 5 miles apart in the north-south direction. The geometry of the AoR is delineated by the maximum lateral extent of the two CO_2 plumes, which modeling shows to be 14 years after the start of injection (i.e. two years after the 12-year injection period has stopped). Figure 96 shows the maximum plume distance from the North and South wells vs. time. Table 13 details the CO_2 plume sizes at 14 years.

The pressure front for AoR delineation was calculated using the EPA-Guidance method for critical pressure calculation in an overpressured reservoir (Nicot, 2009; USEPA, 2013). Calculations indicated that the change in pressure (ΔP) above native reservoir pressure required to potentially impact the expected lowermost USDW (in the Silurian-Devonian Carbonate-Rock Aquifer; see Korose et al., 2022) is 70.4 psi (0.44 MPa).

The input parameters and their sources are provided in Table 14. For the purposes of critical pressure calculation and AoR delineation, the reservoir zone was defined to extend to the base of the primary seal, the Maquoketa Group. Therefore, hydrostatic reservoir zone pressure and depth were extracted from the layer immediately below the Maquoketa Group, the Trenton Limestone. Because the Trenton Limestone was represented in the model by a single layer, and the ΔP reported was from the middle of that layer of grid cells, hydrostatic reservoir zone pressure and depth were also extracted from the middle of the Trenton Limestone layer of grid cells. The depth to the reservoir zone below the lowermost USDW, the Trenton Limestone, was determined using the formation top determined at Wabash #1. The fluid density within the Trenton Limestone was calculated by estimating R_{wa} from the deep resistivity and DPHI logs, and confirmed by calculating R_w from temperature and spontaneous potential logs (Archie, 1952; Asquith, 2004). Finally, fluid density (Table 14) was estimated using the R_w, R_{wa}, formation pressure and temperature, and salinity.

The critical pressure 70.4 psi (0.44 MPa) was scaled by 0.9 to provide a conservative estimate of the pressure-based AoR, and the resulting value of 63.4 psi was applied as a contour to the modeled ΔP in the Trenton Limestone, which is the model layer directly below the primary confining zone. The ΔP pressure front in the Trenton Limestone does not laterally, nor at any modeled time, exceed the estimated critical pressure required to endanger the lowermost USDW in the Silurian-Devonian strata; the maximum pressure reached in the Trenton Limestone was 0.137 psi ($0.9 * 10^{-4}$ MPa). Therefore, the AoR was based only on the extent of the CO_2 saturation plumes using a 1% saturation cutoff.

A map of the hypothetical AoR case (Figure 97) shows the predicted maximum lateral extent of the CO_2 plumes at 14 years after the start of injection (i.e. two years after the 12-year injection period has stopped), based on a 1% gas saturation cutoff. The modeled plumes are shown overlain on a topographic map of the immediate area around the example injection wells. The green/blue blocky shape of the simulation grid results for each well are inscribed within a solid blue polygon outline—which represents a more conservative delineation of the maximum extent of the CO_2 plume for each well; The combined CO_2 plume areas for both wells are used to delineate the AoR.

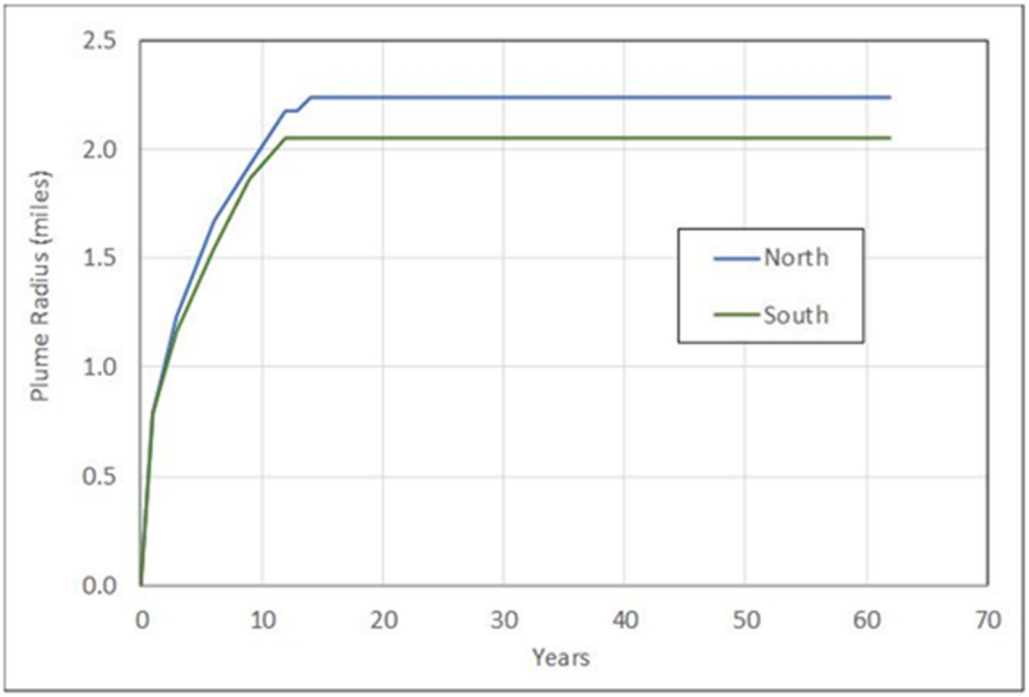

Figure 96. *Maximum (CO_2) plume radius vs. time, based on 1% saturation cutoff.*

Table 13. *Distance from each well to the edge of the CO_2 plume, at the maximum plume size.*

AoR Plume	Extent Direction	Approximte Distance from Well
North Plume	North	2.2 miles
	East	2.0 miles
	South	1.4 miles
	West	1.7 miles
South Plume	North	1.8 miles
	East	2.0 miles
	South	1.8 miles
	West	1.8 miles

Table 14. *Parameters and values used as input in the critical pressure calculation.*

Parameter	Value	Units	Source
Pressure at the base of the lowermost USDW	1,003.14	psi	Calculated using freshwater gradient of 0.433 psi/ft
Depth to base of the lowermost USDW	2,286	ft	Base of Silurian (top of Maquoketa Group), Wabash #1
Depth to reservoir zone below lowermost USDW	2,783	ft	Middle of Trenton Limestone model layer, Wabash #1 well
Hydrostatic reservoir zone pressure below lowermost USDW	1,140	psi	Calculated from Wabash #1 Pressure Fall Off testing fracture gradient
Fluid density within the reservoir zone below lowermost USDW	64.3	lb/ft3	Calculated from formation P and T, and deep resistivity, SP and DPHI logs

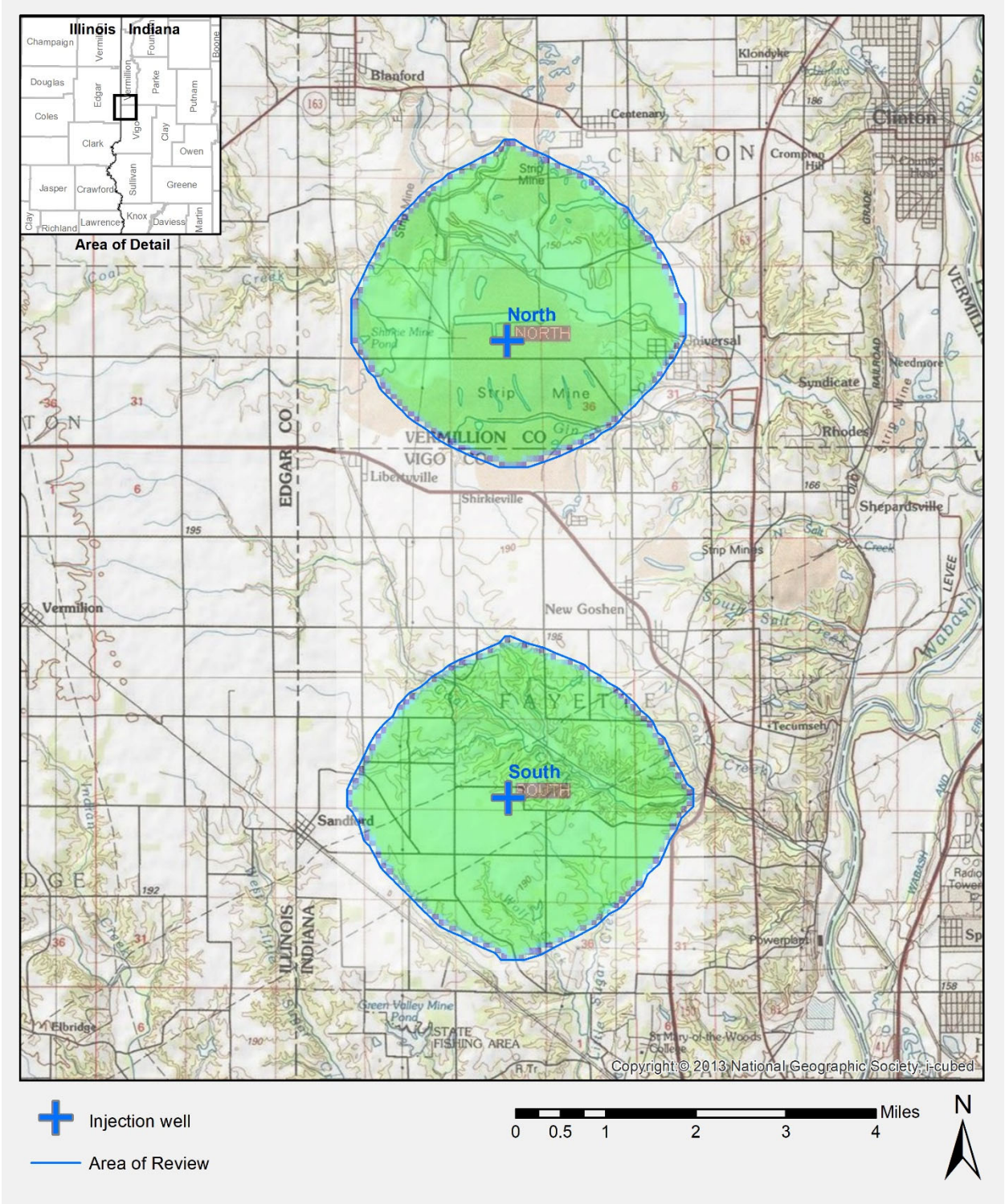

Figure 97. *Hypothetical AoR case showing the predicted maximum lateral extent of the CO_2 plumes at year 14, based on a 1% gas saturation cutoff. The modeled plumes are shown overlain on a topographic map of the immediate area around the example injection wells. A solid blue polygon outlines the green/blue blocky shape of the simulation grid results for each well.*

3.2.5 Summary of Potosi Simulation

Nexus® dynamic simulation models were constructed using the geologic models exported from Petrel™. The models are based on all the available data. A preliminary model, which included the Potosi Dolomite interval only, was used to: assess the CO_2 injectivity of a single well into the Potosi, perform a grid size sensitivity and help frame an injection concept for a 12 year CO_2 injection project.

An updated Potosi model was constructed. The updated model includes the Potosi Dolomite, underlying Davis Formation, and the overburden formations (listed in descending order) the Maquoketa Group, Trenton Limestone, Platteville (Black River) Group, Dutchtown Limestone, St. Peter Sandstone, Shakopee Dolomite, and Oneota Dolomite. The updated Potosi model was used to simulate several injection scenarios. Each simulation includes an injection period of either 12 or 30 years, followed by a 50 year post-injection observation period. The injection scenarios simulated are as follows:

- Two well injection of 1.67 MMTA of CO_2 for 30 years
- Two well injection of 1.67 MMTA of CO_2 for 12 years
- Single well injection of 1.67 MMTA of CO_2 into Wabash #1 for 30 years
- Single well injection of 1.67 MMTA of CO_2 into Wabash #1 for 12 years

Learnings from the Potosi simulation study are as follows:

- The Potosi has adequate injectivity to support a large scale CO_2 injection project at the Wabash site; as it is possible to inject over 5 MMTA for 30 years without exceeding the fracture pressure of the Potosi.
- CO_2 plume radius for injecting 1.67 MMTA for 12 years into Wabash #1 is 2.8 miles.
- CO_2 plume radius for injecting 1.67 MMTA for 30 years into Wabash #1 is 3.8 miles.
- CO_2 plume radius for injecting 1.67 MMTA for 12 years into two wells that are 5 miles apart is 2.2 miles.
- CO_2 plume radius for injecting 1.67 MMTA for 30 years into two wells that are 5 miles apart is 3.0 miles
- The pressure increase from injection does not substantially propagate vertically past the Dutchtown formation; which results in a negligible increase in pressure in any overlying formations above the Dutchtown.
- AoR for the Wabash CarbonSAFE site should be based on the maximum CO_2 plume extent because the pressure change at the base of the Maquoketa (top of the Trenton), which is the primary seal, is negligible and the pressure-based AoR is much smaller than the plume radius.

There are many sources of uncertainty in the model and results, several are listed below:

- The current models are layer cake models, with constant properties within layers, but heterogenous vertically across the layers. Layer cake models were built because of limited nearby well data. The drilling of additional wells in the area would allow for a more heterogenous model.
- Lateral extent and connectivity of the vuggy intervals within the Potosi are uncertain. The model assumes that the vuggy intervals are continuous across the entire 22 x 22 mile model.
- No core measured permeability, relative permeability or capillary pressure data are available for the Potosi matrix and/or vuggy intervals. Laboratory measurements of permeability, relative permeability, and capillary pressure using cores from the Potosi is recommended.
- The permeability and capillary entry pressures for the overlying formations were not measured; published correlations were used to calculate an average permeability from log porosity.
- CO_2 solubility in brine and chemical reactions of the CO_2 with the reservoir rock were not considered in this study.

4. References

Adushita, Y., and Smith, V., 2014. The Potosi Reservoir Model 2013, USDOE Topical Report, Report Number DOE/FE0002068-14, p. 33

Archie, G. E., 1952, Classification of carbonate reservoir rocks and petrophysical considerations: AAPG Bulletin, vol. 36, no. 2, p. 218–298.

Asquith G, Krygowski D (2004) Basic well log analysis. AAPG methods in exploration series, vol. 28. American Association of Petroleum Geologists, Tulsa, p 244.

Bennion, D. Brant, and Stefan Bachu. "Drainage and Imbibition CO_2/Brine Relative Permeability Curves at Reservoir Conditions for Carbonate Formations." Paper presented at the SPE Annual Technical Conference and Exhibition, Florence, Italy, September 2010. doi: https://doi.org/10.2118/134028-MS

Deutsch, C.V., 2002, Geostatistical reservoir modeling: Oxford, UK, Oxford University Press, 350 p.

Dubrule, O., 2003, Geostatistics for seismic data integration in Earth models: Society of Exploration Geophysicists/European Association of Geoscientists and Engineers, Distinguished Instructor Short Course, v. 6, 279 p.

Frailey, Scott M., 2021, Analyses of the Step Rate, Vertical Interference, Pressure Falloff/Buildup, and Multirate Tests of the McMillen #2 in the Eau Claire, Mt. Simon Sandstone, and Precambrian Basement, internal report for the CarbonSAFE Macon County Project (DE-FE0029381), Submitted on May 28, 2021.

Freiburg, J.T., Ritzi, R.W. and Kehoe, K.S., 2016, Depositional and diagenetic controls on anomalously high porosity within a deeply buried CO2 storage reservoir—The Cambrian Mt. Simon Sandstone, Illinois Basin, USA. *International Journal of Greenhouse Gas Control*, *55*, pp.42-54.

Khosravi, Mansour, Yaghoob Lasemi, Zohreh Askari, Hannes Leetaru, Scott Frailey, Oladipupo Babarinde, Donna Willette, Curt Blakley, Charles Monson, Carl Carman, Steve Whittaker, Chris Korose, 2022 (antic.), Geologic Analysis of the Potosi Dolomite Reservoir Interval and Potential Confining Units – Wabash CarbonSAFE Subtask 7.2, Technical Report for DOE-FE0031626. U.S Department of Energy.

Korose, Christopher, John Koenig, Curt Blakley, January 31, 2022, Wabash CarbonSAFE Policy, Regulatory, Legal, and Permitting Evaluation – Task 6.0, Technical Report: DOE-FE0031626-6. U.S Department of Energy.

Krevor, S.C.M., Pini R., Zuo L. and Benson S.M., 2012. Relative permeability and trapping of CO_2 and water in sandstone rocks at reservoir conditions. Water Resources Research, 48, W02532.

Lasemi, Y., and Khorasgani, Z. A., 2020, Stratigraphic variability, secondary porosity development, and correlation of the Cambrian Potosi Dolomite across the Illinois Basin, Annual GSA Meeting, abstract no.29-7.

Lemmon, Eric W., Mark O. McLinden and Daniel G. Friend, "Thermophysical Properties of Fluid Systems" in NIST Chemistry WebBook, NIST Standard Reference Database Number 69, Eds. P.J. Linstrom and W.G. Mallard, National Institute of Standards and Technology, Gaithersburg MD, 20899, https://doi.org/10.18434/T4D303, (retrieved November 16, 2021).

Lucia, F. J., 1983, Petrophysical parameters estimated from visual description of carbonate rocks: a field classification of carbonate pore space: Journal of Petroleum Technology, March, v. 35, p. 626-637.

Lucia, F. J., 1995, Rock-fabric/petrophysical classification of carbonate pore space for reservoir characterization: American Association of Petroleum Geologists Bulletin, v. 79, p. 1275-1300.

McCain, W.D.. "Reservoir-Fluid Property Correlations-State of the Art (includes associated papers 23583 and 23594)." *SPE Res Eng* 6 (1991): 266–272. doi: https://doi.org/10.2118/18571-PA

Newman, G.H., Chevron Oil Field Research Co., 1973. Pore-Volume Compressibility of Consolidates, Friable, and Unconsolidated Reservoir Rocks under Hydrostatic Loading. SPE 3835. Presented at SPE Rocky Mountain Regional Meeting, held in Denver, Colorado, 10-12 April 1972.

Nicot, J., Oldenburg, C., Bryan, S., and Hovorka, S., 2009. Pressure perturbations from geologic carbon sequestration: Area-of-Review boundaries and borehole leakage driving forces. Energy Procedia, 1, pp. 47-54.

USEPA. (2013). Geologic Sequestration of Carbon Dioxide Underground Injection Control (UIC) Program Class VI Well Area of Review Evaluation and Corrective Action Guidance. Office of Water (4606M) EPA 816-R-13-005 May 2013.